

The relationship between fallout radionuclides
and soil organic carbon in coniferous forest

January 2014

Mengistu, Teramage Tesfaye

The relationship between fallout radionuclides
and soil organic carbon in coniferous forest

Dissertation Submitted to
the Graduate School of Life and Environmental Sciences,
the University of Tsukuba
in Partial Fulfillment of the Requirements
for the Degree of Doctor of Philosophy in Science
(Doctoral Program in Integrative Environmental Sciences)

Mengistu, Teramage Tesfaye

Table of Contents

Abstract	iv
List of Tables.....	vii
List of Figures	viii
Chapter 1: General Introduction.....	1
1.1 Carbon storage in the environment and global warming.....	1
1.2 Forest, carbon cycle and soil erosion.....	3
1.3 Study approaches	5
1.4 Objectives and the structure of the study	11
References	12
Chapter 2: The relationship of soil organic carbon to $^{210}\text{Pb}_{\text{ex}}$ and ^{137}Cs during surface soil erosion in a hillslope forested environment	16
2.1 Introduction.....	16
2.2 Materials and Methods	18
2.2.1 Study site	18
2.2.2 Sampling procedures	21
2.2.3. Laboratory procedures and analysis.....	24
2.3 Results and Discussion.....	25
2.3.1 Soil and SOC displacement rates estimated from runoff plot.....	25
2.3.2 Comparison of radionuclides and SOC concentrations in eroded sediment	26
2.3.4 The relationship between displaced SOC and radionuclides	29
2.3.5 The relationship between displaced SOC and Pb/Cs ratio.....	32
2.3.6 $^{210}\text{Pb}_{\text{ex}}$ as a tracer of displaced SOC.....	34
2.4 Conclusions	36
References	37
Chapter 3: Atmospheric $^{210}\text{Pb}_{\text{ex}}$ and soil organic carbon in coniferous forest.....	43
3.1 Introduction.....	43
3.2 Material and methods	45
3.2.1 Site description	45
3.2.2 Data collection and analysis	46
3.3 Results and Discussion.....	49
3.3.1 Local reference inventory and annual atmospheric $^{210}\text{Pb}_{\text{ex}}$ flux.....	49
3.3.2 Inverted U-shaped bi-box compartment model	50
3.3.3 $^{210}\text{Pb}_{\text{ex}}$ and organic carbon input via litter.....	54
3.3.4 Litter-fed $^{210}\text{Pb}_{\text{ex}}$ deposition flux and its MRT in forest soil.....	56
3.3.5 $^{210}\text{Pb}_{\text{ex}}$ and SOC inventories, and their depth distribution profiles	62
3.4 Conclusions	69

References	69
Chapter 4: The migration of radiocesium in coniferous forest after Fukushima nuclear power plant accident	73
4.1 Introduction	73
4.2 Study site	76
4.3 Materials and methods	78
4.3.1 Litterfall sampling	78
4.3.2 Soil sampling	78
4.3.3 Laboratory analysis.....	80
4.4 Parameters for radiocesium depth profile	81
4.5 Characterizing the pre-Fukushima ¹³⁷Cs	82
4.6 Diffusion and migration rates of radiocesium in mineral soil	83
4.7 Results and discussion	84
4.7.1 Radiocesium in litterfall and on tree canopy	84
4.7.2 Radiocesium in forest soil.....	89
4.7.3 Depth distribution of radiocesium inventory and Of- horizon.....	96
4.7.4 The distribution of pre-Fukushima ¹³⁷ Cs in soil profile.....	98
4.7.5 The distribution of Fukushima-origin radiocesium in soil profile	101
4.7.6 Characteristics of the vertical distribution of radiocesium in soil profile	104
4.7.7 Diffusion and migration rates of radiocesium in the soil profile	105
4.8 Conclusions	109
References	109
Chapter 5: The use of ¹³⁴ Cs: ¹³⁷ Cs ratio to trace the migration of surface materials since the Fukushima accident.....	117
5.1 Introduction	117
5.2 Study site	120
5.3 Materials and methods	121
5.3.1 Litterfall sampling	121
5.3.2 Soil sampling	122
5.3.3 Laboratory analysis.....	125
5.4 Results and discussion	126
5.4.1 ¹³⁴ Cs: ¹³⁷ Cs ratio in litterfall.....	126
5.4.2 Vertical distribution of radiocesium in soil profiles over time	130
5.5 Conclusions	135
References	136
Chapter 6: General discussion and Conclusions	139
6.1 Main Findings of the study and their intra-linkage	139
6.2 Conclusions	142

References 146
Acknowledgments 147

Abstract

Despite the seriousness of erosion especially in forested areas, few isotope-based soil erosion studies exist, and information on soil organic carbon (SOC) in particular is limited and inadequate. Beside, the current lack of understanding of soil system forms is a bottleneck and sources of uncertainty in terrestrial carbon cycle predictions. Therefore, methods to precisely observe and monitor SOC are necessary. The behavior of radionuclides and SOC have been investigated using: (1) Runoff plots in three different forest types to observe the relationship between erosion-induced displaced SOC to discharged $^{210}\text{Pb}_{\text{ex}}$ and ^{137}Cs in a hillslope forested area. (2) Core soil samples and litter-derived deposits were monitored, collected and analyzed to investigate characteristics of the spatial and depth distribution of $^{210}\text{Pb}_{\text{ex}}$ and SOC in coniferous plantation forest. Simple bi-box compartment model was employed to estimate a stepwise deposition pattern of $^{210}\text{Pb}_{\text{ex}}$ with litter in Kochi prefecture. (3) The behavior of Fukushima-derived radiocesium is being investigated in coniferous forest in Karasawayama (Tochigi prefecture) using litter traps, runoff plots, scraper and core soil sampling techniques. In scraper plate sampling scheme (sampling area = 450 cm²), the soil samples were collected layer by layer to a depth of 30 cm from an undisturbed flat site. The forest floor components (understory plants, litter (Ol-) and fermented layers (Of-) were collected and treated separately.

A significant correlation was found between the displaced SOC and the radionuclides in each examined forest type. Compared with ^{137}Cs , however, the discharge of $^{210}\text{Pb}_{\text{ex}}$ is more closely correlated with the displaced SOC and shows a far low root mean square error (RMSE) value which approximately less by factor of two. This finding suggests that $^{210}\text{Pb}_{\text{ex}}$ and SOC are more likely than ^{137}Cs and SOC to move together in the course of soil erosion processes. Moreover, because ^{137}Cs was introduced in the 1960s by thermonuclear bomb tests and is being depleted, its availability in the environment could be limited in the foreseeable future just before Fukushima accident.

For detailed analysis Inverted-U shape bi-box compartment (IUS) model was proposed to easily illustrate the flow pathways of radiolead in both hillslope and stable forest area and helps to determine the $^{210}\text{Pb}_{\text{ex}}$ depositional partitioning in a stepwise pattern. Following this and assuming a constant $^{210}\text{Pb}_{\text{ex}}$ deposition flux in undisturbed site, the annual deposition of $^{210}\text{Pb}_{\text{ex}}$ in the study area was estimated about $614 \text{ Bq m}^{-2} \text{ year}^{-1}$. Of canopy-reside $^{210}\text{Pb}_{\text{ex}}$, litterfall transports about 53 % of it to forest floor. Along with, it also provides about $117 \text{ g m}^{-2} \text{ year}^{-1}$ organic carbon onto forest soil, implying that litterfall dynamics can influences the distribution of $^{210}\text{Pb}_{\text{ex}}$ and SOC in forest soil matrix. My results revealed that $^{210}\text{Pb}_{\text{ex}}$ tends the follow the behavior of SOC and both have shown identical profile shapes and strong correlation along the examined soil depth that explains 99% of its spatial variability. In addition, $^{210}\text{Pb}_{\text{ex}}$ is continuously replenished from its ubiquitous natural source as does SOC from fallen organic materials (e.g., litter); all together suggesting $^{210}\text{Pb}_{\text{ex}}$ can be a potential candidate to understand SOC redistribution and related processes.

Fukushima-derived radiocesium showed a general decreasing trend in litter regardless of the litterfall flux due to weathering and decaying. Higher concentration and very dynamic of Fukushima-derived radiocesium on forest floor revealed that a faster remobilization of radiocesium in this particular soil section. The raw organic layer (Ol+Of) holds 52% (5.3 kBq m^{-2}) of Fukushima-derived and 25% (0.7 kBq m^{-2}) pre-Fukushima radiocesium at the time of first soil sampling (16 January 2012) and the rest is distributed in soil below Of-layer. Including the pre-Fukushima ^{137}Cs , 99% of the total inventory was found in the upper ~10 cm in which the organic matter (OM) content was greater than 10%, suggesting the subsequent distribution is more likely to depend on the dynamics of OM. The $^{134}\text{Cs}:^{137}\text{Cs}$ ratio profiles showed a general decreasing trend along the depth; typically due to the presence of pre-Fukushima ^{137}Cs . Recent migration of surface material can be related and matched to the evolution of the $^{134}\text{Cs}:^{137}\text{Cs}$ ratio excluding the rapid phase of initial radiocesium migration. Soon after rapid-phase, the migration pattern shifts to passive

type that could depend on the migration of the OM. Hence, the answer of many key questions laid on the radiocesium behavior during decomposition process and its evolution over time. This needs further study so as to understand its migration in soil matrix and soil forming processes therein provide SOC migration in soil profile and can complement the $^{210}\text{Pb}_{\text{ex}}$ approach discussed in this study.

Key words: Erosion, Migration, Litterfall, Radiocesium, Radiolead, SOC, ^{134}Cs , ^{137}Cs , $^{210}\text{Pb}_{\text{ex}}$

List of Tables

Chapter 2

Table 2.1 Description of the runoff plots in study forest watersheds	22
Table 2.2 Soil particle compositions and estimated SOC and soil erosion rates	26
Table 2.3 Means of SOC proportion, radionuclide activities and inventories in sediments collected from runoff plots	27
Table 2.4 Comparison of $^{210}\text{Pb}_{\text{ex}}$ and ^{137}Cs based linear regression models for SOC and Root Mean Square Error (RMSE)	30

Chapter 3

Table 3.1 $^{210}\text{Pb}_{\text{ex}}$ inventory and SOC contents at the sampling points	50
Table 3.2 Seasonal distribution of litter driven inputs	51
Table 3.3 Measured $^{210}\text{Pb}_{\text{ex}}$ (activities and inventories), SOC (content and density) and litter-fed $^{210}\text{Pb}_{\text{ex}}$ MRT at each sampling point in the study hillslope.....	57

Chapter 4

Table 4.1 Deposition of radiocesium onto forest floor via Rainfall, Throughfall (TF), Stemflow (SF) and Litterfall (LF) at different sampling period	85
Table 4.2 Physiochemical properties in each soil layer	91
Table 4.3 The retention ^{137}Cs in the litter layer in different locations affected by Chernobyl power plant accident (% of the total soil inventory).....	94
Table 4.4 Values of diffusion and migration coefficients.....	107

Chapter 5

Table 5.1 The amount of litterfall and associated radiocesium activity	127
Table 5.2 The proportion of radiocesium inventory in forest soil over time	132

List of Figures

Chapter 1

- Figure 1.1 Schematic diagram on major global carbon pools and cycle 1
- Figure 1.2 The types of greenhouse gasses and their contribution to global warming... 2
- Figure 1.3 Summary of the distribution of global carbon in different pools. SOC= Soil organic carbon; SIC= Soil inorganic carbon; SC = Soil carbon 4
- Figure 1.4 The schematic sketch of sources and depositional pathways of fallout radionuclides (FRN) in the environment 8
- Figure 1.5 The structure of the study. SOC = soil organic carbon; OM = organic matter 10

Chapter 2

- Figure 2.1 Map of the study catchments and location of runoff plots 20
- Figure 2.2 Photographs of the floor surface condition of erosion plots established in three different forest types (a) BLF; (b) Japanese cedar; (c) Japanese cypress. ... 23
- Figure 2.3 Comparison histogram of sediment loads with previously reported results. 25
- Figure 2.4 Relationship of discharge amount between SOC and $^{210}\text{Pb}_{\text{ex}}$ and between SOC and ^{137}Cs in the eroded sediment collected from erosion plots in three forest types: (a, b) BLF; (c, d) Japanese cedar; (e, f) Japanese cypress..... 31
- Figure 2.5 The correlation between the inventories $^{210}\text{Pb}_{\text{ex}}$ and ^{137}Cs in sediment driven from different forest types: (a) BLF; (b) Japanese cedar; (c) Japanese cypress 33
- Figure 2.6 The relationship between eroded SOC and $^{210}\text{Pb}_{\text{ex}}/^{137}\text{Cs}$ ratio: (a) BLF, (b) Japanese cedar and (c) Japanese cypress 35

Chapter 3

- Figure 3.1 Map of the study site, the position and photographs of the sampling points (filled circles), litter traps (squares) and location of reference sites (filled stars) in Japanese cypress forest. 47
- Figure 3.2 Inverted U-shape $^{210}\text{Pb}_{\text{ex}}$ model for stable site scenario. The model illustrates the pathways and the fates of atmospheric $^{210}\text{Pb}_{\text{ex}}$ in reference site. The simplified framework of the model is shown in the right side and the indicated values are calculated based on the assumption discussed in the text..... 55
- Figure 3.3 The cumulative atmospheric $^{210}\text{Pb}_{\text{ex}}$ flux over the forest age..... 56
- Figure 3.4 One-to-one relationship between $^{210}\text{Pb}_{\text{ex}}$ inventory ratios (inventory of the i^{th} sampling point, I_{ith} , to reference inventory, I_{ref}) and MRT of litter-fed $^{210}\text{Pb}_{\text{ex}}$ 60
- Figure 3.5 Schematic diagram of $^{210}\text{Pb}_{\text{ex}}$ inverted U-shape flow path in erosion prone hillslope scenario. 61
- Figure 3.6 The depth distribution profiles of (a) radiolead and (b) SOC concentrations at the reference site..... 63

Figure 3.7 The depth distribution profiles of radiollead at each sampling point (SP- <i>i</i> 's) in the study watershed.....	65
Figure 3.8 The depth distribution profile of SOC at each sampling point (SP- <i>i</i> 's) in the study watershed.....	66
Figure 3.9 The relationship between $^{210}\text{Pb}_{\text{ex}}$ and SOC at (a) Reference site; (b) Hillslope	68

Chapter 4

Figure 4.1 Map of the study area and location of the sampling point	76
Figure 4.2 Monthly (bars) and cumulative (bold line) precipitation for one year duration at the study site. = indicates arrival of the radionuclide plume at the study site on mid-March (2011) and the wet deposition was expected due to the precipitation from March 15 to the first two weeks April, 2011.	77
Figure 4.3 Comparison on deposition of radiocesium onto forest floor via literfall route in coniferous forest. The deposition in an old spruce forest was obtained from literature (<i>Bunzl et al. 1989</i>) studied immediately after Chernobyl power plant accident (April 1986) and compared to cypress forest investigated following FDNPP accident (March 2011).....	86
Figure 4.4 Deposition of radiocesium onto forest floor via different routes over time in cypress forest after the FDNPP accident. The net area under each respective curve roughly represents the cumulative deposition of radiocesium by each depositional route.....	88
Figure 4.5 Retained ^{137}Cs in litter layer in different forest ecosystems over time. It compares my result to the reported values from different locations that were contaminated by Chernobyl accident (see also Table 4.3)	95
Figure 4.6 The vertical distribution of radiocesium inventory along the soil depth. The position of the peak is at Of -horizon. The ^{137}Cs inventory line runs above ^{134}Cs inventory more clearly in the deeper soil sections.....	97
Figure 4.7 Total and pre-Fukushima ^{137}Cs depth distribution profile	99
Figure 4.8 Pre-Fukushima ^{137}Cs depth profile (a) concentration distribution; (b) the corresponding inventory proportion	100
Figure 4.9 Depth distribution of Fukushima-derived radiocesium activity concentration below the Of-horizon of the forest soil; (a) ^{137}Cs and (b) ^{134}Cs concentrations profile. The black solid line shows the measured, gray solid line shows pre-Fukushima remains and the broken line is the fitting results by Eq.4.1. ..	102
Figure 4.10 Comparative position of the input parameters used for determination of Diffusion (D) and Migration rate (v) coefficients in soil depth profile distribution of Pre- and Fukushima-derived radiocesium.....	108

Chapter 5

Figure 5.1 Simple pictorial model representing radiocesium depositions via litterfall and its subsequent possible pathways in stable site. (<i>US</i> : understory vegetation; <i>Ol</i> :- litter horizon and; <i>Of</i> :- fermented horizon)	118
Figure 5.2 Expected ^{134}Cs : ^{137}Cs ratio over time along the vertical strata of forest	119
Figure 5.3 The model of initial theory. The direction of arrows shows the trends of the level. (OM stands for organic matter).....	120
Figure 5.4 Map of the study area and location of the sampling point	121
Figure 5.5 Photographs of the components of forest floor collected during soil sampling	123
Figure 5.6 Photographs of litter trap and scraper soil sampling setups in coniferous forest at references site.....	124
Figure 5.7 Laboratory procedures for soil and litter samples for radioactivity analysis	126
Figure 5.8 Temporal and spatial deposition pattern of litter and associated radiocesium after Fukushima accident. The red and broken line represents the weighted mean of the four litter traps during each respective observation period and the solid line show the cumulative deposition.	129
Figure 5.9 The depth distribution of the radiocesium activities (a) and the corresponding inventory (b) at the reference soil profiles in four different sampling dates. The number indicates the order of sampling time step sequence.....	131
Figure 5.10 Vertical distribution of ^{134}Cs : ^{137}Cs ratio and the corresponding OM fraction along fine soil depth resolution over time. LF stands for the ratio in the falling litter which assumed to be constant across the sampling dates.	134
Figure 5.11 The evolution of ^{134}Cs : ^{137}Cs ratio and SOM fraction in coarse soil section over time	135

Chapter 1: General Introduction

1.1 Carbon storage in the environment and global warming

The global carbon is stored in three fundamental pools in different proportion and forms (Figure 1.1). Namely, *Oceanic pool* (38,000Pg), *terrestrial pool* (including soil (SOC- 1550 and SIC 750Pg), vegetation- 560Pg, excluding carbonated sedimentary rock of geologic bands -5000Pg of which coal- 4000Pg, oil- 500Pg, gas- 500Pg) *atmospheric pool*- 760Pg with increasing rate of 3.2 Pg C year⁻¹ (Lal, 2003). All these pools are interconnected (Lal, 2003), and the exchange carbon flux among these components is to depend on the combination of natural and man-made driven forces like volcanic eruption, soil erosion, and deforestation, fire, burning of fossil fuel, land use changes and the like. As it is an important element that makes life possible in planet earth, equally it has also the potential to hamper (through onsite and offsite impact) and challenge life when it is relocated improperly and unwisely for example its accumulation in the atmosphere leads to global warming.

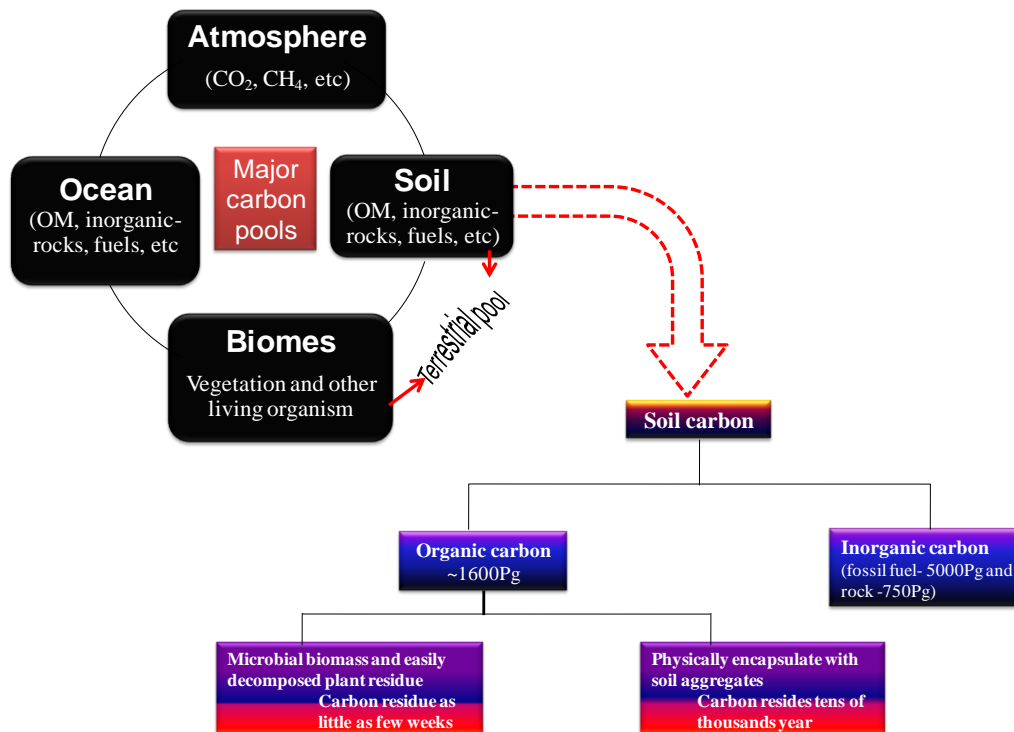


Figure 1.1 Schematic diagram on major global carbon pools and cycle

Global climate change is one of the most serious environmental problems to my living planet triggered by carbon based greenhouse gasses. Carbon dioxide (CO_2) takes the leading (60%) share with an increasing trend as a major cause of global warming followed by Chlorofluorocarbon (CFC), Methane (CH_4) and others (N_2O , NO_x , tropospheric O_3 , CO and water vapor)(Figure 1.2) (Christopherson, 1994). This issue is dominating international agendas since mid-1990s due to an increase of the world temperature by ever-increasing anthropogenic-driven carbon emission (Mole, 2012). In response, many working documents and strategies are proposed, being developed and to some extent started implementing to mitigate the problem (IPCC, 1995; 2003). Therefore, understanding the carbon in my environment is crucial step toward to understand and efficiently contribute for the solution.

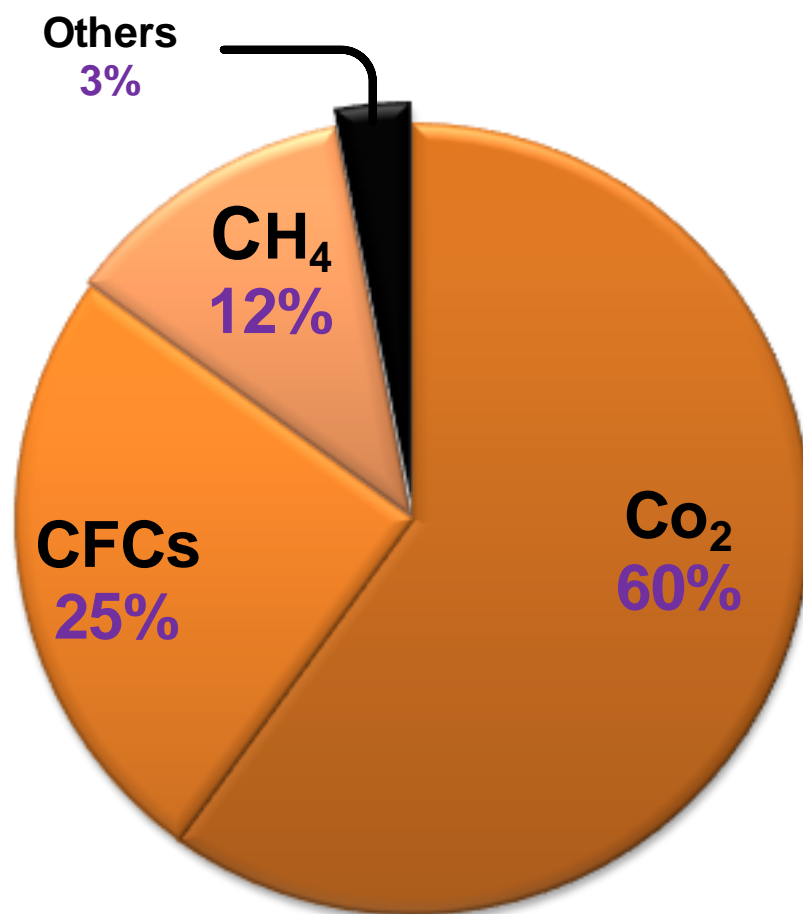


Figure 1.2 The types of greenhouse gasses and their contribution to global warming

1.2 Forest, carbon cycle and soil erosion

Among the terrestrial carbon pools, world soils are the major doorknob in global carbon cycle (Lorenz et al., 2006) and the largest store house of organic carbon (Schuman et al., 2002; Yanai et al., 2003; Lal, 2003). As it can be seen from the chart displayed in Figure 1.3, soil contains two to three times larger carbon than its amount in atmospheric pool and five times larger than biotic pool (Garten et al., 1999; Lal, 2003; Lorenz et al., 2006; Dinakaran and Krishnaya, 2008). Four billion hectare of the planet's forest land which is equivalent to 30% of the total terrestrial surface (Lal, 2005; FOA, 2006) holds 40% of the global soil carbon (Garten et al., 1999) of which most of the soil organic carbon (SOC) is located on the vicinity of soil surface. This made it the most sensitive carbon portion that could be impacted by different soil surface processes such as soil erosion.

Soil erosion is the natural process that rides and shapes the earth surface evolution since its creation and is governed by interactive and complex geomorphology and bio-physio-chemical factors. In amid of human interference on nature, accelerated erosion which is considered as a destructive process (Lal, 2003) modifies and affects the basic biogeochemistry processes of my planet. Carbon cycle is one of the basic process which directly and indirectly affected by soil erosion. In fact soil erosion causes various environmental problems particularly by affecting the largest global carbon pool (in soil) that ultimately aggravate global warming by releasing carbon to the atmosphere. This effect can be serious particularly in forested area where 40% the global soil carbon is reside (Garten et al., 1999; Lal, 2005) which in most cases are hills and mountainous part of the world.

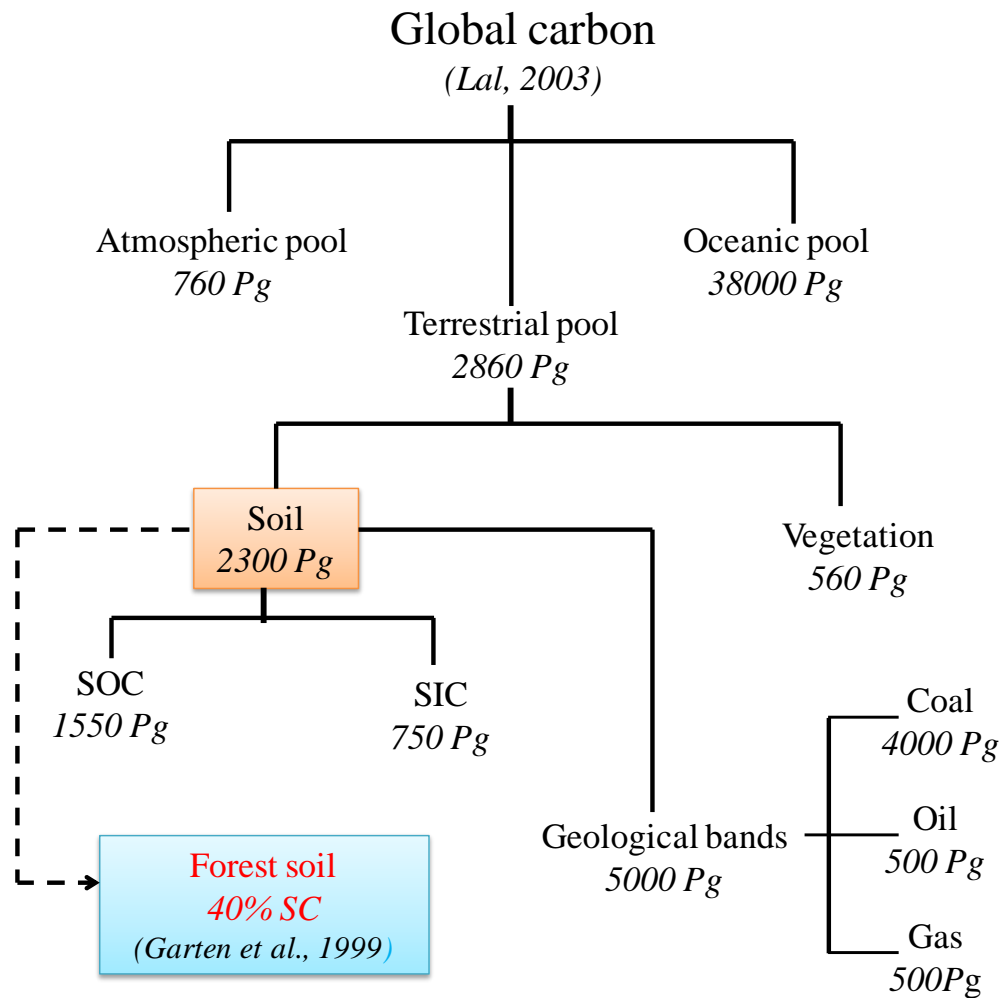


Figure 1.3 Summary of the distribution of global carbon in different pools. SOC= Soil organic carbon; SIC= Soil inorganic carbon; SC = Soil carbon

Given this considerable land cover that has huge carbon plus soil-forest as fundamental path that carbon has to pass-through in the global carbon networks, understanding particularly the very susceptible soil carbon component - soil organic carbon (SOC) in forested area in relation to water induced soil erosion is important. SOC is not only the key determinant of soil quality to biomass productivity but also a chief node of global carbon cycle which has the potential to influence the global climate and environmental moderating capacity (Polyakov and Lal, 2004; Ito, 2007). However, the current lack of understanding of soil system forms is a bottleneck and sources of uncertainty in terrestrial carbon cycle predictions (Braakhekke et al., 2013). Therefore, developing

methods to understand and therein manage soil erosion and SOC movement at field and watershed level are the two key factors to maintain and improve the soil quality to catch the ultimate objectives of human desires from it and may contribute to mitigate greenhouse effects.

1.3 Study approaches

Various natural and artificial radionuclides are present as abiotic component in our living environment and have a complex interaction with biotic elements including human beings. As the knowledge and understanding of radionuclides advances, the application and use out of them particularly to understand different environmental processes has emerged and is being developed.

In fact soil related process like erosion has been studied using a traditional techniques including erosion plots, erosion pin and indirectly from sediment discharge in the outlet of the target catchments. Nowadays, the application of nuclear techniques for the same purpose becomes common. This approach is cheaper and faster than the traditional one (Poreba, 2006). It can also provide the spatial distribution with its magnitude and even help to identify the sources of sediments as compare to the laborious and time consuming traditional techniques. Radionuclide application in soil sciences backs to 1960s, which started by measuring the relationship between the movement of fallout radionuclides and soil redistribution (Ritchie and McHenry, 1990). Since then the methods, approaches, protocols and models have been magnificently progressing for various land forms, mainly focusing on agricultural soils. The two most popular radionuclides that are serving for such purpose are radiocesium from artificial fallout radionuclides and Lead-210 in excess from natural fallout radionuclides.

Radiocesium (^{134}Cs : $t_{1/2} = 2$ years and ^{137}Cs : $t_{1/2} = 30.2$ years) was introduced to the atmosphere in three major episodes: first through detonation of atomic bomb test that lasts from mid-1950s to 1970s (peaked fallout in 1964) followed by Chernobyl nuclear power plant (ChNPP) accident (26 April 1986 in Ukraine) and more recently, Fukushima nuclear power plant (FNPP)

accident in North-east Japan on March 11, 2011, triggered by mega earth quake and the following tsunami. Three Mile Island nuclear accident (28 March 1979 in USA) can be taken as nuclear incident but its contribution to radioactive materials in the environment are negligible. Although the inherited behaviors of radiocesium released in three major episodes are common, the amount, the mechanisms of discharge, composition and distribution of radioactive materials from each radionuclide injection episode are more likely different. This is mainly due to the difference in the nature of the accident, methods applied to control over and available safety system, and local bio-physio-oro-graphy variability that plume crossover, meteorological parameters (temperature, wind and precipitation) at time of accident and subsequent peak deposition periods. For example, bomb radiocesium fallout was circulated globally as it was injected into the stratosphere and deposited back in spatial and temporal variable pattern depending on latitude, local precipitation pattern (Ritchie and McHenry, 1990) and particle size (Hirose, 2011) and was falling for quite extended period over broader part of earth surface. While the Chernobyl fallout, mainly composed of large particles and soot, was injected in to only few kilometers above the surface and had fallen back within about four weeks due to high post-release precipitation (Dorr and Munnich, 1991). In the case of FNPP accident, the radionuclides materials were associated with large particles that could limit to the lower part of troposphere (Hirose, 2011) and deposited back quickly. According to the reported atmospheric residence time of radionuclides that released from three major radionuclide discharge episodes, the following order can be identified: Atomic bomb (30 days) > Chernobyl (25 days) > Fukushima (8 days) (Hirose, 2011) of which Fukushima-driven is the shortest.

Lead-210 (^{210}Pb) is a naturally occurring fallout radionuclide (FRN) with a half-life ($t_{1/2}$) of 22.3 years. It is a direct α -decay progeny of ^{222}Rn ($t_{1/2} = 3.8$ days) formed in the ^{238}U ($t_{1/2} = 4.5 \times 10^9$ years) decay chain (Figure 1.4), which is found in almost all soils (EI-Daoushy, 1988; Dorr, 1995; Likuku, 2009). When ^{222}Rn decays to a series of short-lived ($t_{1/2} = 104 \mu\text{s} - 26.8$ min)

progenies, it eventually produces the long-lived isotope ^{210}Pb through α -decay. ^{210}Pb is produced both in situ in the soil air (pore space), and ex situ in the atmosphere when it is released from solid soil particles through α -recoil and diffusion along concentration gradients. To differentiate atmospheric ^{210}Pb from its terrigenous species (also called supported ^{210}Pb), the term “unsupported ^{210}Pb ” or ^{210}Pb in excess (hereafter expressed as $^{210}\text{Pb}_{\text{ex}}$ or radiolead unless stated otherwise) is used. Since $^{210}\text{Pb}_{\text{ex}}$ rapidly attaches to aerosols, it immediately participates in mixing and transport processes in the atmosphere. It is then re-deposited with tagged aerosols within 5 to 10 days to the soil surface by dry and wet deposition (Dorr, 1995; Fowler et al., 1995).

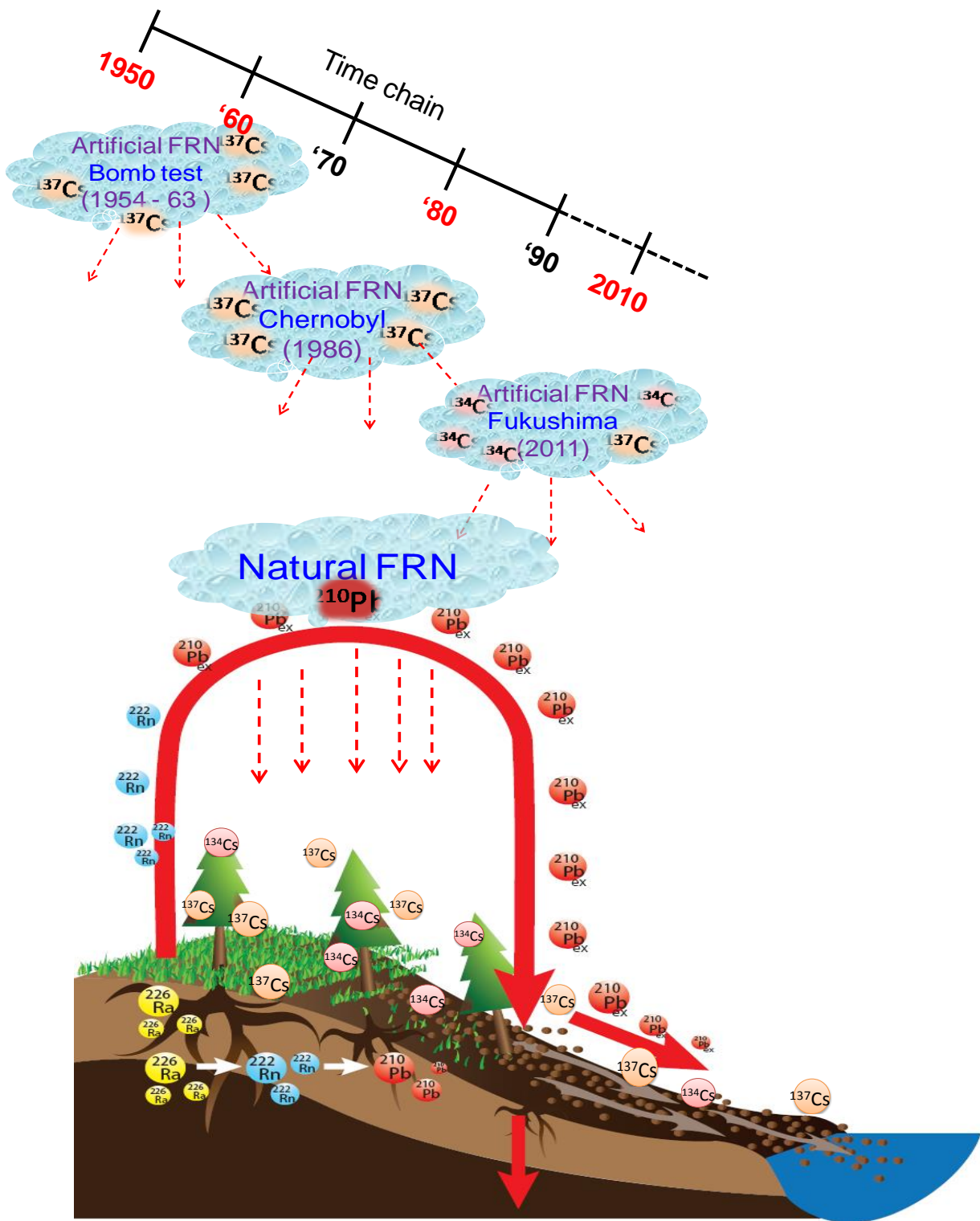


Figure 1.4 The schematic sketch of sources and depositional pathways of fallout radionuclides (FRN) in the environment

Both radiocesium and radiolead are fallout radionuclides (FRN) deposit from atmosphere onto earth surface. However, they differ in their deposition pattern: as radiocesium is artificially introduced, it has a starting point time and continuously reducing over time following pulse type of deposition pattern and are limited to the northern hemisphere where most of the emission had occurred. On the other hand, $^{210}\text{Pb}_{\text{ex}}$ follows a continuous type of input from its ubiquitous natural source. After deposition on land surfaces, both radionuclides are strongly adsorbed by organic matter (OM) and fine soil particles (Hancock et al., 2010; Zheng et al., 2007). Therefore, their subsequent movements are totally dependent on the movement of these components of the soil, is the basic concept where their application laid on. Accordingly, they have been used to document soil erosion in wide range of environments (Onda et al, 2003; Quine and Walling, 1996) but focusing in agricultural soils. their applications to processes in forested environmental in general and soil organic carbon (SOC) cycle in particular are so limited and inadequate, particularly information on the application of $^{210}\text{Pb}_{\text{ex}}$ is lacking mainly due to the complex nature of forested environment that might add difficulties at the initial stage of the study. Therefore, the possible approach can be started by looking at the basic and simple relationship between radionuclides and SOC in the complex forested environment and step on forward to deepen the knowledge horizon.

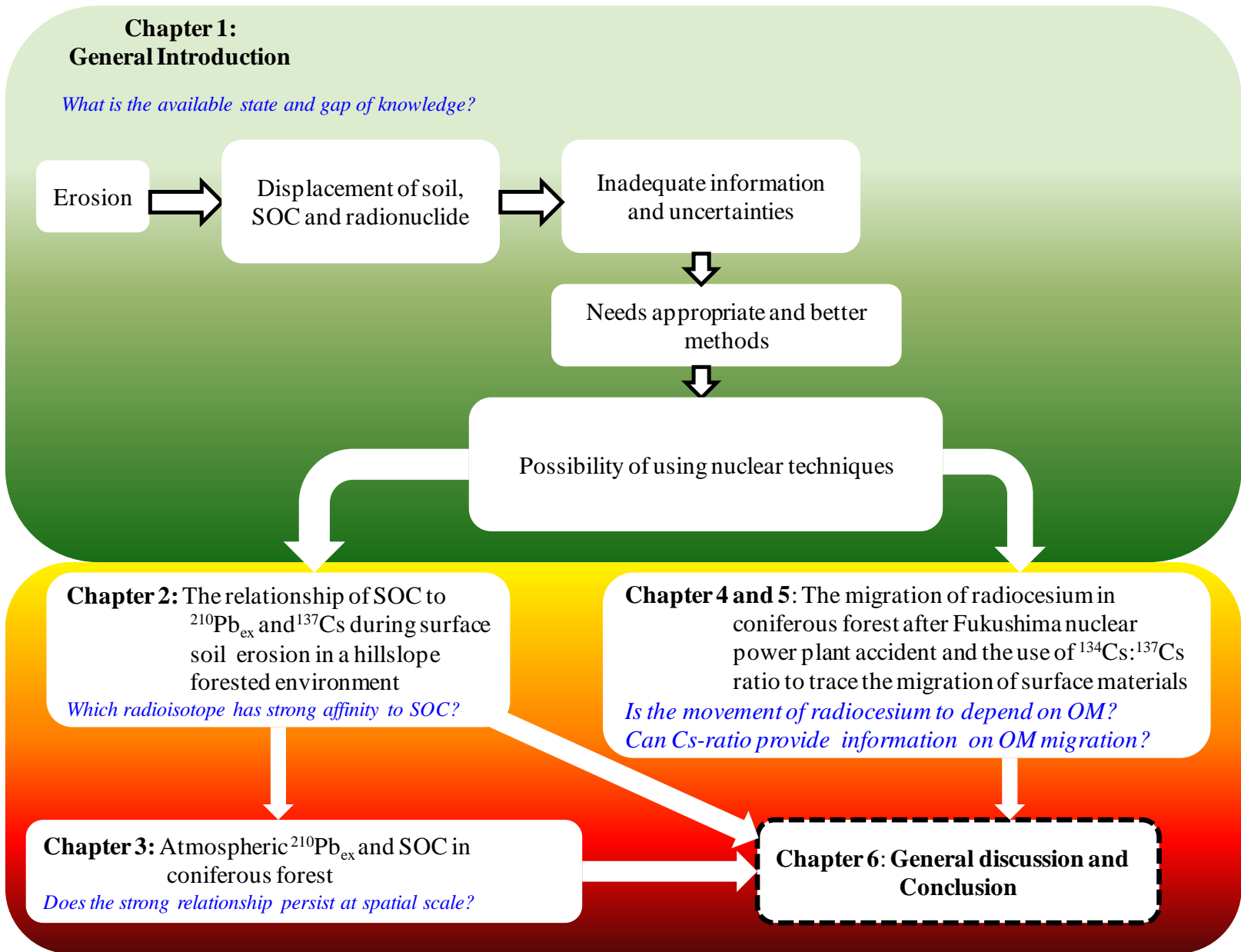


Figure 1.5 The structure of the study. SOC = soil organic carbon; OM = organic matter

1.4 Objectives and the structure of the study

The goal of the study was to evaluate the relationship between FRN and SOC in forested environment starting with simple processes based relationship. Comparison between observed relationships of SOC to the two major FRN has been done to screen out the best tracer. Using the opportunity of Fukushima-derived radiocesium, additional analysis was carried out to look at the migration of radionuclides in forest ecosystem and their possible uses to trace the sedimentation of surface organic materials along soil profile.

The general logical framework of the study is illustrated in Figure 1.5. The detail outlines of each chapter are highlighted as follow. In Chapter 2 the relationship of SOC to ^{137}Cs and $^{210}\text{Pb}_{\text{ex}}$ has been evaluated during soil erosion on physical basis. Three different hillslope forested environment has been used. The classical runoff plots were installed in each forest type to collect sediments during erosion events and the contents of radionuclides and SOC with the eroded materials were used for the purpose.

In Chapter 3 based on the results obtained from Chapter 2, the relationship and dynamics of SOC and $^{210}\text{Pb}_{\text{ex}}$ has be examined to deepen the knowledge and understanding at watershed scale. Their deposition from forest canopy on to forest floor was measured. Their relationship in both spatial and depth distribution across the watershed has been evaluated and comparison against their values at reference site (neither eroded nor deposited area) has been carried out and discussed. A qualitative model to represent their dynamics in forested environment was proposed.

In Chapter 4 the initial deposition and migration of Fukushima-derived radiocesium in Japanese cypress forest was studied. The radiocesium in forest floor was also determined. The deposition of radiocesium via litterfall and its contribution for soil inventory against hydrological pathway was discussed. The migration and diffusion coefficients along soil profile were determined

and compared with available values in literatures. The dependence of radiocesium on the organic matter (OM) also motivates to launch the next chapter.

In Chapter 5 the evolution of ^{134}Cs : ^{137}Cs ratio along soil profiles was evaluated based on four sampling dates at reference site following the Fukushima Daiichi Nuclear Power Plant (FDNPP) accident. A scenario was evaluated for the use of the ratio to understand the recent movement of surface organic material therein SOC along soil profile.

In chapter 6 the summary of main findings from each chapter is described. The prospective and final conclusions of the study are also presented.

References

- Braakhekke, M.C., Wutzler, T., Reichstein, M., Kattge, J., Beer, C., Schrumpf, M., Schoning, I., Hoosbeek, M.R., Kruijt, B., Kabat, P., 2013. Modeling the vertical soil organic matter profile using Bayesian parameter estimation. *Biogeosciences* **10**, 399 - 420
- Christopherson, R.W. 1994. An Introduction to Physical Geography. 2nd edition. New York, Macmillan.
- Dinakaran J., Krishnaya N., 2008. Variations in type of vegetal cover and heterogeneity of soil organic carbon in affecting sink capacity of tropical soils. *Current Science* **94** (9), 1144 – 1150
- Dorr, H., 1995. Application of ^{210}Pb in soils. *Paleolimnol* **13**, 157 – 168.
- Dorr, H., Munnich, O.K., 1991. Lead and Cesium transport in European Forest soils. *Water, air, and Soil Pollution* **57 – 58**, 809 – 818.
- EI-Daoushy, F., 1988. A summary on the lead-210 cycle in nature and related applications in Scandinavia. *Environment International* **14**, 305 – 319

- FAO, 2006. Global forest resources assessment 2005 progress towards sustainable forest Management. *Forest paper –147*
- Fowler, D., Mourne, R., Branford, D., 1995. The application of ^{210}Pb inventories in soil to measure long-term average wet deposition of pollutants in a complex terrain. *Water, Air and Soil Pollution* **85**, 2113 – 2118.
- Garten, C., Post, W., Hanson, J., Cooper, L., 1999. Forest soil carbon inventories and dynamics along an elevation gradient in the southern Appalachian mountains. *Biogeochemistry* **45**, 115 –145.
- Hancock, R., Murphy, D., Evans, K., 2010. Hillslope and catchment scale soil organic carbon concentration: an assessment of the role of geomorphology and soil erosion in undisturbed environment. *Geoderma* **155**, 36 – 45.
- He, Q., Walling, D. E., 1996. Interpreting particle size effects in the adsorption of ^{137}Cs and unsupported ^{210}Pb by mineral soils and sediments. *Journal of Environmental Radioactivity* **30** (2), 117 - 137.
- Hirose, K., 2012. 2011 Fukushima dai-ichi nuclear power plant accident: Summary of regional radioactive deposition monitoring results. *Journal of Environmental Radioactivity* **111**, 13 – 17.
- Intergovernmental Panel on Climate Change (IPCC), 1995. IPCC Second Assessment-Climate Change: A Report of the Intergovernmental Panel on Climate Change. Cambridge University Press, Cambridge.
- Intergovernmental Panel on Climate Change (IPCC), 2003. Good practices guidance for land use, land-use change and forestry. Institute for Global Environmental Strategies (IGES), Japan

- Ito, A., 2007. Simulated impacts of climate and land-cover change on soil erosion and implication for the carbon cycle, 1901 to 2100. *Geophysical Research Letters* **34**, doi:10.1029/2007GL029342.
- Lal, R., 2003. Soil erosion and the global carbon budget. *Environmental International* **29**, 437 – 450.
- Lal, R., 2005. Forest Soil and Carbon sequestration. *Forest Ecology and Management* **220**, 242 – 258.
- Likuku, A.S., 2009. Atmospheric transfer and deposition mechanisms of ^{210}Pb aerosols on to forest soils. *Water Air and Soil Pollution* **9**, 179 – 184.
- Lorenz, K., Lal R., Shipitalo M., 2006. Stabilization of organic carbon in chemically separated pools in no-till and meadow soils in North Appalachia. *Geoderma* **137**, 205 – 211.
- Mol, P.J., 2012. Carbon flows, financial markets and climate change mitigation. *Environmental Development* **1**, 10 – 24.
- Onda, Y., Takenaka, C., Furuta, M., Nonoda, T., Hamajima, Y., 2003. Use of ^{137}Cs for estimating soil erosion processes in a forested environment in Japan. *TransJapan Geomorphology Union* **24** (1), 13 – 25.
- Polyako, V., Lal R., 2004. Modeling soil organic matter dynamics as affected by soil water erosion. *Environmental International* **30**: 547 – 556.
- Poreba, G.J., 2006. Caesium-137 as a soil erosion tracer: a review. *Geochronometria: Journal on Methods and application of Absolute Chronology* **25**, 37 - 46.
- Ritchie, J.C., McHenry, J.R., 1990. Application of Radioactive Fallout Cesium-137 for Measuring Soil Erosion and Sediment Accumulation Rates and patterns: A Review. *Environ.Qual.* **19**, 215 – 233
- Schuman, G.E., Janzen H.H., Herrick J.E., 2002. Soil carbon dynamics and potential carbon sequestration by rangelands. *Environmental Pollution* **16** (3), 391 – 396.

Yanai, R.D., Currie, W.S., Goodale, C.L., 2003. Soil carbon dynamics after Forest Harvest: An Ecosystem Paradigm Reconsidered. *Ecosystem* **6**, 197 – 212.

Zheng, J., He X., Walling, D.E., Zhang, X., Flanagan, D., Qi, Y., 2007. Assessing soil erosion rates on manually-tilled hillslopes in the Sichuan hilly basin using ^{137}Cs and $^{210}\text{Pb}_{\text{ex}}$ Measurements. *Pedosphere* **17** (3), 273 – 283.

Chapter 2: The relationship of soil organic carbon to $^{210}\text{Pb}_{\text{ex}}$ and ^{137}Cs during surface soil erosion in a hillslope forested environment

2.1 Introduction

Forested environments lock in large amounts of the global carbon (Garten et al., 1999). However, soil erosion is a major threat in hillslope forested areas. In Japan, for example, many Japanese cypress (*Chamaecyparis obtusa* Sieb. et Zucc.) plantations are located on hillslopes with high stand density and poor ground cover. These slopes experience severe surface erosion and pose major environmental problems, even if a forest appears healthy from a distance (Onda et al., 2010). Recent reports of high soil erosion rates by Wakiyama et al. (2010) and Fukuyama et al. (2008) from different hillslopes of Japanese cypress forest confirm the seriousness of the problem. Mizugaki et al. (2008) demonstrated through radionuclide-based fingerprinting that hillslope forest floors, where SOC is located, are a major source of sediment. Soil erosion can influence SOC by burying it, moving it to the surface, and laterally distributing it across the forest floor. Erosion can also create site-specific quality differences (quality anomalies) by altering the physicochemical properties of the soil. These differences, in turn, can cause disequilibrium in the carbon pool and have far-reaching effects, including global warming. Despite the seriousness of erosion in forested areas, few isotope-based soil erosion studies exist, and information on SOC in particular is limited and inadequate. Therefore, to better understand and manage mountainous forested areas, methods to precisely observe and monitor SOC are necessary (Alewell et al., 2008; Ito, 2007).

In the past few decades, ^{137}Cs ($t_{1/2} = 30.07$ y), an artificial fallout radionuclide (FRN) from aboveground atomic weapons testing during the 1950s, has proven to be an effective trace marker in the study of soil erosion in a wide range of environments (e.g., Afshar et al., 2010; Hancock et al.,

2008; He and Walling, 1996; Kato et al., 2010; Loughran et al., 1990,1993; Mabit *et al*; 2009; Onda et al., 2003; Ritchie et al., 2005; Sac et al., 2008; Walling and He, 1999). In contrast, the naturally occurring $^{210}\text{Pb}_{\text{ex}}$ ($t_{1/2} = 22.3$ y) is a continuing FRN from ^{238}U decay and is commonly used to date sediments. After deposition on land surfaces, both radionuclides are strongly adsorbed by organic matter (OM) and fine soil particles (Hancock et al., 2010; Zheng et al., 2007). Therefore, their subsequent movements are totally dependent on the movement of these components of the soil. It follows from this basic concept that soil erosion rates can be estimated by comparing the radionuclide inventories at the site of interest to those at a local reference site (neither an erosion nor a deposition site) that represents the total FRN. The details of this method have been discussed elsewhere (e.g., Walling et al., 2002). Accordingly, several studies of soil erosion have successfully used ^{137}Cs as a marker, either alone or coupled with $^{210}\text{Pb}_{\text{ex}}$ (Mabit et al., 2009; Nearing et al., 2005; Sac et al., 2008; Walling et al., 2003; Walling and He, 1999). Such studies have tended to focus on agricultural soils. For example, Ritchie et al. (2007) suggested the possibility of linking SOC and ^{137}Cs in soil samples from two Iowa farms. Several studies have also simultaneously investigated the displacement of soil and SOC or soil and OM on cultivated lands using ^{137}Cs as a marker (Mabit and Bernard, 2010; van Oost et al., 2007; VandenBygaart, 2001; Walling et al., 2003). A few studies of soil erosion have used $^{210}\text{Pb}_{\text{ex}}$ as a marker, either alone or as a supplement to ^{137}Cs (Kato et al., 2010; Mabit et al., 2009; Porto et al., 2006; Walling et al., 2003; Walling and He, 1999; Zhang et al., 2006). Nevertheless, the relationship of $^{210}\text{Pb}_{\text{ex}}$ to SOC is still poorly understood, particularly in forested environments.

Although ^{137}Cs has been successfully used to study soil redistribution in the southern hemisphere (Chappell et al., 2011; Hancock et al., 2008, 2010; Loughran et al., 1988,1990,1993; Martinez et al., 2010; Morris and Loughran, 1994), its wider application appears limited to the northern hemisphere, where nuclear weapons testing primarily occurred. This site-specific condition

most likely hampers the potential of ^{137}Cs to cover global-scale issues (Walling et al., 2003). $^{210}\text{Pb}_{\text{ex}}$, on the other hand, has a natural source, ^{222}Rn . For this reason, it is a constituent of soils worldwide. Although it has found little application outside sediment dating and has received little attention in soil erosion studies, $^{210}\text{Pb}_{\text{ex}}$ has been shown to adsorb to soil particles (He and Walling, 1996) and to bind tightly to humic substances (Blake et al., 2009; Dorr, 1995). It has been generally suggested that the dynamics of radionuclides in forest soil may be related to the existence of OM (Dorr and Munnich, 1991; Vaaramaa et al., 2010). Hence, it is possible to infer that because of the continual replacement of $^{210}\text{Pb}_{\text{ex}}$ by new deposition in a manner similar to OM, $^{210}\text{Pb}_{\text{ex}}$ could be an indicator of OM movement in forested areas (Wakiyama et al., 2010). Nevertheless, little is known, and direct evidence is lacking, regarding the relationship between $^{210}\text{Pb}_{\text{ex}}$ and SOC movement in various environments including forested areas. In addition, the existing knowledge of $^{210}\text{Pb}_{\text{ex}}$ applications is limited, and the topic is under-researched.

I postulate that $^{210}\text{Pb}_{\text{ex}}$ can be associated with and directly quantify SOC in forested areas. Hence, I comparatively examined the SOC and radionuclides contained in eroded sediments collected from hillslopes of three different forest types using a classical method of studying erosion (i.e., runoff plots). This study investigated the relationship of SOC with $^{210}\text{Pb}_{\text{ex}}$ and ^{137}Cs with the goals of expanding the frontiers of SOC exploration, either independently or simultaneously with soil erosion assessments, and improving our understanding of the applications of radionuclides to the study of forest systems.

2.2 Materials and Methods

2.2.1 Study site

The study was conducted in three forest types located in two subwatersheds (downstream and upstream) of the Tsuzura River subbasin in Kochi Prefecture, Japan. The climate of the basin is classified as humid, temperate monsoon with a mean rainfall of 2735 mm y^{-1} and a mean

temperature of 14.6°C. The elevation ranges from 175 to 560 m asl. The soil of the subbasin was categorized as brown forest soil. Both subwatersheds can be characterized as steep slopes with a narrow range of gradients (34 - 40°) and more or less similar geomorphic properties.

The upstream subwatershed (33°08'N, 132°55'E, Figure 2.1a) consists of the first two study forest types. The first type was a natural broadleaf forest (BLF). The second type was a forest of Japanese cedar (*Cryptomeria japonica* D. Don.), commonly called *sugi* (these two terms will be used interchangeably in this paper). The BLF covered 4.9 ha and was composed of native species such as *Quercus acuta*, *Q. glauca*, and *Q. aslicina* on the slopes and *Abies firma*, *Tsuga sieboldii*, and *Chamaecyparis obtusa* on the ridge tops. The 30- to 40-year-old monoculture of Japanese cedar covered 2.4 ha. A litter layer covered the forest floor during the study period.

A third forest type, Japanese cypress (*Chamaecyparis obtusa* Sieb.et Zucc.) forest, locally termed *hinoki* (these two terms will be used interchangeably in this paper), covered 2.1 ha in the downstream subwatershed (33°10'N, 132°57'E, Figure 2.1b). The forest was planted between 1965 and 1969, and the stand density at the time of the study was estimated to range from 1400–2750 stems ha⁻¹. Most of the forest floor of the stand was bare due to the closed canopy. Figure 2.1c illustrates the runoff plot setup and its major components (as an example). These runoff plots were installed in each type of study forest.

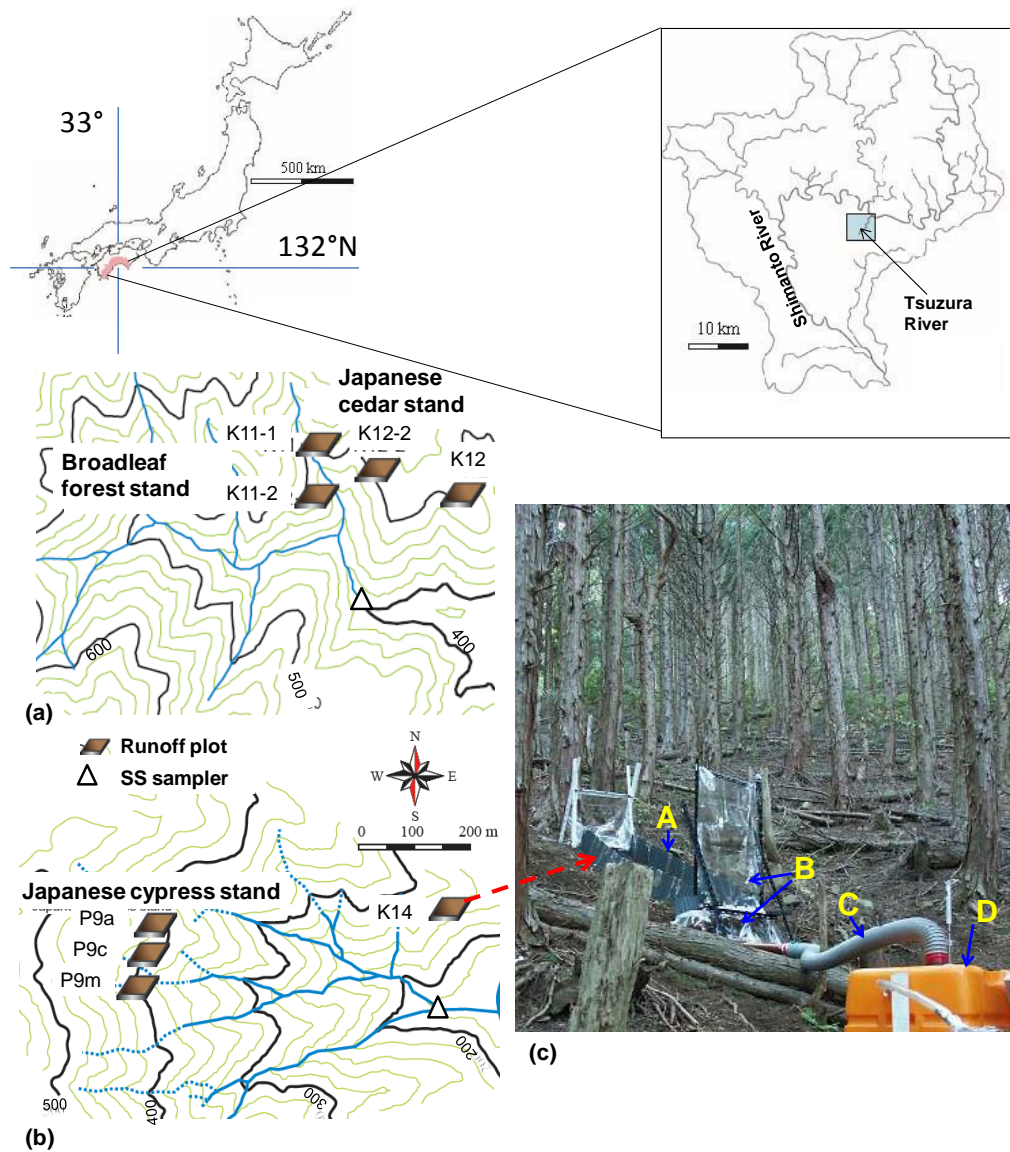



Figure 2.1 Map of the study catchments and location of runoff plots indicated by square box () at (a) upstream site; (b) downstream site and the triangle symbol(Δ) at the confluence point of the catchment was the location of suspended sediment sampler (SS) installed by Mizugaki et al. (2008); (c) the basic setup of the runoff plot and its component which was installed in each forest stand (An example photo of a runoff plot (0.5*1.7m) from hinoki forest stand). The main components are indicated as A = corrugated plastic plot boundary wall; B = sediment capturing aluminum gutter and its protecting plastic cover; C = overland flow transferring pipe; D = overland flow collecting reservoir tank.

2.2.2 Sampling procedures

Size and number of runoff plots

It has been noted that interrill erosion is the common erosion process in most unmanaged mountainous plantation forests of Japan (Onda et al., 2003). Specifically, Miura et al. (2002) indicated that because raindrop splash erosion tends to be the dominant soil transport factor on forested hillslopes, the effect of slope length could be ignored, but the effect of ground cover should be considered. Kitahara et al. (2000) also indicated that among the parameters of USLE for forested hillslopes, including plantation forest, the amount of soil erosion is primarily dependent on the litter cover ratio, followed by the rainfall intensity and the steepness factor. These statements indirectly imply that the influence of slope length could at least occupy a rank lower than those of the three listed factors. Further, Fukuyama et al. (2008) indicated that on Japanese forested slopes, where raindrop erosion dominates, the occurrence of an overland flow, which mainly depends on the local gradients and the contributing area, is less probable. In addition, Gomi et al. (2008) compared the plot scaling effect on the runoff connectivity of overland flow and demonstrated that the runoff amount captured at the outlet of a plot is relatively independent of slope length due to the discontinuous nature of overland flow on forested hillslopes, whereas ground cover is crucial. Consequently, it is reasonable to assume that the effect of slope length is relatively low in a particular environment of this type. In light of this assumption and given the high annual rainfall at the study site, similar runoff plots of approximately the same dimension were installed in the three different forest stands for this study. Table 2.1 provides detailed descriptions of the runoff plots, including the size and number of erosion plots in each type of study forest.

Table 2.1 Description of the runoff plots in study forest watersheds

	Forest type	Plot code	Runoff plot		Watershed area (ha)	Mean altitude (m a.s.l.)
			Dimension (m)	Slope (°)		
Upstream site	Broad-leaved forest (<i>BLF</i>)	K11	0.5*1.8	36.6	7.3	520
		K11-2	0.5*2	38.9		
	Japanese cedar or Sugi (<i>Cryptomeria japonica</i>)	K12	0.5*1.8	37.6		
		K12-2	0.5*2	38		
Downstream site	Japanese cypress or Hinoki (<i>Chamaecyparis obtusa</i>)	K14	0.5*1.7	37.6	2.1	368
		P9A	0.5*2	38.8		
		P9C	0.5*2	34.8		
		P9M	1*2	36.7		

The number of plots was based on the status of each forest floor cover (Figure 2.2) described in the preceding section. Two runoff plots were established in the BLF and two in the sugi forest stands because the floors of these forests were almost uniformly covered by leaf litter throughout the study period (Figure 2.2a, b). However, four runoff plots were installed in the hinoki forest stand to minimize the variability of the observed parameters that might result from non-uniform and poor forest floor cover (Figure 2.2c).

Slope gradient, plot setup and sediment sampling

As indicated in Table 2.1, the slopes of the plots can be characterized as steep slopes with a narrow range of gradients (34° to 40°). In this context, the effect of the slope of the plots on the observations could be assumed to be nearly constant or could be neglected. However, previous studies had indicated that the different slope angles associated with bulk density could affect splash detachment, the initial stage of the soil erosion process (Mizugaki et al., 2010). Therefore, to reduce the slope-driven variability of my observations from the very beginning, the plots were designed to have similar slopes.



Figure 2.2 Photographs of the floor surface condition of erosion plots established in three different forest types. This example demonstrates the degree of differences in the surface cover conditions among erosion plots installed in each forest type: (a) BLF; (b) Japanese cedar; (c) Japanese cypress.

To collect eroded sediments from each runoff plot, a sediment-collecting gutter was inserted between the A and A₀ soil horizons at the outlet of each plot (Figure 2.1c). Corrugated plastic boards (aluminum for some plots) were inserted vertically to form the rectangular boundary walls of the plots. Eroded soils were collected for five continuous months from July to November 2006 using a plankton net (pore size: 0.075 mm) and a reservoir tank connected through a hose pipe to trap fine soil particles. Because the atmospheric input of ²¹⁰Pb_{ex} is nearly constant and continuous, the sediment-collecting gutter was roofed from the very beginning with plastic sheet to avoid the direct deposition of the radionuclide into the sediments.

The samples of eroded soil were used in a direct investigation of the relationship between SOC and each radionuclide in the lateral soil movements. The measurements and the averages calculated for the plots were extrapolated to a hectare base to estimate the erosion and SOC displacement rates in each investigated forest type.

2.2.3. Laboratory procedures and analysis

The sediments were oven-dried at 110°C for 24 h, disaggregated by gentle grinding, and then passed through a 2-mm sieve. A soil fraction of < 2 mm was placed in a plastic bin, sealed, and stored for 21 days prior to assaying to achieve equilibrium between *in situ* ^{226}Ra and its daughter ^{222}Rn before measurement of $^{210}\text{Pb}_{\text{ex}}$, which was determined by subtracting ^{214}Pb from the total measured ^{210}Pb . The activities of ^{137}Cs (at 662 keV) and $^{210}\text{Pb}_{\text{ex}}$ (at 46.5 keV) were quantified by gamma ray spectrometry using coaxial n-type germanium detectors (EGC-200-R and EGC 25-195-R of EURYSIS, Canberra, Meriden, USA) at the University of Tsukuba, Japan, which had participated in independent calibration checks during the worldwide open proficiency test in 2006 (IAEA/AL/171) prepared by the International Atomic Energy Agency (IAEA). The absolute counting efficiencies of the detectors were calibrated using various weights of IAEA-2006-03 standard soil samples that were background corrected. The experimental samples were measured for 43,200 to 86,400 s. The measured radionuclides (Bq kg^{-1}) were converted to an inventory (Bq m^{-2}) using the soil weight of < 2 mm and the plot areas. The corresponding SOC_s were determined directly using a highly sensitive nitrogen-carbon analyzer (SumGraph NC-900). The total soil carbon was considered SOC because the soil pH was less than 7.

The variabilities of SOC, $^{210}\text{Pb}_{\text{ex}}$ and ^{137}Cs were analyzed and compared. A simple linear regression model was used to establish the relationships between these variables, and a Pearson correlation was used to compare the behavior and potential of SOC and the strength of the relationship of SOC to $^{210}\text{Pb}_{\text{ex}}$ and ^{137}Cs . The means of the variables were compared among the forest types with a paired-sample t test. The validity of the linear models was compared and cross-checked by analyzing the root-mean-square errors (RMSEs).

2.3 Results and Discussion

2.3.1 Soil and SOC displacement rates estimated from runoff plot

Table 2.2 shows the soil texture composition, soil erosion, and displaced SOC for each forest type, calculated and extrapolated based on the erosion-plot data on a dry weight base. The values of sediment load obtained from the erosion plots were more or less consistent with the results of previous studies from the same area, as illustrated in Figure 2.3 (Wakiyama et al., 2010). The highest SOC loss rate was found in the Japanese cypress forest ($1.2 \pm 0.3 \text{ t}\cdot\text{ha}^{-1}\cdot\text{y}^{-1}$), followed by the BLF ($0.6 \pm 0.1 \text{ t}\cdot\text{ha}^{-1}\cdot\text{y}^{-1}$) and Japanese cedar forest ($0.2 \pm 0.2 \text{ t}\cdot\text{ha}^{-1}\cdot\text{y}^{-1}$).

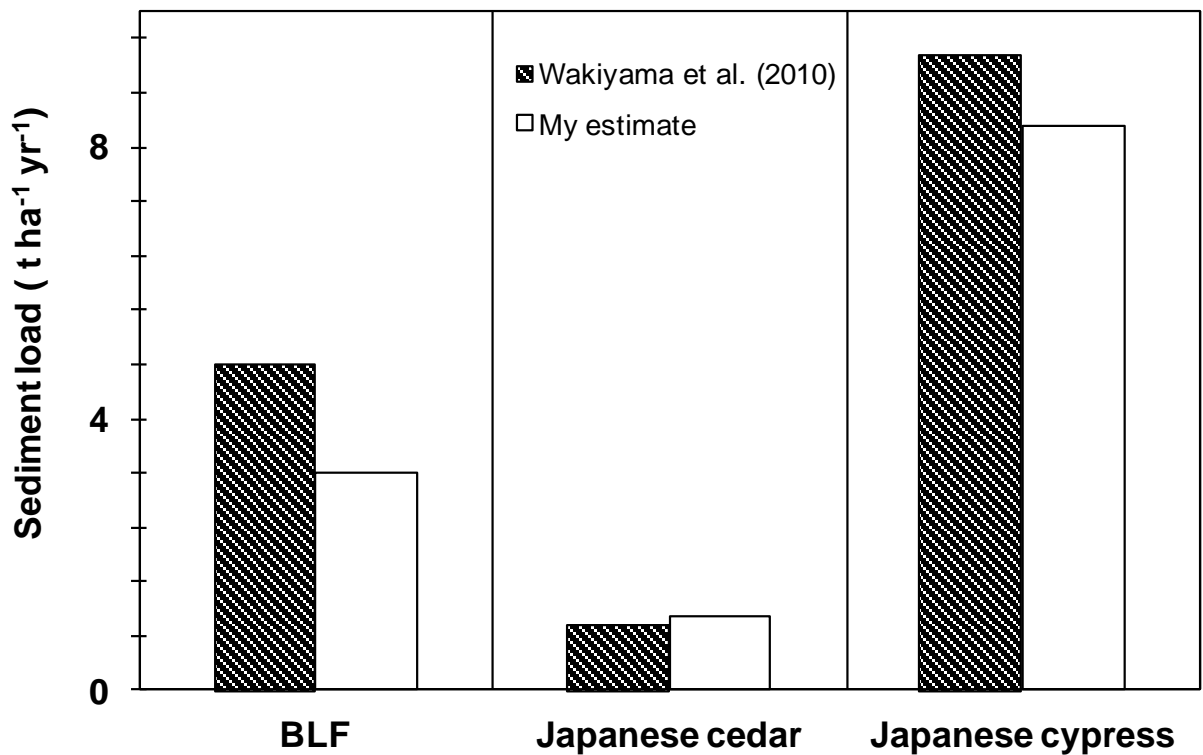


Figure 2.3 Comparison histogram of sediment loads with previously reported results.

The result from the Japanese cypress forest supports the conclusions drawn by Onda et al. (2003) and Fukuyama et al. (2008) that because of the high stand density, closed canopy, and easily fragmented leaves of cypress trees, the forest floors are bare and soil erosion is accelerated. It is

clear from Figure 2.2 that the forest floor in the Japanese cypress plots was almost denuded, whereas the forest floor in the BLF and cedar plots was covered with thick leaf litter and branches.

Table 2.2 Soil particle compositions and estimated SOC and soil erosion rates

Forest types	Soil Composition			Erosion ($\text{t ha}^{-1} \text{y}^{-1}$)				SOC displacement ($\text{t ha}^{-1} \text{y}^{-1}$)			
	Sand (%)	Silt (%)	Clay (%)	Minimum	Maximum	Mean*	CV (%)	Minimum	Maximum	Mean*	CV (%)
BLF	29	60	24	2.4	4	3.2	36	0.4	0.7	0.6	19
Sugi	24	66	11	0.4	1.9	1.1	84	0.1	0.4	0.3	94
Hinoki	23	63	16	5.9	10	8.3	26	1.2	1.4	1.2	26

* The average value of the erosion events (n) that observed in the study period at each forest type and directly extrapolated from plot area per observation period to hectare per year scale: BLF ($n = 20$), Sugi ($n = 20$) and hinoki ($n = 27$)

The eroded sediment from the cedar forest showed the highest SOC content (21%), compared with 15% in the cypress forest and 20% in the BLF. However, the cypress forest exhibited the greatest SOC loss due to its high soil erosion rate resulting from the poor ground cover. The observations of the combined soil and SOC losses showed that the soil degradation in the three forest types followed the order cypress > BLF > cedar, whereas the SOC content in the eroded sediments generally showed the reverse order. These findings indicate that SOC and soil erosion are intimately but inversely interrelated and that the magnitude of loss depends on the forest type.

2.3.2 Comparison of radionuclides and SOC concentrations in eroded sediment

The average concentration of ^{137}Cs was slightly lower in sediments from the cedar ($33 \pm 29 \text{ Bq g}^{-1}$) and cypress ($32 \pm 9.3 \text{ Bq g}^{-1}$) forests than in the BLF ($38 \pm 29 \text{ Bq g}^{-1}$), regardless of the trend in SOC content (Table 2.3). In contrast, the average $^{210}\text{Pb}_{\text{ex}}$ concentration followed a similar pattern to the SOC content but with different magnitudes: cedar (714 Bq g^{-1} , 21%) > BLF (635 Bq g^{-1} , 20%) > cypress (374 Bq g^{-1} , 15%). These results suggest that higher values of SOC content are

associated with higher concentrations of $^{210}\text{Pb}_{\text{ex}}$, but the same relationship does not hold for ^{137}Cs . The inventories (Bq m^{-2}) of both radionuclides were dependent on the quantity of eroded soil and were highest in the eroded soils of the cypress forest, followed by the BLF and the cedar forest.

Table 2.3 Means of SOC proportion, radionuclide activities and inventories in sediments collected from runoff plots

Forest type	Variability	SOC (%)	Radionuclides			
			Activity (Bq g^{-1})		Inventory (kBq m^{-2})	
			$^{210}\text{Pb}_{\text{ex}}$	^{137}Cs	$^{210}\text{Pb}_{\text{ex}}$	^{137}Cs
Broad-leaved forest (BLF)		20 ± 13	635 ± 363	38 ± 29	75.5 ± 15	6.8 ± 4.1
		64	57	76	20	60
Japanese cedar (Sugi; <i>Cryptomeria japonica</i>)	Mean \pm SD	21 ± 3.5	714 ± 411	33 ± 29	32 ± 30.8	2.4 ± 2.4
	CV%	16	58	88	96	104
Japanese cypress (Hinoki; <i>Chamaecyparis obtusa</i>)		15 ± 3	374 ± 83	32 ± 9.3	111 ± 48	8.6 ± 2.7
		20	22	29	43	32

The variabilities of SOC, ^{137}Cs , and $^{210}\text{Pb}_{\text{ex}}$ differed among the forest types. The coefficient of variation (CV) of the SOC content of the eroded sediment from all forest types was moderately to highly variable, according to the classification scheme of Li et al. (2006), with the cedar forest showing the least (CV = 16%) variation. The CVs of the activities and inventories of $^{210}\text{Pb}_{\text{ex}}$ (22–58%; 20–96%) and ^{137}Cs (29–88%; 37–104%) of the sediments were also moderately to highly variable. The heterogeneity of the ^{137}Cs inventories (CV = 104%) in sediment from the cedar forest was found to exceed 100%, whereas the SOC content exhibited relatively low variation. However, the CVs of both the activities and inventories of $^{210}\text{Pb}_{\text{ex}}$ were less than those of ^{137}Cs in the sediments from all forest types except cypress (Table 2.3).

It has been reported that stemflow could be a potential source of local variability for ^{137}Cs in woodland sites (Onda et al., 2003). Note that because both radionuclides are associated with

atmospheric fallout, they could be influenced in equivalent ways by any deposition pathways. However, previous studies have indicated that the contribution of stemflow relative to other mechanisms, in terms of both rain water delivery and the deposition of the associated radionuclides, appears to be insignificant. For example, Gomi et al. (2008) reported that stemflow represents 1 to 10% of the precipitation, and Rafferty et al. (2000) demonstrated that ^{137}Cs deposition via stemflow is far lower ($0.6 \text{ Bq m}^{-2} \text{ y}^{-1}$) than other mechanisms (throughfall = $65 \text{ Bq m}^{-2} \text{ y}^{-1}$; litter fall = $45 \text{ Bq m}^{-2} \text{ y}^{-1}$). Specifically, Bunzl et al. (1989) and Takenaka et al. (1998) showed no systematic differences between ^{134}Cs (surrogate of ^{137}Cs) and ^{137}Cs activities deposited around spruce and Japanese cypress tree stems, respectively. Therefore, the different degrees of variability shown by the two radionuclides could result from their inherited behavior toward the overall complex processes in the soil matrix. For example, Dorr and Munnich (1991) reported that continuous litter fall and the subsequent decomposition process in the surface soil could contribute to the permanent fixation of $^{210}\text{Pb}_{\text{ex}}$ to organic complexes and could result in storage in the topmost organic layer of the soil. Hence, one potential explanation for the observed variation could be the relatively uniform and continuous deposition of $^{210}\text{Pb}_{\text{ex}}$ on the erodible surface floor. This process can yield more or less moderately even $^{210}\text{Pb}_{\text{ex}}$ activities in the eroded materials, a different outcome from that found for the time-restricted fallout ^{137}Cs . The finding that the variability in the sediments of both SOC and $^{210}\text{Pb}_{\text{ex}}$ was relatively lower than that of ^{137}Cs supports the following hypothesis: due to their location in the upper soil horizon, where both are renewed continuously from the canopy, the $^{210}\text{Pb}_{\text{ex}}$ and SOC components of the soil can be preferentially sorted, removed from the soil matrix, and moved together during water-induced soil erosion on forested hillslopes.

The means of each parameter for the forest types were compared and examined with a paired-sample t test. Statistically, the mean SOC content of the sediments differed significantly between cypress and cedar ($p < 0.001$) and between the BLF and cypress ($p < 0.03$). The mean

activity of $^{210}\text{Pb}_{\text{ex}}$ also differed significantly between the BLF and cypress ($p < 0.002$) and between cedar and cypress ($p < 0.001$). The mean inventories of both $^{210}\text{Pb}_{\text{ex}}$ and ^{137}Cs in the sediments were markedly dissimilar for cedar vs. cypress ($^{210}\text{Pb}_{\text{ex}}$: $p < 0.026$; ^{137}Cs : $p < 0.005$) and for BLF vs. cedar ($^{210}\text{Pb}_{\text{ex}}$: $p < 0.013$; ^{137}Cs : $p < 0.033$). These results imply that the examined parameters are highly sensitive to forest type regardless of the similarity in the geo-climatic parameters of the study sites. Moreover, the results indirectly demonstrate the variation in the interception and residence time of radionuclide fallout among the forest types. This among-forest variation may contribute to the observed inventory differences in the soil and could add a unique dimension of complexity to radioecology studies in forest ecosystems.

2.3.4 The relationship between displaced SOC and radionuclides

I examined the relationship between SOC and the two radionuclides contained in the eroded sediment from each forest type by plotting the values of all observations during the study period. The linear relationship and correlation strength of SOC to $^{210}\text{Pb}_{\text{ex}}$ and ^{137}Cs are shown in Figure 2.4. Linear regression models show a positive and strong correlation ($p < 0.01$) between displaced SOC (g) and the quantities of $^{210}\text{Pb}_{\text{ex}}$ (R^2 range: $0.93 - 0.97$) or ^{137}Cs (R^2 range: $0.5 - 0.93$) (Bq) in all forest types. The results suggest that ^{137}Cs is correlated with 50%, 95%, and 75% of the SOC variation in the BLF, cedar forest, and cypress forest, respectively (Figures 2.4b, d, f). In contrast, $^{210}\text{Pb}_{\text{ex}}$ is correlated with 96% (BLF), 97% (cedar), and 93% (cypress) of the variation in SOC (Figures 2.4a, c, e). Table 2.4 lists the slopes and intercepts of the simple linear regression models for each forest type based on $^{210}\text{Pb}_{\text{ex}}$ and ^{137}Cs activities and show the relative variability of the model results in terms of the RMSE. The results indicate that the ability of the ^{137}Cs -based model to predict the SOC in the BLF and Japanese cypress sediments was half that of the $^{210}\text{Pb}_{\text{ex}}$ -based model (RMSE ratio 2:1).

Table 2.4 Comparison of $^{210}\text{Pb}_{\text{ex}}$ and ^{137}Cs based linear regression models for SOC and Root Mean Square Error (RMSE)

Forest type	Linear regression model						RMSE		
	$^{210}\text{Pb}_{\text{ex}}$ model			^{137}Cs model			$^{210}\text{Pb}_{\text{ex}}$	^{137}Cs	Cs/ Pb Ratio
	Slope (Bq)	Intercept (Bq)	r^2	Slope (Bq)	Intercept (Bq)	r^2	prediction (Bq)	prediction (Bq)	
BLF	0.0003	-0.0035	0.96	0.002	0.86	0.50	1	2	2
Japanese cedar	0.0003	-0.0111	0.97	0.004	0.13	0.95	0.3	0.3	1
Japanese cypress	0.0003	0.5795	0.93	0.003	1.17	0.74	1	2	2

Conversely, for the cedar forest, both models had a fairly similar proportion of unexplained variation, most likely due to a low erosion rate (weak causal variation). The $^{210}\text{Pb}_{\text{ex}}$ -based model appears to be a better predictor of SOC than the ^{137}Cs -based model despite differences in erosion rate and vegetation type. This finding may imply that $^{210}\text{Pb}_{\text{ex}}$ is potentially applicable to a wider range of forest environments.

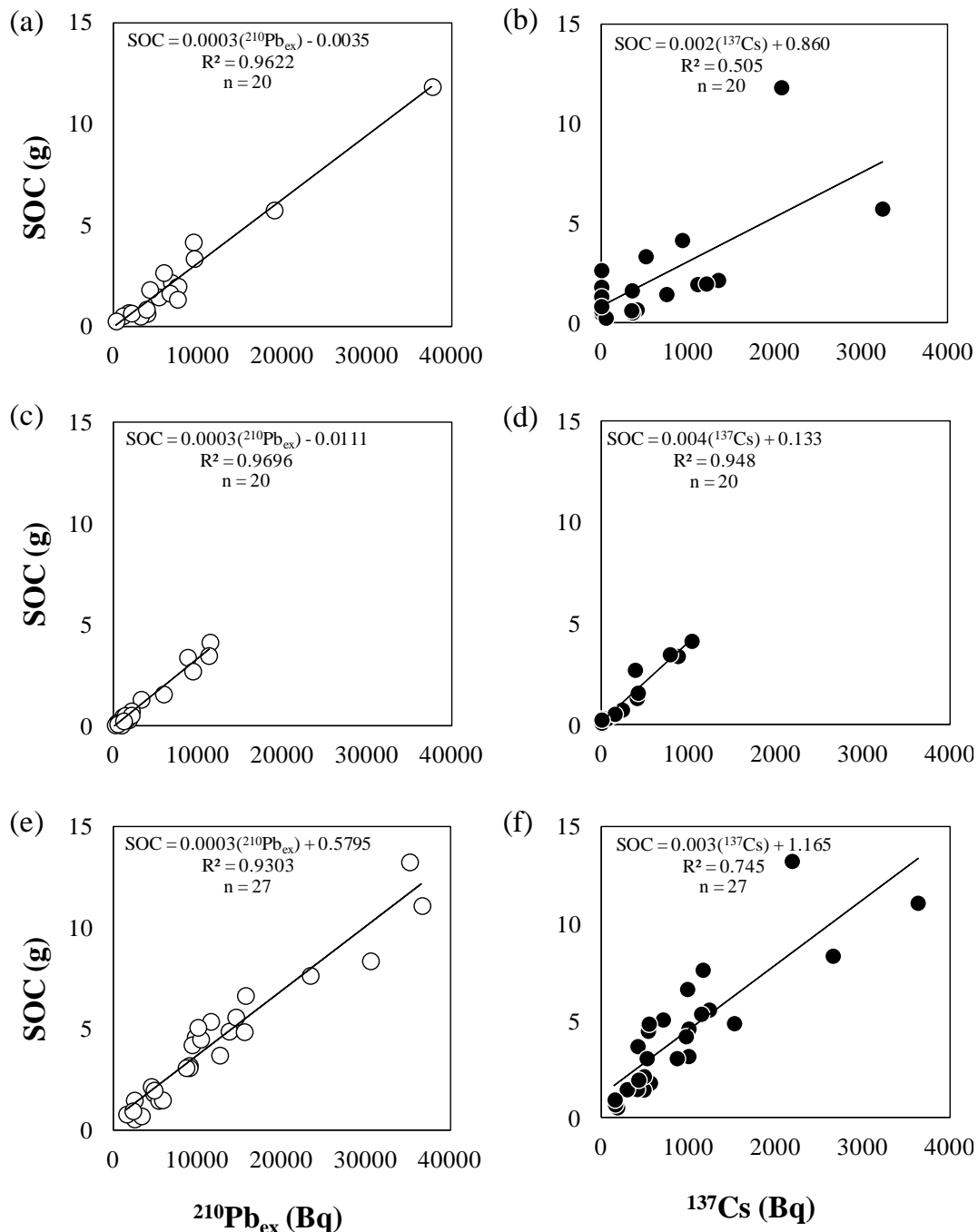


Figure 2.4 Relationship of discharge amount between SOC and $^{210}\text{Pb}_{\text{ex}}$ and between SOC and ^{137}Cs in the eroded sediment collected from erosion plots in three forest types: (a, b) BLF; (c, d) Japanese cedar; (e, f) Japanese cypress

The results suggest that $^{210}\text{Pb}_{\text{ex}}$ can remain more tightly bound to the SOC within the soil matrix than can ^{137}Cs . Consequently, $^{210}\text{Pb}_{\text{ex}}$ and SOC could move together laterally in the course of soil erosion.

2.3.5 The relationship between displaced SOC and Pb/Cs ratio

I examined the relationship between the two radionuclides in the eroded material from the three forest floors. Figure 2.5 shows the linear regression between the $^{210}\text{Pb}_{\text{ex}}$ and ^{137}Cs inventories in the sediments. The slopes of the equations represent the inventory ratios of the radionuclides. The results show that the inventory ratios of the radionuclides varied across the forest types. The Pb/Cs ratio showed a large dispersion and poor correlation in the BLF (Figure 2.5a) but was comparatively stronger in the coniferous forests (Figures 2.5b, c). This result suggests that if the fallout of one radionuclide in the soil is known, it is possible to obtain a reasonable estimate of the other radionuclide from the regression equations, particularly in coniferous forests. It is probable that the variations in the concentrations of the radionuclides in the soils of coniferous forests vs. the BLF are related to the differences in the litter surface area and transfer dynamics of the two types of forest. These factors could cause differences in the efficiency with which the radionuclides are delivered to the soil matrix upon decomposition of the forest litter.

Wallbrink and Murray (1996) demonstrated that in stable sites, the ratio of the two radionuclides shows less spatial variability than do the individual radionuclides. For this reason, they proposed to estimate soil erosion rates using the ratios instead of the mono-radionuclide method. Although I speculated that a similar pattern would be found for SOC, I found an extremely poor relationship between SOC and the Pb/Cs ratio in all three forest stands, as shown in Figure 2.6.

Although such differences could occur for many reasons, different sampling dates

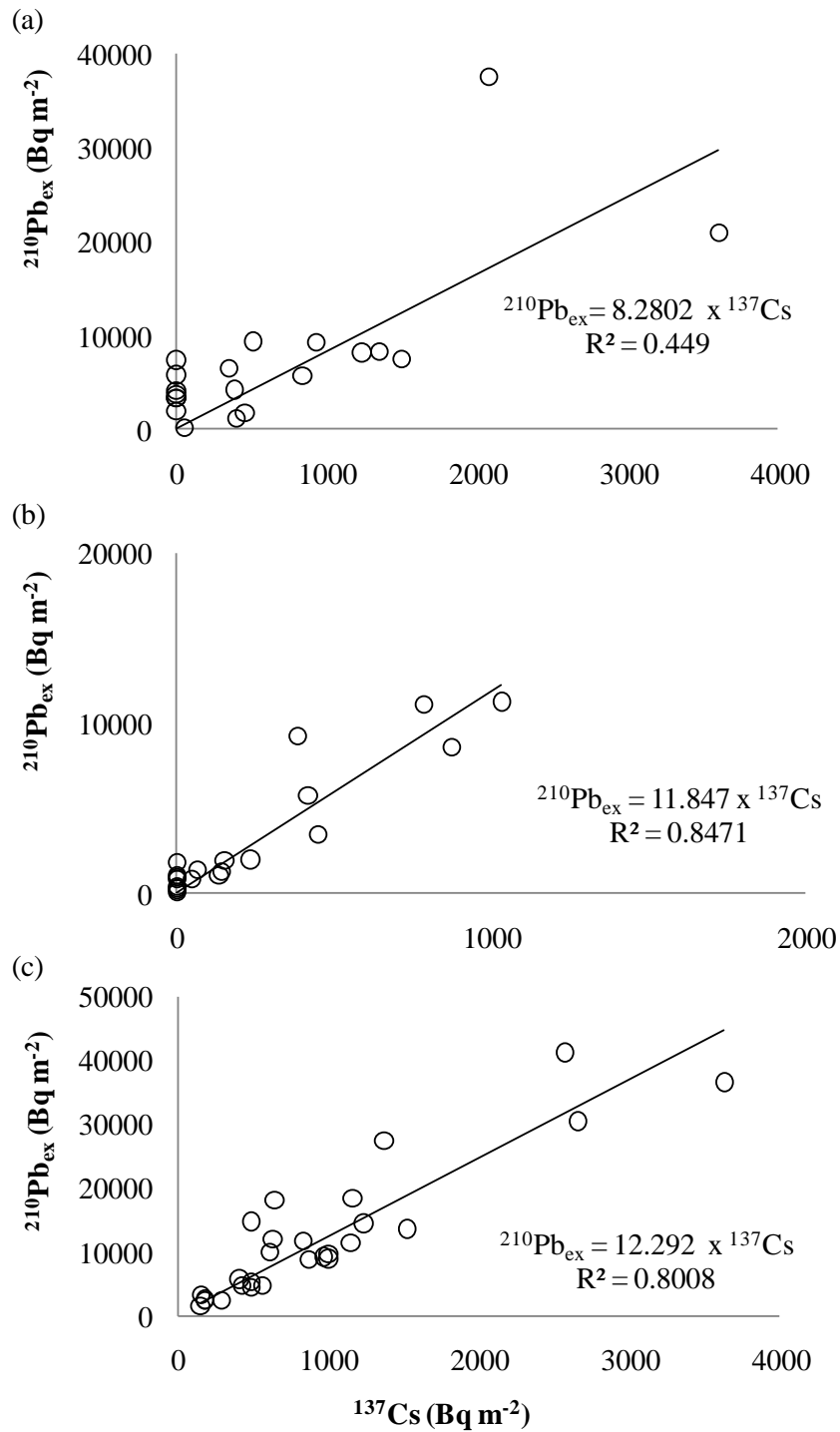


Figure 2.5 The correlation between the inventories $^{210}\text{Pb}_{\text{ex}}$ and ^{137}Cs in sediment driven from different forest types: (a) BLF; (b) Japanese cedar; (c) Japanese cypress

and site differences may particularly influence the amount of artificial ^{137}Cs deposition. In particular, the more recent the sampling date and the more eroded the sampling site, the higher the Pb/Cs ratio would be, assuming a continuous deposition and redistribution of ^{210}Pb and no further ^{137}Cs input. Another potential reason could be that the SOC might be influenced by additional factors associated with the soil erosion process. Nevertheless, my results do not resolve the question of the adequacy of the Pb/Cs ratio for predicting SOC on forested hillslopes. Further studies and independent validation are required.

2.3.6 $^{210}\text{Pb}_{\text{ex}}$ as a tracer of displaced SOC

Generally, my results have provided practical evidence of a strong, positive linear relationship between SOC and $^{210}\text{Pb}_{\text{ex}}$ in lateral transport, compared with ^{137}Cs . This result may be due to differences in the chemical natures of the radionuclides, particularly their behavior with respect to the cation adsorption properties of exchange sites in the soil matrix, such as the OM. OM in soil is a negatively charged plate with a high cation exchange/adsorption capacity (CEC). The single largest component of soil OM is SOC. The physical and chemical behaviors of OM are therefore dominated by, if not originating from, the nature of SOC. In addition, the CEC of OM depends on the rate of replacement of hydrogen in carboxylic acid and phenol functional groups by metallic ions; many factors, in turn, influence the metals' transportation, deposition, and bioavailability to the environment (e.g., Herzog et al., 1996). Hence, the tendency of a radionuclide to replace hydrogen and bind to the OM plate depends on the metal's valence, ionic radius, and hydration properties (Hillel, 1998). Owing to its monovalence, larger atomic radius, and strong hydration property, ^{137}Cs could be replaced more easily in the course of soil erosion by other cations, such as K^+ , Ca^{2+} , and Mg^{2+} , than would $^{210}\text{Pb}_{\text{ex}}$. Similarly, numerous studies have reported that $^{210}\text{Pb}_{\text{ex}}$ is strongly fixed to and transported with OM (Dorr, 1995; Vaaramaa et al., 2010).

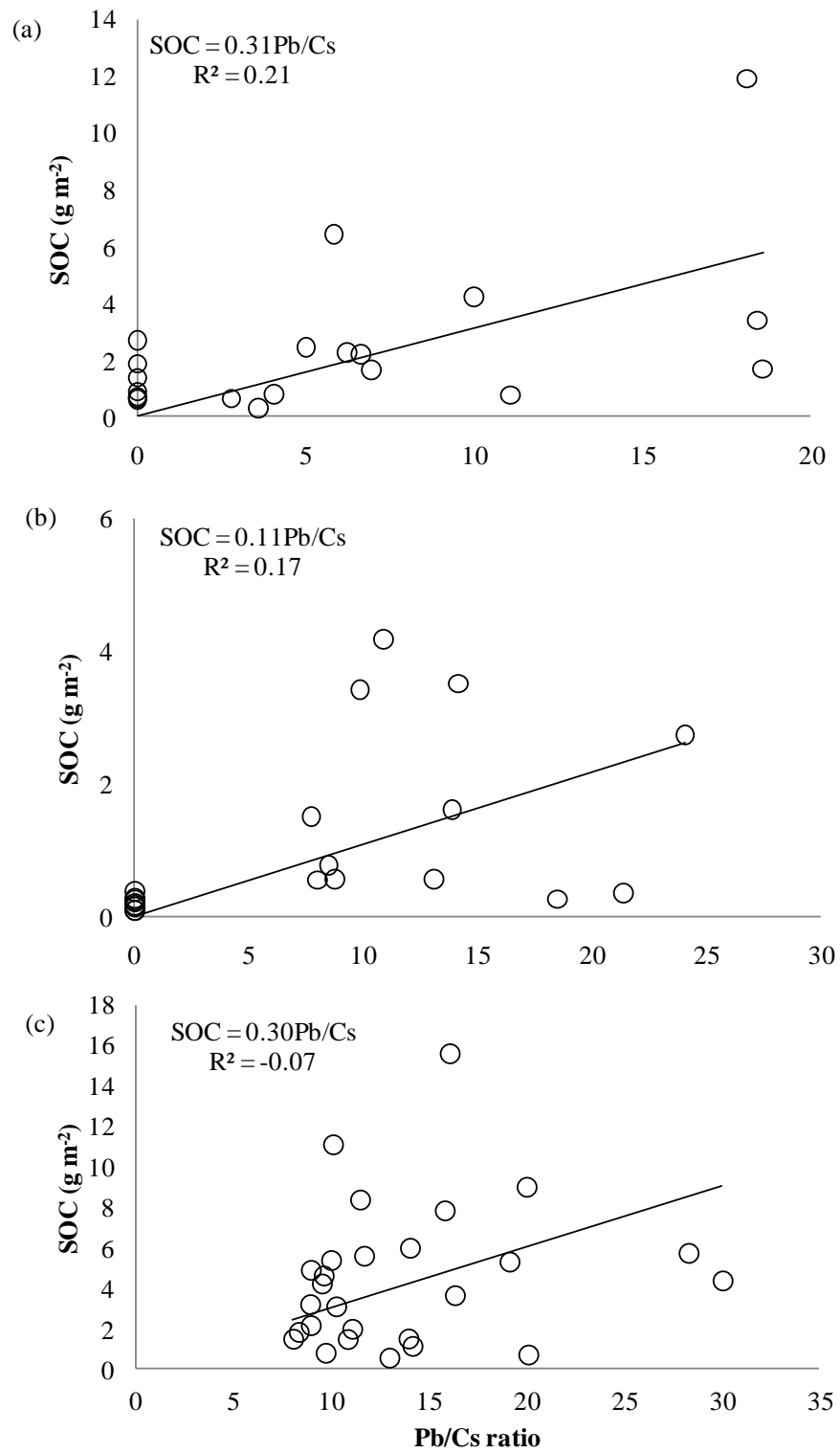


Figure 2.6 The relationship between eroded SOC and ²¹⁰Pb_{ex}/¹³⁷Cs ratio: (a) BLF, (b) Japanese cedar and (c) Japanese cypress

Furthermore, Roy et al. (2010) reported a strong correlation ($R^2 = 0.806$) between SOC and CEC. In agreement with these principles, my results confirm and provide field evidence that $^{210}\text{Pb}_{\text{ex}}$ is more tightly fixed to SOC than is ^{137}Cs in forest soil. Thus, measurements of $^{210}\text{Pb}_{\text{ex}}$ may potentially quantify the dynamics of the lateral distribution of SOC as a complement to or in place of ^{137}Cs measurements if ^{137}Cs is inadequate or difficult to detect. In a wider scenario, $^{210}\text{Pb}_{\text{ex}}$ can provide relevant and precise information to understand the dynamics and transfer patterns of SOC in forests of the study region as well as around the world.

2.4 Conclusions

$^{210}\text{Pb}_{\text{ex}}$ and ^{137}Cs show different variabilities and behaviors toward SOC in forest soil. A greater amount of SOC in the eroded material indicates that erosion can seriously affect the SOC stock. In addition, high concentrations and inventories of $^{210}\text{Pb}_{\text{ex}}$ and lower RMSE values confirm a stronger attachment of $^{210}\text{Pb}_{\text{ex}}$ than ^{137}Cs with SOC in lateral movements. Unlike ^{137}Cs , both SOC and $^{210}\text{Pb}_{\text{ex}}$ have natural input sources that are continuously replenishing the surface soil via forest litter and emanated ^{222}Rn , respectively. From these practical considerations, $^{210}\text{Pb}_{\text{ex}}$ could be used independently to document SOC movements on forested hillslopes where ^{137}Cs application is limited. Therefore, $^{210}\text{Pb}_{\text{ex}}$ would be a valuable tool for quantifying SOC as a component of global carbon dynamics with better precision, providing high-quality input for the complex equations describing carbon-induced climate changes. Although further investigation and validation studies are required to fully understand the potential of $^{210}\text{Pb}_{\text{ex}}$ as a marker for SOC redistribution, the results presented here may lay the groundwork for the development of a $^{210}\text{Pb}_{\text{ex}}$ -based model for studying forest systems.

References

- Afshar, F.A., Ayoubi, S., Jalalian, A., 2010. Soil redistribution rate and its relationship with soil organic carbon and total nitrogen using ^{137}Cs technique in a cultivated complex hillslope in western Iran. *Journal of Environmental Radioactivity* **101**, 606 – 614.
- Alewell, C., Meusburger, K., Brodbeck, M., Banniger, D., 2008. Methods to describe and predict soil erosion in mountain regions. *Journal of Land and Urban Planning* **88**, 46 – 53.
- Blake, W., Wallbrink, P., Wilkinson, S., Humphreys, G., Doerr, S., Shakesby, R., Tomkins, K., 2009. Deriving hillslope sediment budgets in wildfire-affected forests using fallout radionuclide tracers. *Geomorphology* **104**, 105 – 116.
- Bunzl, K., Schimmack, W., Kreutzer, K., Schierl, R., 1989. Interception and retention of Chernobyl-derived ^{134}Cs , ^{137}Cs and ^{106}Ru in a spruce stand. *Science of the Total Environment* **78**, 77 – 87.
- Chappell, A., Hancock, R., Raphael, A., Rossel, V., Loughran, R., 2011. Spatial uncertainty of ^{137}Cs reference inventory for Australian soil. *Journal of Geophysical Research* **116**, doi:10.1029/2010JF001942.
- Dorr, H., 1995. Application of ^{210}Pb in soils. *Paleolimnol* **13**, 157 - 168.
- Dorr, H., Munnich, O.K., 1991. Lead and Cesium transport in European Forest soils. *Water, air, and Soil Pollution* **57 – 58**, 809 – 818.
- Fukuyama, T., Onda, Y., Takenaka, C., Walling, D., 2008. Investigating erosion rates within a Japanese cypress plantation using ^{137}Cs and $^{210}\text{Pb}_{\text{ex}}$ measurements. *Journal of Geophysical Research, Earth Surface* **113**, doi:10.1029/2006JF000657.
- Garten, C., Post, W., Hanson, J., Cooper, L., 1999. Forest soil carbon inventories and dynamics along an elevation gradient in the southern Appalachian mountains. *Biogeochemistry* **45**, 115 – 145.

- Gomi, T., Sidle, R.C., Miyata, S., Kosugi, K., Onda, Y., 2008. Dynamic of runoff connectivity of overland flow on steep forested hillslopes: Scale effects and runoff transfer. *Water Resources Research* **44**, W08411, doi:10.1029/2007WR005894.
- Hancock, R., Loughran, R., Evans, K., Balog, R., 2008. Estimation of soil erosion using field and modelling approaches in an undisturbed Arnhem Land catchment, Northern Territory, Australia. *Geographical Research* **46**(3), 333 – 349.
- Hancock, R., Murphy, D., Evans, K., 2010. Hillslope and catchment scale soil organic carbon concentration: an assessment of the role of geomorphology and soil erosion in undisturbed environment. *Geoderma* **155**, 36 – 45.
- He, Q., Walling, D. E., 1996. Interpreting particle size effects in the adsorption of ^{137}Cs and unsupported ^{210}Pb by mineral soils and sediments. *Journal of Environmental Radioactivity* **30** (2), 117 –137.
- Herzog, H., Burba, P., Buddrus, J., 1996. Quantification of hydroxylic groups in river humic substance by ^{29}Si -NMR. *Journal of Anal Chemistry* **354**, 375 – 377.
- Hillel, D., 1998. Environmental Soil Physics. Academic press, New York.
- Ito, A., 2007. Simulated impacts of climate and land-cover change on soil erosion and implication for the carbon cycle, 1901 to 2100. *Geophysical Research Letters* **34**, doi:10.1029/2007GL029342.
- Kato, H., Onda Y., Tanaka Y., 2010. Using ^{137}Cs and $^{210}\text{Pb}_{\text{ex}}$ measurements to estimate soil redistribution rates on semi-arid grassland in Mongolia. *Geomorphology* **114**, 508 – 519.
- Kitahara, H., Okura, Y., Sammori, T., Kawanami, A., 2000. Application of Universal Soil Loss Equation (USLE) to mountainous forests in Japan. *Journal of Forest Research* **5**, 231 – 236.
- Lal, R., 2003. Soil erosion and the global carbon budget. *Environmental International* **29**, 437– 450.

- Lal, R., 2005. Forest Soil and Carbon sequestration. *Forest Ecology and Management* **220**, 242 – 258.
- Li, Y., Zhang, Q.W., Recosky, D.C., Bai, L.Y., Lindstorm, M.J., Li, L., 2006. Using ^{137}Cs and $^{210}\text{Pb}_{\text{ex}}$ for quantifying soil organic carbon redistribution affected by intensive tillage on steep slopes. *Soil and Tillage* **86**, 176 – 184.
- Loughran, R.J., Elliott, G.L., Campbell, B.L., Curtis, S.J., Cummings, D., Shelly D.J., 1993. Estimation of erosion using the radionuclide caesium-137 in three diverse areas in eastern Australia. *Applied Geography* **13**, 169 – 188.
- Loughran, R.J., Campbell, B.L., Elliott, G.L., Shelly D.J., 1990. Determination of the rate of sheet erosion on grazing land using caesium-137. *Applied Geography* **10**, 125 – 133.
- Loughran, R.J., Elliott, G.L., Campbell, B.L., Shelly D.J., 1988. Estimation of soil erosion from caesium-137 measurements in a small, cultivated catchment in Australia. *International Journal of Radiation Applications and Instrumentation. Part A. Applied Radiation and Isotopes* **39** (11), 1153 – 1157.
- Mabit, L., Bernard C., 2010. Spatial distribution and content of soil organic matter in agricultural field in eastern Canada, as estimated from geostatistical tools. *Earth Surface process and Land Forms* **35**, 278–283. doi: 10.1002/esp.1907
- Mabit, L., Klik, A., Benmansour, M., Toloza, A., Geisler, A., Gerstmann, U.C., 2009. Assessment of erosion and deposition rates within an Austrian agricultural watershed by combining ^{137}Cs and $^{210}\text{Pb}_{\text{ex}}$ and conventional measurements. *Geoderma* **150**, 231 – 239
- Martinez, C., Hancock, R., Kalma J.D., 2010. Relationships between ^{137}Cs and Soil organic carbon (SOC) in cultivated and never-cultivated soils: An Australian example. *Geoderma* **158**, 137 - 147 doi:10.1016/j.geoderma.2010.04.019.

- Miura, S., Hirai, K., Yamada, T., 2002. Transport rates of surface materials on steep forested slopes induced by raindrop splash erosion. *Journal of Forest Research* **7**, 201 – 211.
- Mizugaki, S., Nanko, K., Onda, Y., 2010. The effect of slope angle on splash detachment in an unmanaged Japanese cypress plantation forest. *Hydrological Processes* **24**, 576 – 587.
- Mizugaki, S., Onda, Y., Fukuyama, T., Koga, S., Asai, H., Hiramatsu, S., 2008. Estimation of suspended sediment sources using ^{137}Cs and $^{210}\text{Pb}_{\text{ex}}$ in unmanaged Japanese cypress plantation watersheds in southern Japan. *Hydrological Processes* **22**, 4519 – 4531.
- Morris, C.D., Loughram, R.J., 1994. Distribution of Caesium-137 in soils across a hillslope hollow. *Hydrological Processes* **8**, 531 – 541.
- Nearing, M., Kimoto, A., Nichols, M., Ritchie, J., 2005. Spatial patterns of soil erosion and deposition in two small, semiarid watersheds. *Journal of Geophysical Research* doi: 10.1029/2005JF000290
- Onda, Y., Takenaka, C., Furuta, M., Nonoda, T., Hamajima, Y., 2003. Use of ^{137}Cs for estimating soil erosion processes in a forested environment in Japan. *TransJapan Geomorphology Union* **24** (1), 13 – 25.
- Onda, Y., Gomi, T., Mizugaki, S., Nonoda, T., Sidle, R., 2010. An overview of the field and modeling studies on effects of forest devastation on flooding and environmental issues. *Hydrological Processes* **24**, 527 – 534.
- Porto, P., Walling, D. E., Callegari, G., Catona, F., 2006. Using Fallout Lead-210 measurements to estimate soil erosion in three small catchments in south Italy. *Water, Air and Soil Pollution* **6**, 657– 667
- Rafferty, B., Brennan, M., Dawson, D., Dowding, D., 2000. Mechanisms of ^{137}Cs migration in coniferous forest soils. *Journal of Environmental Radioactivity* **48**, 131 – 43.

- Ritchie, C., McCarty, G., Venteris, E., Kaspar, T., 2007. Soil and soil organic carbon redistribution on the landscape. *Geomorphology* **89**, 163 - 171.
- Ritchie, C., Nearing, A., Nichols, H., Ritchie, A., 2005. Patterns of soil erosion and redistribution on Lucky Hills watershed, Walnut Gulch experimental watershed, Arizona. *Catena* **61**, 122 - 130
- Roy, K., Samai, N., Roy, M., Mazumdar, A., 2010. Soil carbon and nutrient accumulation under forest plantations in Jharkhand state of India. *Clean-Soil Air Water* **38**(8), 706 - 712.
- Saç ,M. Uğur, A., Yener, G., Özden, B., 2008. Estimates of soil erosion using Cesium-137 tracer models. *Environmental Monitoring and Assessment* **136**, 461– 467, doi: 10.1007/s10661-007-9700-8
- Takenaka, C., Onda, Y., Hamajima, Y., 1998. Distribution of cesium-137 in Japanese forest soil: Correlation with the contents of organic carbon. *Science of the Total Environment* **222**, 193 - 199.
- Vaaramaa, K., Lasse, A., Solatie, D., Lehto, J., 2010. Distribution of ²¹⁰Pb and ²¹⁰Po in boreal forest soil. *Science of the Total Environment* **408**, 6165 - 6171.
- VandenBygaar, J. 2001. Erosion and deposition history derived by depth stratigraphy of ¹³⁷Cs and soil organic carbon. *Soil & Tillage Research* **61**, 187 - 192.
- Van Oost, K., Quine, T., Govers, G., De Gryze, S., Six, J., Harden, J., Ritchie, J., McCarty, G. Heckrath, G., Kosmas, C., Giraldez, J., Marques da Silva, J., Merckx, R., 2007. The impact of agricultural soil erosion on the global carbon cycle. *Science* **318**, 626 - 229.
- Wakiyama, Y., Onda, Y., Mizugaki, S., Asai, H., Hiramatsu, S., 2010. Soil erosion rates on forested mountain hillslopes estimated using ¹³⁷Cs and ²¹⁰Pb_{ex}. *Geoderma* **159**, 39 - 52.
- Wallbrink, P., Murray, A., 1996. Determining Soil Loss Using the Inventory Ratio of Excess Lead-210 to Cesium-137. *Soil Science Society of America Journal* **60**, 1201 – 1208.

- Walling, D.E, Collins, A., Sickingabula, H., 2003. Using unsupported Lead-210 measurements to investigate soil erosion and sediment delivery in a small Zambian catchment. *Geomorphology* **52**, 193 - 213.
- Walling, D. E., He, Q., 1999. Using Fallout lead-210 Measurements to Estimate Soil Erosion on Cultivated Land. *Soil Science Society of America Journal* **63**, 1404 – 1412
- Walling, D. E., He, Q., Appleby, P.G., 2002. Conversion models for use in soil-erosion, soil-redistribution and sedimentation investigation, in: Zapata, F. (Ed), Handbook for the Assessment of Soil Erosion and Sedimentation Using Environmental Radionuclides. Kluwer academic polishes, Dordrecht, pp. 111 – 162.
- Zhang, X., Qi, Y., Walling, D.E., He, X., Wen, A., Fu, J. 2006. A preliminary assessment of the potential for using $^{210}\text{Pb}_{\text{ex}}$ measurement to estimate soil redistribution rates on cultivated slopes in the Sichuan Hilly basin of China. *Catena* **68**, 1 - 9
- Zheng, J., He, X., Walling, D.E., Zhang, X., Flanagan, D., Qi, Y., 2007. Assessing soil erosion rates on manually-tilled hillslopes in the Sichuan hilly basin using ^{137}Cs and $^{210}\text{Pb}_{\text{ex}}$ Measurements. *Pedosphere* **17** (3), 273-283.

Chapter 3: Atmospheric $^{210}\text{Pb}_{\text{ex}}$ and soil organic carbon in coniferous forest

3.1 Introduction

Lead-210 (^{210}Pb) is a naturally occurring radionuclide with a half-life ($t_{1/2}$) of 22.3 years. It is a direct α -decay progeny of ^{222}Rn ($t_{1/2} = 3.8$ days) formed in the ^{238}U ($t_{1/2} = 4.5 \times 10^9$ years) decay chain, which is found in almost all soils (EI-Daoushy, 1988; Dorr, 1995; Likuku, 2009). When ^{222}Rn decays to a series of short-lived ($t_{1/2} = 104 \mu\text{s} - 26.8$ min) progenies, it eventually produces the long-lived isotope ^{210}Pb through α -decay. ^{210}Pb is produced both *in situ* in the soil and air, and *ex situ* in the atmosphere when it is released from solid soil particles through α -recoil and diffusion along concentration gradients. To differentiate atmospheric ^{210}Pb from its terrigenous species (also called supported ^{210}Pb), the term “unsupported ^{210}Pb ” or ^{210}Pb in excess (hereafter expressed as $^{210}\text{Pb}_{\text{ex}}$ or radiollead unless stated otherwise) is used. Since $^{210}\text{Pb}_{\text{ex}}$ rapidly attaches to aerosols, it immediately participates in mixing and transport processes in the atmosphere. It is then re-deposited with tagged aerosols within 5 to 10 days to the soil surface by dry and wet deposition (Dorr, 1995; Fowler et al., 1995).

In forested environment, $^{210}\text{Pb}_{\text{ex}}$ can reach the forest floor directly through litterfall, rainwater (throughfall and stemflow) and dry deposition between canopy openings, similar to other land use systems. However, Dorr (1995) found that the ^{210}Pb inventory in the forest is about six times higher than in meadow sites. This may be due to large interception area provided by leaves, twigs and branches, which makes forest an important sink and removal zone of atmospheric aerosols ($^{210}\text{Pb}_{\text{ex}}$ in particular). This suggests that the forest canopy intercepts and retains most atmospheric $^{210}\text{Pb}_{\text{ex}}$ deposition for a short time (short stay) and transfers it to the ground surface through litterfall. This unique process directs most radionuclide-base studies to agricultural areas, which involve

simple land use systems (Fukuyama et al., 2008). Few previous studies have explored the transfer, behavior and deposition of $^{210}\text{Pb}_{\text{ex}}$ and other atmospheric radionuclides in coniferous, broad-leaved forests and grasslands, focusing on wet (rain water) deposition mechanisms (e.g. Osaki et al., 2003, 2007; Likuku, 2009).

Deposition of forest litter and its subsequent complex biogeochemical processes determine the chemical capital and quality of forest soil. It is also the primary aboveground input source of soil organic carbon (SOC) and numerous other chemical elements (both nutrients and contaminants), which are closely related to atmospheric carbon dioxide levels (climate change), soil quality (productivity) and environmental health (sanitation). Therefore, litter functions as a primary mechanism of canopy-trapped $^{210}\text{Pb}_{\text{ex}}$ deposition to forest soil. In soil, as several studies have shown, $^{210}\text{Pb}_{\text{ex}}$ has a strong association with organic matter, of which litter input is the main source. Lewis (1977) showed that the atmospheric flux of $^{210}\text{Pb}_{\text{ex}}$ is efficiently scavenged by organic-rich horizons of soil and is only lost from the system by soil erosion. Other studies found a dependence of $^{210}\text{Pb}_{\text{ex}}$ movement on organic matter, which acts as a physical carrier (e.g. Dorr and Munnich, 1989, 1991; Dorr, 1995; Kaste et al., 2011). Vaaramaa et al. (2010) confirmed the association of $^{210}\text{Pb}_{\text{ex}}$ with humic substances in Scots pine-dominated forest soil in Finland. Apparently, soil organic matter (SOM) itself is a mixture of various chemical compounds dominated by organo-carbon functional groups to which $^{210}\text{Pb}_{\text{ex}}$ and other organo-metallic complexes are more likely fixed on. However, little is known on radilead deposition, redistribution and its relationship, particularly to SOC in forested environment.

Soil erosion from hillslope can adversely affect both on- and off-site resources (Pricope, 2009). Using ^{137}Cs technique, Ritchie et al. (2007) have shown that SOC tends to accumulate in soils of depositional areas (concave slopes, bottom slopes) and it decreases as the gradient slope increases. This implies that, beside onsite effects, soil erosion can transport considerable amount of

eroded materials including SOC and radiolead that damage waterways, reservoirs, rivers, streams, lakes, riparian zones, estuarine, aquatic and marine environments that may pose additional costs like for water treatments (Lal, 1998, 2003). The problem is more likely pronounced in those water networks that are closed enough to steeper slopes with poor surface cover landforms such as those of this study site. On the other hand there is an increasing demand for accurate assessment of soils as a carbon sink or source potential in many international environmental programs (e.g IPCC, 2003). However, the dilemma on soil erosion as a carbon sink or source is still unsolved though some recent studies rejected both notions (e.g van Oost et al., 2007). This implies the existing states of knowledge is not adequate enough and indicate the need of further study and develop alternative approaches. More recently, Teramage et al. (2013) have shown the existence of strong affinity between SOC and $^{210}\text{Pb}_{\text{ex}}$ than does between SOC and ^{137}Cs during surface soil erosion in forested hillslope environment. Therefore, I hypothesized that understanding the behavior and redistribution of radiolead can be used as a possible diagnostic tool to understand the redistribution of SOC on forested hillslope at local and global scales.

Thus, this study (1) investigated the role of the litter continuum in transferring atmospheric radiolead to coniferous forest soil and (2) determined the depth distribution behavior of $^{210}\text{Pb}_{\text{ex}}$ and quantified its relationship with SOC by isolating it from complex SOM components of the soil matrix.

3.2 Material and methods

3.2.1 Site description

Samples were collected from the downstream of the Tsuzura River sub-basin in Kochi prefecture, southern Japan ($33^{\circ}10'N$, $132^{\circ}57'E$) (Figure 3.1). The climate of the area is classified as a temperate monsoon humid type, with a mean annual rainfall of 2735 mm and temperature of 14.6°C . The elevation of the watershed ranges from 175 m to 560 m asl. Brown forest soil dominates

in the watershed, which was formed *in situ* from sedimentary rock and alternate mudstone and sandstone layers. The bedrock is made mainly of sedimentary rocks from the Shimanto belt. The forest consists of Japanese cypress (*Chamaecyparis obtusa* Sieb. Et Zucc.) species planted between 1965 and 1969. The stand density was estimated at 1400 – 2750 stems ha⁻¹, and the forest floors were lightly covered by undergrowth during the study period.

3.2.2 Data collection and analysis

Three litter traps (1 m² each) were suspended one meter above the ground in representative regions of the catchment to monitor annual litterfall. The ²¹⁰Pb_{ex} and organic carbon proportion in litter were measured to estimate ²¹⁰Pb_{ex} and carbon input onto forest soil by litter. To determine the vertical soil profile of ²¹⁰Pb_{ex} and SOC in the study catchment, 16 composited core soil samples were collected (i.e. three cores per sampling point to account for spatial variability; a total of 48 cores) for direct measurement and determination of ²¹⁰Pb_{ex} and SOC. Several previous studies have used 30 cm depth which was enough to fully describe ²¹⁰Pb_{ex} depth distribution (e.g Fukuyama et al., 2008; Kato et al., 2010; Wakiyama et al., 2010). On this basis, the core samples were collected using manual percussion of a steel core tube (internal diameter 5 cm and length of 30 cm) vertically to the ground. The cores were sliced in to depth classes of 0 - 2, 2 - 5, 5 - 10 and 10 - 30 cm to examine the vertical distribution of ²¹⁰Pb_{ex} and SOC. The three replicate cores a sampling point was mixed at the same depth classes to better representation.

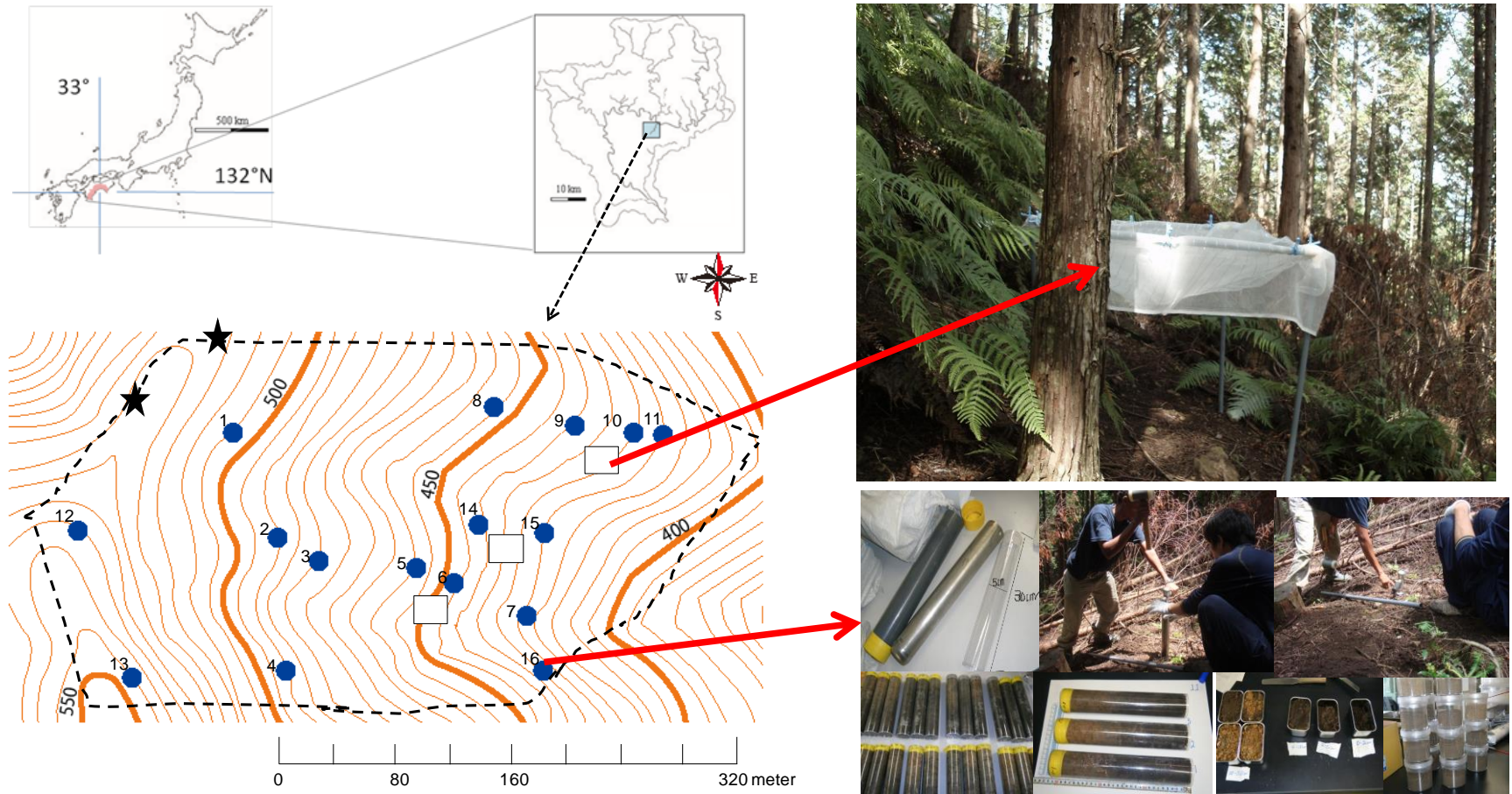


Figure 3.1 Map of the study site, the position and photographs of the sampling points (filled circles), litter traps (squares) and location of reference sites (filled stars) in Japanese cypress forest.

Soil samples were oven-dried at 110°C for 24 hrs, gently grinded to disaggregate the soil, and passed through a 2-mm sieve. A representative soil fraction from less than a 2 mm soil portion of each sample was then placed in a plastic bin, sealed and stored for 21 days prior to the assay to achieve equilibrium between ^{226}Ra and its daughter ^{222}Rn to measure ^{214}Pb . Corrections were then made for *in situ*-produced ^{210}Pb by subtracting ^{214}Pb from total ^{210}Pb to quantify atmospheric $^{210}\text{Pb}_{\text{ex}}$. The analysis was conducted in the laboratory of the University of Tsukuba, which was authorized for independent calibration checks during the worldwide open proficiency test in 2006 (IAEA/AL/171) prepared by the International Atomic Energy Agency (IAEA). The activities were determined using gamma ray spectrometry from a high purity n-type germanium coaxial gamma ray detector (EGC 25-195-R, Canberra-Eurysis, Meriden, USA) connected to an amplifier (PSC822, Canberra, Meriden, USA) and multichannel impulse separator (DSA1000, Canberra, Meriden, USA). The absolute counting efficiency of the detector and self-absorption of the sample itself were calibrated and corrected using various weights of IAEA-2006-03 standard soil samples with background correction. The specific activities (Becquerel per kilogram, Bq kg^{-1}) were obtained based on their gamma radiation at 46.5 keV (^{210}Pb), 351.9 keV (^{214}Pb) and 609.3 keV (^{214}Bi) using n-type coaxial low-energy HPGe gamma detectors with an efficiency of 30% at the University of Tsukuba (Tsukuba City, Japan). Counting times for each packed soil sample were 43, 200 – 86, and 400 s to obtain better accuracy ($\sim \pm 10\%$). The measured activities (Bq kg^{-1}) were converted to inventories (Bq m^{-2}) using dry mass depth (kg m^{-2}) of the < 2mm soil samples from each sampling layer.

Radioactivity in the litter was computed by converting the litter to ash under gradually increasing temperatures (120°C for 16 hrs, 200°C for 1 hr, 300°C for 30 minutes and a hold at 450°C for 4 hrs) using a fully automatic muffle electric furnace (Ikeda, Scientific Co.LTD). The black ash was then pulverized using a mortar and pestle, put in a plastic bin, and gently compacted to increase

the stability and density prior to the assay. The activities were determined directly with similar procedure as above but not stored for 21 days unlike of the soil samples.

The corresponding SOC for each soil sample and litter was measured directly under high-temperature combustion using a fully automatic high sensitivity nitrogen-carbon (NC) analyzer (SumGraph NC-900. Acetanilide (C_8H_9NO), which is composed of 71.09% (C), 11.84 % (O), 10.36 % (N) and 6.71 % (H), was used as a standard to calibrate the instrument. Total soil carbon was considered to be the SOC since the soil pH value is considerably less than 7. Hence, free carbonate was not expected to be found in the soil, and the soil was not pretreated with acid.

3.3 Results and Discussion

3.3.1 Local reference inventory and annual atmospheric $^{210}Pb_{ex}$ flux

The inventory (I_{refe}) from undisturbed flat site (where $^{210}Pb_{ex}$ deposition is preserved) was adopted from literature (Wakiyama et al., 2010) and used to determine the annual $^{210}Pb_{ex}$ flux (a) deposited on the forest canopy (discus below). In a closed forest canopy, I assumed that all atmospheric $^{210}Pb_{ex}$ flux (a) was deposited on the forest canopy, reduced by decay, transferred and reached the soil through depositional mechanisms (wet, dry and litterfall). I assumed that this process was conserved over extended periods of time. In other words, the canopy accumulated radiolead for a specific amount of time which is often referred to as the mean residence time (MRT).

Table 3.1 $^{210}\text{Pb}_{\text{ex}}$ inventory and SOC contents at the sampling points

	$^{210}\text{Pb}_{\text{ex}}$ (Bq m^{-2})		SOC (%)	
	Reference site ^a	Sampling points ^b	Reference site ^c	Sampling points ^b
Mean	19703	10953	18	9
Maximum		16413		18
Minimum		5310		5
Standard deviation		3094		3
Coefficient of variation (%)		28		33
Number of Samples		16		16

^a Values taken from Wakiyama et al. (2010) that represents area-weighted mean

^b The measured values of core samples for upper 30 cm soil depth. The steel core sampler area was 19.6 cm^2 .

^c Determined from available composited soil samples of the reference site.

3.3.2 Inverted U-shaped bi-box compartment model

Model description

To discuss the information stated in section 3.3.1 in a more quantitative manner, I created an inverted U-shaped bi-box compartment model (IUS-model). This model has two major components. The first component consists of an inverted-U shaped pathway, which represents the $^{210}\text{Pb}_{\text{ex}}$ yielding chain that connects the atmosphere and soil interfaces. For simplicity, the flow direction of the $^{210}\text{Pb}_{\text{ex}}$ yielding chain for the forest setup follows an inverted U-shape path. As letter “U” has the same shape in upper and lower cases, it helps to avoid confusion of using letter “n”. The inverted U-shape flow indicates that the $^{210}\text{Pb}_{\text{ex}}$ -producing isotope is transferred from soil to the atmosphere and is deposited back to the soil through different mechanisms. It is worth to mention that this local fallout model could be affected by a long-distance movement of $^{210}\text{Pb}_{\text{ex}}$ by wind in and out from the specific study site. However, to keep the model as simple as possible, I assumed that inflow and outflow of atmospheric $^{210}\text{Pb}_{\text{ex}}$ from the study site are counterbalanced.

Table 3.2 Seasonal distribution of litter driven inputs

Season	Dry matter (g m ⁻²)	Carbon (g m ⁻²)	²¹⁰ Pb _{ex}	
			(Bq kg ⁻¹)	Bq m ⁻² (%)
Summer	18 ± 1.7	10 ± 0.9	1548 ± 825	28 ± 15(8.8)
Fall	119 ± 4.4	63 ± 2	1333 ± 309	159 ± 31(50)
Winter	36 ± 21	19 ± 11	1325 ± 280	47 ± 38(14.8)
Spring	47 ± 7.3	25 ± 4	1778 ± 817	84 ± 35(26.4)
Annual	220	117	1496	318

*Note: ± is error of 1σ among three litter traps.
Values in the parenthesis are the proportions of litter-fed ²¹⁰Pb_{ex} input for each season.*

In the soil, it is typically lost through physical decay and/or is displaced mechanically by erosion (see Figure 3.2 and 3.5). In addition, the process is represented as an inverted-U shape because that it does not form a complete cycle since plant roots rarely absorb ²¹⁰Pb_{ex} as indicated in some studies. For example, Osaki et al. (2003) reported that ²¹⁰Pb_{ex} is not found in xylem tissue of cedar trees since it is a heavy metal that is tightly fixed to soil particles, unlike ¹³⁷Cs. Therefore, the absorption of ²¹⁰Pb by plants is almost negligible, which the inverted U-shape model accurately explains.

The second component of the model is *Bi-box* compartment. To determine the input of ²¹⁰Pb_{ex} through litter to forest soil, I created two ideal (but practically inseparable) transfer boxes. These transfer boxes allowed us to follow a step-wise pattern to estimate each subsequent depositional flux. Initially, the atmosphere was considered the feeder and the canopy the receiver. In the second step, the canopy was considered the feeder and the forest floor the receiver (Figure 3.2 and 3.5). Over longer periods of time, these depositional groups achieved their own respective equilibrium.

Model results and explanation

Table 3.1 describes the $^{210}\text{Pb}_{\text{ex}}$ inventory and SOC contents for the reference sites and the sampling points. Previous study reported 19703 Bq m⁻² of weighted mean reference inventory of $^{210}\text{Pb}_{\text{ex}}$ for the study site (Wakiyama et al. 2010). The authors stated that the reference sites were located on flat ridge top of the watershed (Figure 3.1) under matured deciduous and coniferous tree canopies. The ground was covered with litter and the vegetation were dominated by old and large diameter (up to 30cm) trees, altogether indicating less recent human disturbance that made it an ideal site for reference site. They have calculated the reference value from area-weighted mean of 15 core samples (19.6 cm² each) and 2 scraper (450 cm⁻² each) soil samples to account for the difference in sampling areas of the core and scraper sampler. The coefficient of variation for core samples was about 35%. Comparatively, the authors suggested that the reference inventory value of the site is appeared to be appropriate. The details are given by Wakiyama et al. (2010). Using this value, the annual atmospheric $^{210}\text{Pb}_{\text{ex}}$ flux (in steady state) deposited on the forest canopy and the portion that reaches to the forest floor were determined as:

$$a = I_{\text{refe}} \lambda \quad (3.1)$$

$$a_c = a - a\lambda = a(1-\lambda) \quad (3.2)$$

Where a is the annual $^{210}\text{Pb}_{\text{ex}}$ flux from atmosphere to canopy; a_c is the net $^{210}\text{Pb}_{\text{ex}}$ density in the canopy after decay (Bq m⁻² year⁻¹), I_{refe} is the local reference soil inventory (Bq m⁻²) and λ represents $\ln 2/t_{1/2}$ (0.03114 year⁻¹), which is the decay constant of $^{210}\text{Pb}_{\text{ex}}$.

The first equation has been used in several previous studies (e.g. Fowler et al., 1995; Branford et al., 2004), but the second equation was generated to determine the contribution of the litterfall path in delivering $^{210}\text{Pb}_{\text{ex}}$ to the soil. Accordingly, the annual atmospheric (a) and canopy (a_c) fluxes of $^{210}\text{Pb}_{\text{ex}}$ were estimated to be approximately 614 and 595 Bq m⁻² year⁻¹, respectively. In previous studies, the reported annual $^{210}\text{Pb}_{\text{ex}}$ deposition ranged from 135 to 267 Bq m⁻² in central Japan (Fukuyama et al., 2008), which was significantly lower than value in this study. Besides the

local orographic variation, this study area receives higher annual rainfall (2735 mm year⁻¹) than cities in central Japan, such as Mie (2069 mm year⁻¹, 267 Bq m⁻² year⁻¹), Tokyo (1466 mm year⁻¹, 200 Bq m⁻² year⁻¹) and Osaka (1306 mm year⁻¹, 135 Bq m⁻² year⁻¹). Therefore, high rainfall of the study area may be responsible for larger observed depositional flux compared to the above sites. And over longer periods of time, this depositional pattern is assumed to be fairly similar in all sampling points of the study catchment, which the subsequent calculation and explanation are made on.

The net ²¹⁰Pb_{ex} from the forest canopy ($F_{C_{Pb}}$, Bq m⁻²) box as an output is transported to the forest soil ($F_{S_{Pb}}$, Bq m⁻²) box as an input. In the “*No soil erosion*” scenario, radioactive decay is the only output from $F_{S_{Pb}}$. Thus, the transported amount of ²¹⁰Pb_{ex} from $F_{C_{Pb}}$ at a constant transport rate (τ) and radioactive decay loss rate (λ , year⁻¹) from $F_{S_{Pb}}$ should be equivalent at a given time point:

$$\tau F_{C_{Pb}} = \lambda F_{S_{Pb}} \quad (3.3)$$

Next, the MRT ($1/\tau$, year) of ²¹⁰Pb_{ex} in the forest canopy (F_c) can be calculated assuming a stationary state using Eq.3.3. Accordingly, the MRT of ²¹⁰Pb_{ex} in the Japanese cypress forest canopy was estimated to be approximately 354 days. Compared to the MRT of ²¹⁰Pb_{ex} of the Japanese cedar forest (730 and 1010 days) reported by Osaki et al. (2003), ²¹⁰Pb_{ex} has shorter residence time in the canopy of Japanese cypress trees by more than a factor of 2. This is probably due to differences between the sites and the nature of the species. For example, Nagakura et al. (2004) showed that the Japanese cypress tree has higher water-saving tendencies than the Japanese cedar tree. This could be directly related to differences in leaf abscission and designs existed between the two species, which in turn could affect the residence time of ²¹⁰Pb_{ex}. Therefore, canopy architecture, stand density, leaf abscission amounts and rates, and specific physiological setups of the species may contribute to the indicated variation.

3.3.3 $^{210}\text{Pb}_{\text{ex}}$ and organic carbon input via litter

The seasonal distribution of litter, SOC and associated $^{210}\text{Pb}_{\text{ex}}$ input in the study forest watershed are shown in Table 3.2. The values represent the mean and standard deviation of three litter traps (1 m² each) except winter season when litter trap number three was found empty due to physical damage. The data indicate that the annual litterfall rate of 220 g m⁻² deposits 117 g m⁻² of organic carbon and 318 Bq m⁻² of $^{210}\text{Pb}_{\text{ex}}$ to the forest soil. A simple bi-box compartment model was used to estimate the contribution of litter to soil's $^{210}\text{Pb}_{\text{ex}}$ inventory beneath the forest canopy. To use the bi-box model, the following two assumptions were made. First, in an equilibrium state, the input and output of $^{210}\text{Pb}_{\text{ex}}$ in a closed forest canopy (as a radiolabel transit box) are equal. Second, the distribution of $^{210}\text{Pb}_{\text{ex}}$ in a closed forest canopy (the case in this study) could cause lodging and dislodging of the radionuclide on its way to the ground. During this time, the canopy intercepts a considerable amount of rainwater that evaporates back from the canopy surface before it reaches the ground. For example, Osaki et al. (2007) reported that a substantial amount of rainwater is retained and evaporated back from coniferous forest canopies. Thus, for simplicity it is reasonable to classify the depositional pathways into two broad categories; litter-fed and other mechanisms-fed (including wet and dry pathways).

My observations show that litter transports 318 Bq m⁻² year⁻¹ (53.4% of the net canopy holdings) of $^{210}\text{Pb}_{\text{ex}}$ to the forest floor while other mechanisms (wet and dry) collectively account 46.6% (Figure 3.2). In agreement, similar trends have been reported by Osaki et al. (2007) for Japanese cedar forest. They demonstrated that 51% of radiolabel deposited via dry deposition (litter fall) and 29.1% through hydrological processes (throughfall = 26% and stemflow = 3.1%) and remaining lost through decay at the canopy. These results therefore demonstrated that litter tends to be a robust transporter of $^{210}\text{Pb}_{\text{ex}}$ to forest floor in a congested forest canopy. Tree phytomass to seasonal climate interaction results in different litterfall yields and it in turn determines the $^{210}\text{Pb}_{\text{ex}}$

deposition flux. Hence, according to the seasonal litterfall pattern, half of the annual litter-fed $^{210}\text{Pb}_{\text{ex}}$ deposition occurred during the fall (50%), followed by spring (26%), winter (15%) and summer (9%). Over longer periods of time, this depositional pattern could influence the vertical distribution of $^{210}\text{Pb}_{\text{ex}}$ and SOC in the soil profile along with seasonal climatic variables which could affect the activities of decomposing biological communities to turnover $^{210}\text{Pb}_{\text{ex}}$ containing litters. The process demands its own time-scale, which ranges from less than a year to several decades. However, this was not explored in this study.

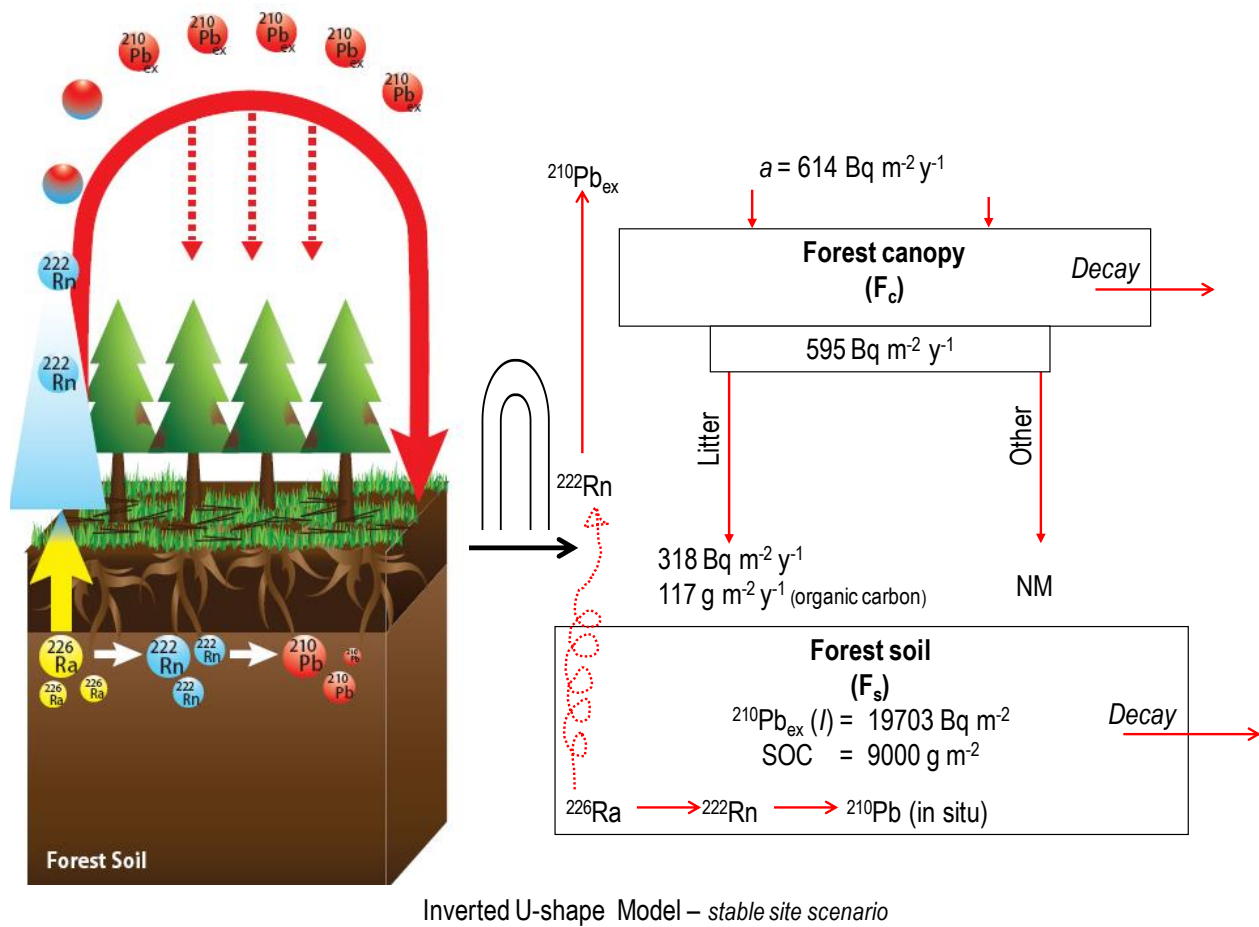


Figure 3.2 Inverted U-shape $^{210}\text{Pb}_{\text{ex}}$ model for stable site scenario. The model illustrates the pathways and the fates of atmospheric $^{210}\text{Pb}_{\text{ex}}$ in reference site. The simplified framework of the model is shown in the right side and the indicated values are calculated based on the assumption discussed in the text

3.3.4 Litter-fed $^{210}\text{Pb}_{\text{ex}}$ deposition flux and its MRT in forest soil

The current concentrations and inventories of $^{210}\text{Pb}_{\text{ex}}$, and the corresponding SOC content of the upper 30 cm of soil at 16 sampling points, were measured (Table 3.3). $^{210}\text{Pb}_{\text{ex}}$ inventories range from 5310 Bq m^{-2} at sampling point 4 to 16413 Bq m^{-2} at sampling point 8 with an average value of $10953 \pm 3094 \text{ Bq m}^{-2}$. This indicates that the $^{210}\text{Pb}_{\text{ex}}$ inventory at each sampling point across the study watershed was lower than the local reference inventory (19703 Bq m^{-2}), qualitatively suggesting each sampling point is an eroded spot.

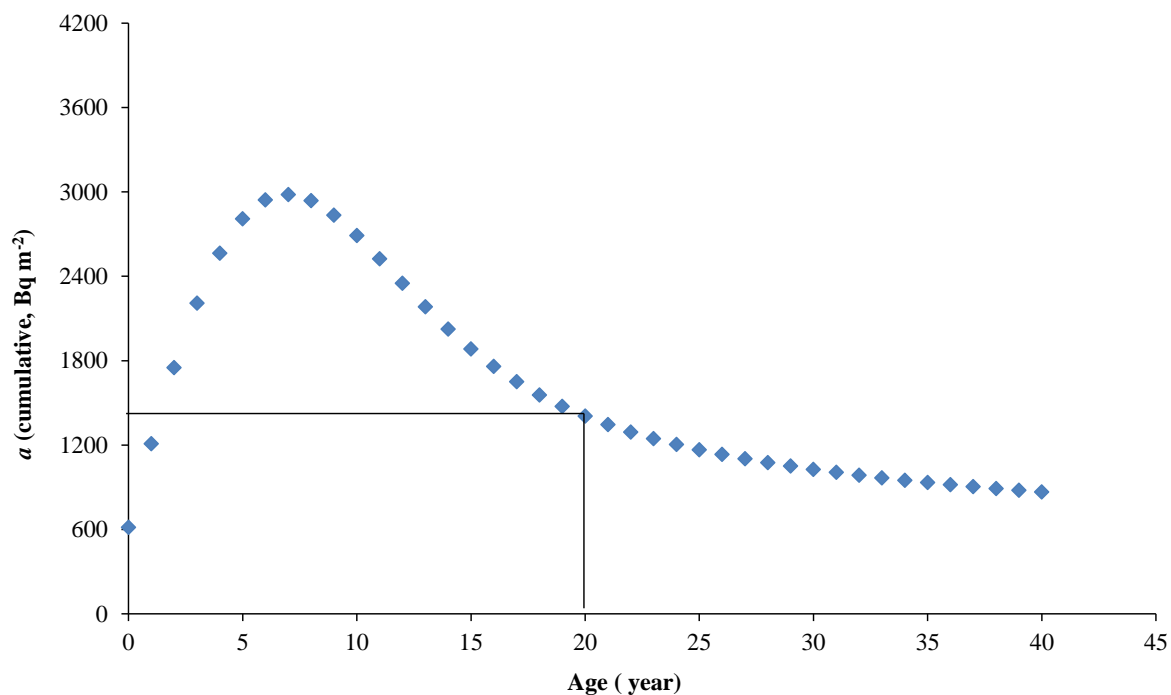


Figure 3.3 The cumulative atmospheric $^{210}\text{Pb}_{\text{ex}}$ flux over the forest age. The assumption here is that forest demands some time to reach climax stage to deliver litter to soil compartment in consistent manner. The atmospheric $^{210}\text{Pb}_{\text{ex}}$ deposition (considering the decay loss at the rate of λ per year) on forest canopy is approaching stable at the age of 20. Hence, it is possible to infer that the forest might reach at full canopy closure growing stage at this age. This gives a clue click start to estimate the MRT of the litter-fed $^{210}\text{Pb}_{\text{ex}}$ in the forest soil

Table 3.3 Measured $^{210}\text{Pb}_{\text{ex}}$ (activities and inventories), SOC (content and density) and litter-fed

$^{210}\text{Pb}_{\text{ex}}$ MRT at each sampling point in the study hillslope

Sampling point	$^{210}\text{Pb}_{\text{ex}}$ Activity (Bq kg ⁻¹)	$^{210}\text{Pb}_{\text{ex}}$ Inventory (Bq m ⁻²)	SOC (%)	SOC (g m ⁻²)	Litter-fed $^{210}\text{Pb}_{\text{ex}}$ MRT ($1/q_i$) (year)
1	220	12292	8	7267	17
2	192	13272	9	7473	18
3	129	11525	5	6964	16
4	86	5310	6	7848	7
5	110	10013	7	8018	14
6	241	10191	12	7404	14
7	197	9021	10	7980	12
8	429	16413	18	10251	23
9	211	8595	10	8802	12
10	236	14234	11	11419	20
11	126	7247	7	7507	10
12	231	13330	13	9851	18
13	185	10261	9	7416	14
14	157	15288	6	6735	21
15	165	11082	8	8885	15
16	139	7176	7	6640	10

Despite a time constant $^{210}\text{Pb}_{\text{ex}}$ flow from forest canopy, erosion disrupted the $^{210}\text{Pb}_{\text{ex}}$ equilibrium and budget by removing it from the soil box, in addition to decay loss. Therefore, I removed the “*No erosion*” scenario assumption applicable at the reference site and included the erosion component as an additional outlet in equation 3.3 for erosion-prone hillslope condition, as follows:

$$\frac{dF_{SPbi}}{dt} = \tau F_{CPb} - \lambda F_{SPbi} - qE_{Pbi} \quad (3.4)$$

Where F_{SPbi} (Bq m^{-2}) is the current soil radiolead inventory of i 's sampling point, E_{Pbi} (Bq m^{-2}) is the difference in radiolead inventory of the i^{th} sampling point to that of reference inventory (I_{refe}), q is the erosion coefficient.

Under a given erosion-induced disequilibrium scenario, the canopy-delivered $^{210}\text{Pb}_{\text{ex}}$ to the forest floor at a sampling point (i) should be equivalent to the sum of the losses by decay (λF_{SPbi}) and erosion (qE_{Pbi}) in the soil compartment. Therefore, the erosion constant (q) at a sampling point (i) can be calculated, as follows:

$$q_i = \frac{\tau F_{Cpb} - F_{SPbi}(1+\lambda)}{E_{Pbi}} \quad (3.5)$$

Where τF_{Cpb} is the cumulative $^{210}\text{Pb}_{\text{ex}}$ deposition from the canopy since the forest reached a stable growing age or age of optimum growth (n). To account for this, I assumed and determined the optimum growth age of the forest, n , as an age when the cumulative annual atmospheric $^{210}\text{Pb}_{\text{ex}}$ flux (a) on the forest canopy approaches the equilibrium condition:

$$\tau F_{Cpb} = a(1 + e^{-\lambda n} + e^{-\lambda n!}) \quad (3.6)$$

Hence, equation 3.5 can be rewritten as:

$$q_i = \frac{a(1+e^{-\lambda n}+e^{-\lambda n!})-F_{SPbi}(1+\lambda)}{E_{Pbi}} \quad (3.7)$$

To determine the age when $^{210}\text{Pb}_{\text{ex}}$ inventory in the forest canopy become constant, I plotted the cumulative atmospheric flux deposition for the entire age of the forest (40 years) (see Figure 3.3). Based on this graph, the cumulative inventory showed a constant tendency starting from age 20 with the corresponding inventory value of 1405 Bq m^{-2} . Next, this value was used to recalculate the cumulative litter-fed $^{210}\text{Pb}_{\text{ex}}$ deposition (the main source of $^{210}\text{Pb}_{\text{ex}}$ in the soil) from age 20 years to the sampling time. Thus, litter-fed $^{210}\text{Pb}_{\text{ex}}$ MRT ($1/q_i$), at least in part, can be estimated based on the net cumulative inventory of litter-fed (L_{pb} , Bq m^{-2}) to the current radiolead inventory (I_{Pbi} , Bq m^{-2}) for the upper 30 cm soil layer of the sampling points, as follows:

$$q_i = L_{Pb} \left[\frac{1 + e^{-\lambda n} + e^{-\lambda n!}}{I_{Pbi}} \right] \quad (3.8)$$

Table 3.3 also summarizes the inventories and their corresponding MRTs of radiolead in the soil at each sampling point. As aforementioned, the inventories of each sampling points are below the reference value indicating erosion is very possible to be generated shortly after rain due to poor ground cover associated with steep slope condition of the study site. In agreement, Onda et al. (2010) reported that most hillslope Japanese forests are left unattended resulting high density and poor ground cover that erosion is the potential threat. More specifically, Wakiyama et al. (2010) and Teramage et al. (2013) have demonstrated high erosion rates ($> 8 \text{ t ha}^{-1} \text{ year}^{-1}$) from this study site. Considering these findings, qualitatively it is possible to infer that all sampling points are eroded points and the difference among them shows the spatial variability of soil erosion across the watershed. The strength of the difference, at least partly can be explained by the MRT of $^{210}\text{Pb}_{\text{ex}}$ at each sampling point calculated based on the value erosion coefficient obtained from Eq. 3.8. Accordingly, the average MRT (I/q_i) of litter-fed $^{210}\text{Pb}_{\text{ex}}$ in the upper 30 cm soil layer was estimated to be approximately 15 years (ranged from 7 to 23 years). This provides additional evidence that clearly shows the impact of erosion on litter-fed radiolead inventory in the study hillslope that shortens its MRT by a magnitude of 8 (at maximum radiolead inventory which is taken an analogue to less eroded site) to 24 years (at minimum radiolead inventory which is taken an analogue to highly eroded site)(Table 3.3).

Figure 3.4 represents the absolute relationship between litter-fed $^{210}\text{Pb}_{\text{ex}}$ MRT and ratios of measured inventory at sampling points to the references site. The results revealed that the higher the ratio value (less eroded site), the longer the litter-fed $^{210}\text{Pb}_{\text{ex}}$ remained in the sampling point, and vice-versa. Therefore, using the $^{210}\text{Pb}_{\text{ex}}$ to MRT ratio, it is possible to estimate the litter-fed based erosion factor for a given study site. This can be used as an indicator of the intensity of litter-fed

$^{210}\text{Pb}_{\text{ex}}$ contamination of vulnerable resources beneath at the downstream side of the watershed, such as water bodies.

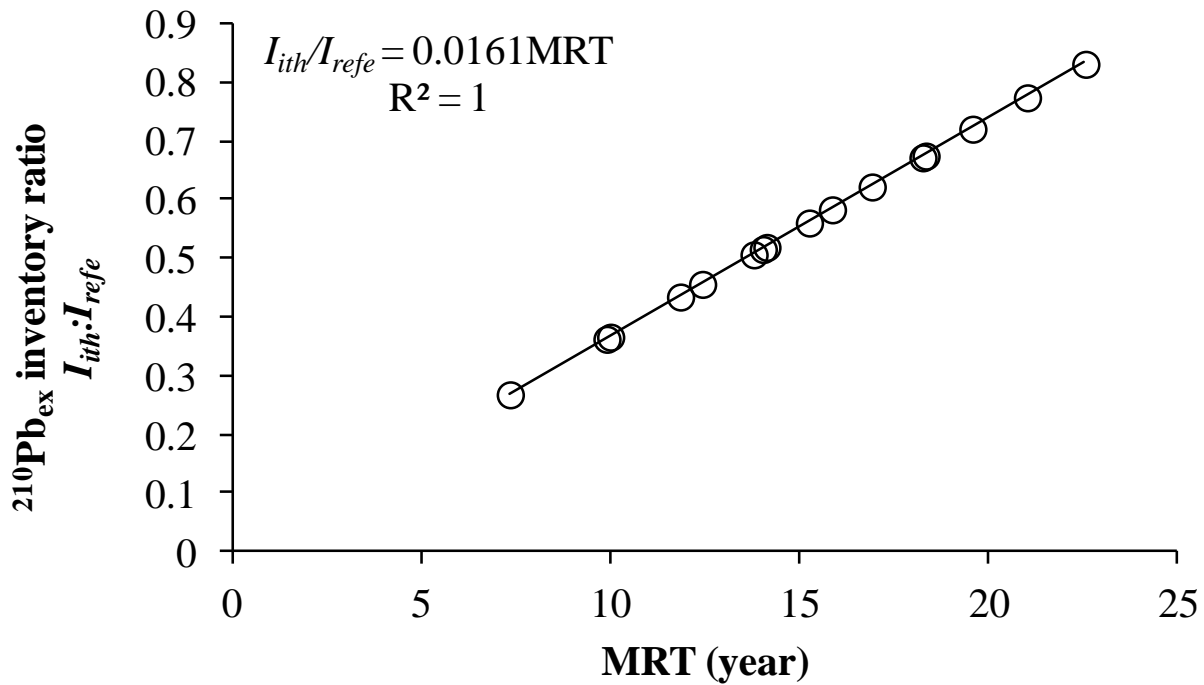
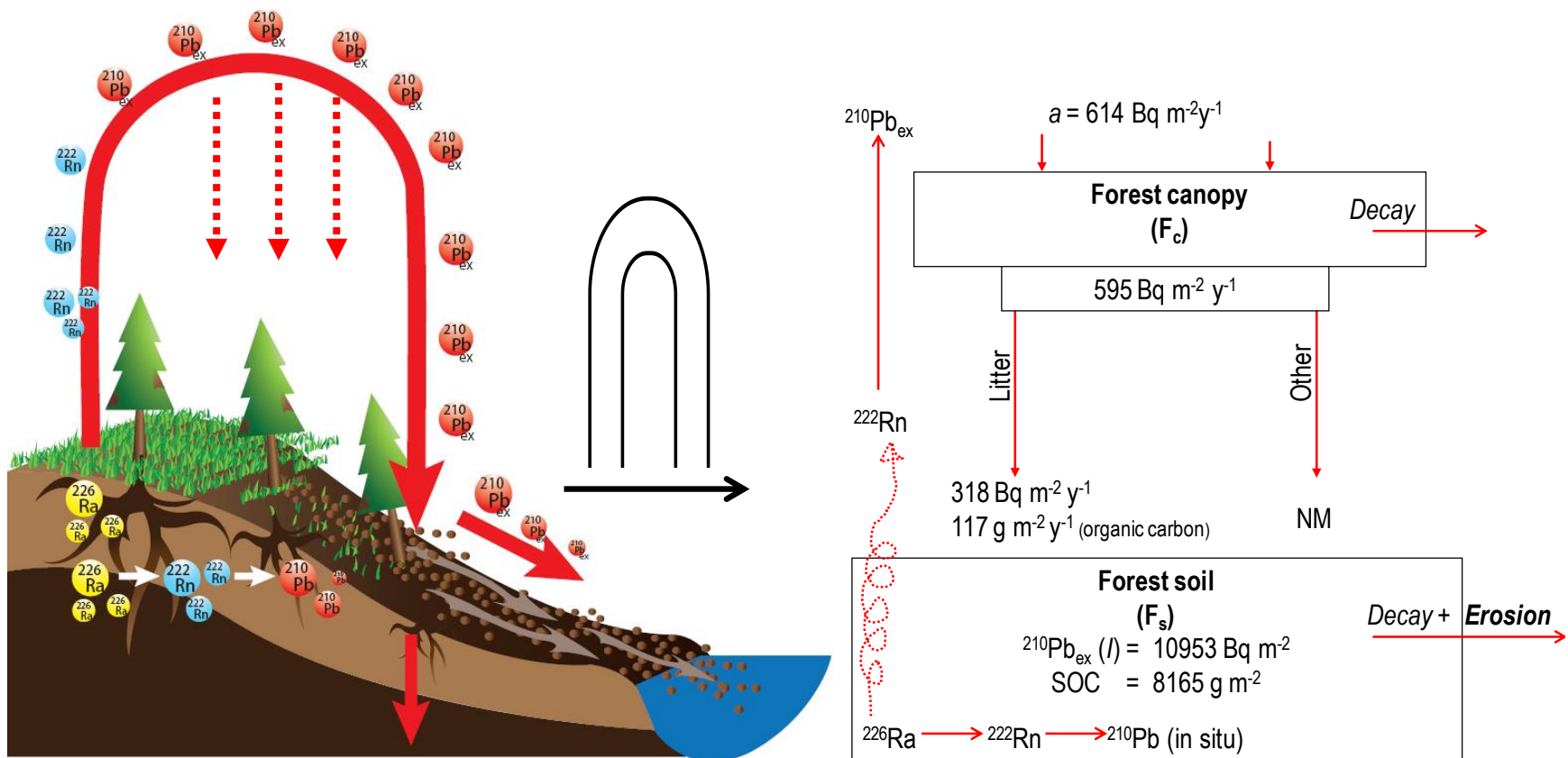


Figure 3.4 One-to-one relationship between $^{210}\text{Pb}_{\text{ex}}$ inventory ratios (inventory of the i^{th} sampling point, I_{ith} , to reference inventory, I_{refe}) and MRT of litter-fed $^{210}\text{Pb}_{\text{ex}}$. Qualitatively discourse, the ratio inventory of $^{210}\text{Pb}_{\text{ex}}$ at a sampling point to local reference site can provide qualitative information about erosion at a given sampling point; eroded site (< 1); deposited site (> 1) and stable site ($=1$). The slope of the equation, inventory-ratio to MRT, can provide the litter-fed $^{210}\text{Pb}_{\text{ex}}$ loss factor per unit time (e.g. per year, year^{-1}).

The modified conceptual model of the $^{210}\text{Pb}_{\text{ex}}$ inverted U-shaped pathways that include erosion as an outlet for the hillslope site scenarios is illustrated in Figure 3.5. Although the flow of litter and its associated inputs ($^{210}\text{Pb}_{\text{ex}}$ and SOC) from the canopy to forest soil are assumed to be uniform, erosion removes and alters their proportion in the soil compartment.



Inverted U-shape Model – hillslope scenario

Figure 3.5 Schematic diagram of $^{210}\text{Pb}_{\text{ex}}$ inverted U-shape flow path in erosion prone hillslope scenario. It represents the situation that erosion dislocates the flow of both $^{210}\text{Pb}_{\text{ex}}$ and SOC and affect the state of equilibrium unlike of the reference site. The simplified framework of the model is shown in the right side that includes erosion as one outlet for both $^{210}\text{Pb}_{\text{ex}}$ and SOC from the system under consideration.

This is clearly illustrated in the conceptual models (Figure 3. 2 and 3.5) for the reference and hillslope scenarios, respectively. And erosion in average removed about 9.2 % of the SOC capital and 44.4% of the $^{210}\text{Pb}_{\text{ex}}$ budget of the hillslope soil compared to the reference site.

3.3.5 $^{210}\text{Pb}_{\text{ex}}$ and SOC inventories, and their depth distribution profiles

The depth distributions of $^{210}\text{Pb}_{\text{ex}}$ (Bq kg^{-1}) and SOC (%) at the reference sites were concentrated on the upper soil horizon where they were continuously replenished from natural sources, mainly via litterfall. The depth distributions of $^{210}\text{Pb}_{\text{ex}}$ and SOC decreased exponentially with increasing depth (Figure 3.6a and b). The relaxation depth ratio of $^{210}\text{Pb}_{\text{ex}}$ to SOC (1.2) demonstrated that both have similar reduction momentum of the surface concentrations by e^{-1} at similar depths in undisturbed soil. This provides evidence that $^{210}\text{Pb}_{\text{ex}}$ and SOC have very comparable depth distribution patterns.

The values of $^{210}\text{Pb}_{\text{ex}}$ inventories and SOC contents did not differ significantly among the sampling points. However, SOC (CV=33%; range: 5 – 18%) showed a relatively larger spatial variability than $^{210}\text{Pb}_{\text{ex}}$ (CV=28%; range: 5310 – 15288 Bq m^{-2}) in the studied watershed. The maximum SOC value was more than 72% higher than the minimum value; whereas $^{210}\text{Pb}_{\text{ex}}$ was only 65% higher (see Table 3.1 and 3.3), implying SOC is relatively variable than $^{210}\text{Pb}_{\text{ex}}$.

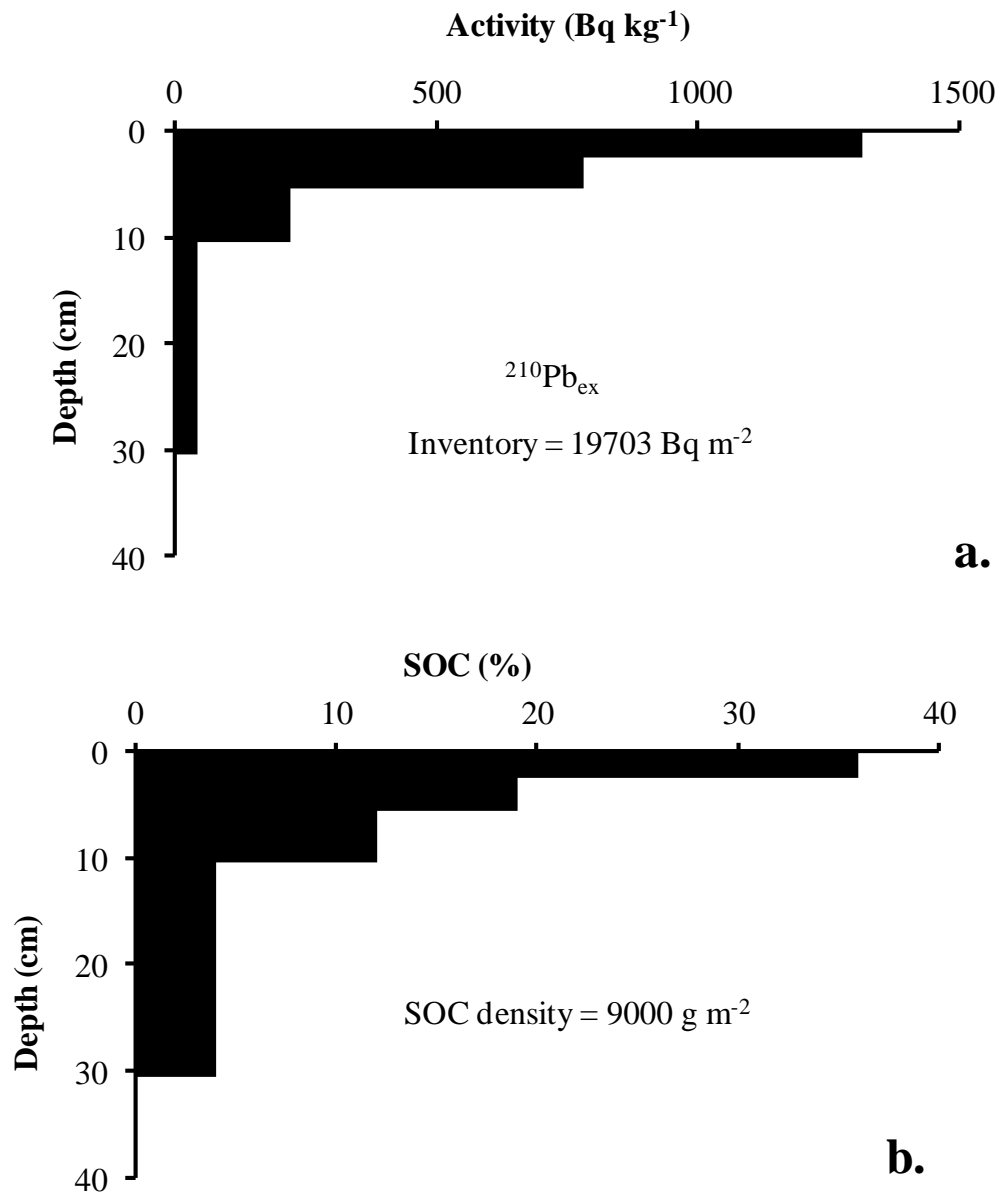


Figure 3.6 The depth distribution profiles of (a) radiollead and (b) SOC concentrations at the reference site. The calculated relaxation depth (\hat{z}) ratio of SOC: $^{210}\text{Pb}_{\text{ex}}$ is 1.2, i.e the depth at which the concentration of SOC decreases to e^{-1} of its concentration at the soil surface is 1.2 times of that of $^{210}\text{Pb}_{\text{ex}}$. This implies that both possess similar depth migration pattern in the vertical soil shelf in undisturbed soil condition. Thus, knowing the concentration $^{210}\text{Pb}_{\text{ex}}$ and its relaxation depth in such environment can give a hint on the SOC content

After deposition of litter and radiolabel, the migration and redistribution of $^{210}\text{Pb}_{\text{ex}}$ and SOC depends on how fast the litter integrates into the soil column. The depth distribution profiles of $^{210}\text{Pb}_{\text{ex}}$ and SOC at each sampling point during the study period are illustrated in Figure 3.7 and 3.8, respectively. Among the depth profile of $^{210}\text{Pb}_{\text{ex}}$ (Figure 3.7), at four sampling points (SP4,7,9 and 11) the lower tails of the profiles were declined to zero around 10 cm depth, indicating 30 cm depth is fairly enough to fully estimate $^{210}\text{Pb}_{\text{ex}}$ inventory in the study site.

Unlike of the reference site, 19% of the sampling points (SP3, 14 and 15) showed minor differences in the shape of their depth distribution profile. Otherwise, most (>80%) had fairly similar shapes, which were concentrated in the topsoil and decline exponentially with increasing depth though SOC and $^{210}\text{Pb}_{\text{ex}}$ follow different disintegration patterns. The former depends on suite of biological decomposition complexes while the latter depends on a constant physical decaying. Regardless of this difference I found a strong relationship between measured SOC and $^{210}\text{Pb}_{\text{ex}}$ along the depth profile. Figure 3.9a shows the relationship between SOC and $^{210}\text{Pb}_{\text{ex}}$ depth distribution at the reference site. Although the variability is high in the upper soil layers and reduces in lower depth, both have shown strong relationship along the vertical soil profile ($R^2 = 0.96$, $n = 4$, $P < 0.05$), implying interdependence on their downward movement in the soil column. Similarly, I plotted the measured values of SOC (%) and $^{210}\text{Pb}_{\text{ex}}$ (Bq kg^{-1}) of all sampling points taken from the study hillslope and is illustrated in Figure 3.9b. This figure shows the relationship of SOC (%) and $^{210}\text{Pb}_{\text{ex}}$ (Bq kg^{-1}) that combines both the effect of spatial and depth distributions together and demonstrates strong correlation ($R^2 = 0.90$, $n = 64$, $P < 0.01$). This provides additional evidence that both are equally affected by similar mechanism and are almost alike in their distribution pattern.

Similar vertical and lateral distribution of SOC and $^{210}\text{Pb}_{\text{ex}}$ could be partly explained by the role of decomposition processes, as follows: When the $^{210}\text{Pb}_{\text{ex}}$ -containing litter begins to breakdown during the different stages of decomposition, $^{210}\text{Pb}_{\text{ex}}$ makes a positional shift from mechanically

external attachment at the canopy and litters to chemically internal attachment, where it is permanently fixed through strong bonds with chains of organic carbon compounds and substances released during the process.

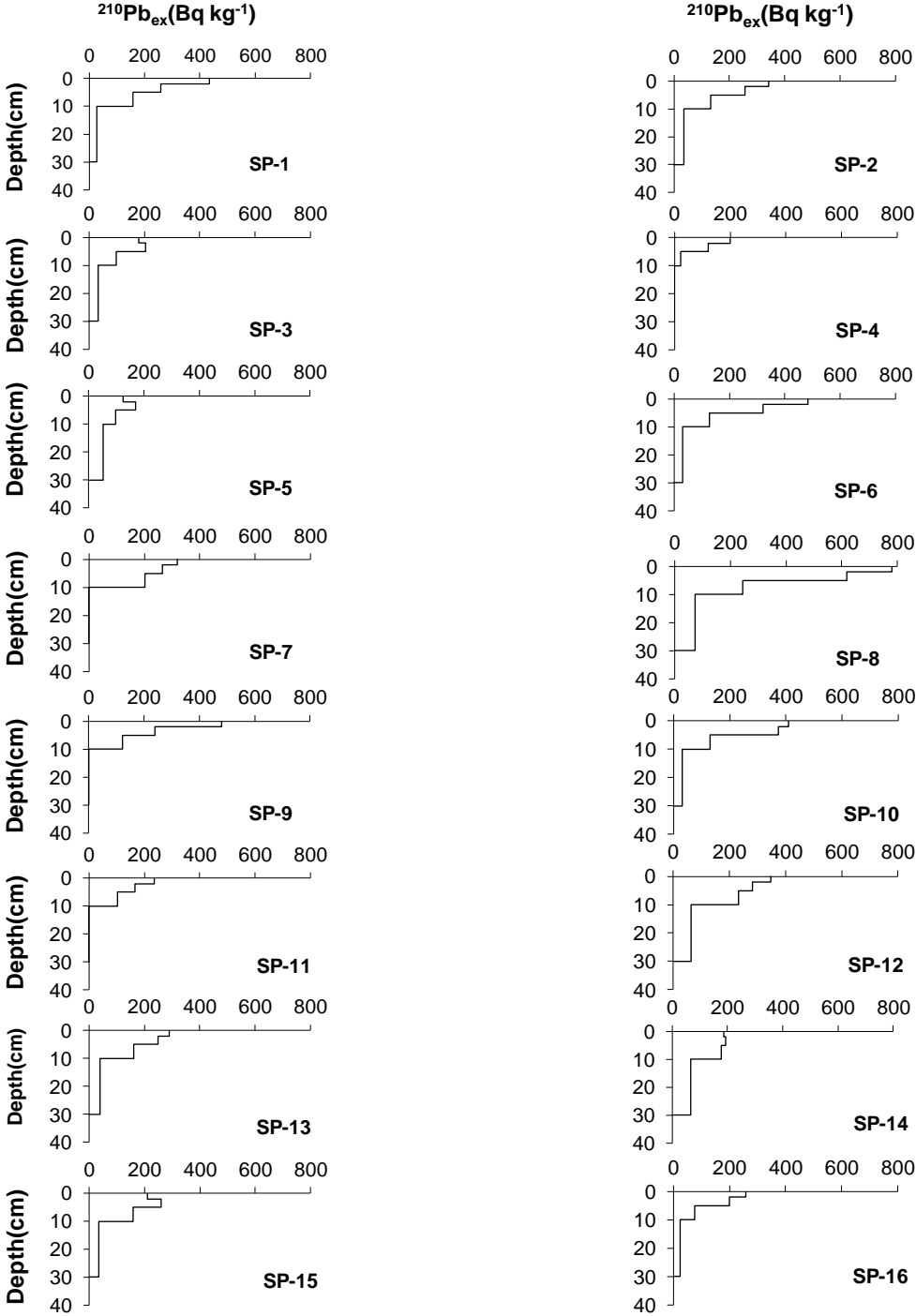


Figure 3.7 The depth distribution profiles of radiopb at each sampling point (SP-*i*'s) in the study watershed

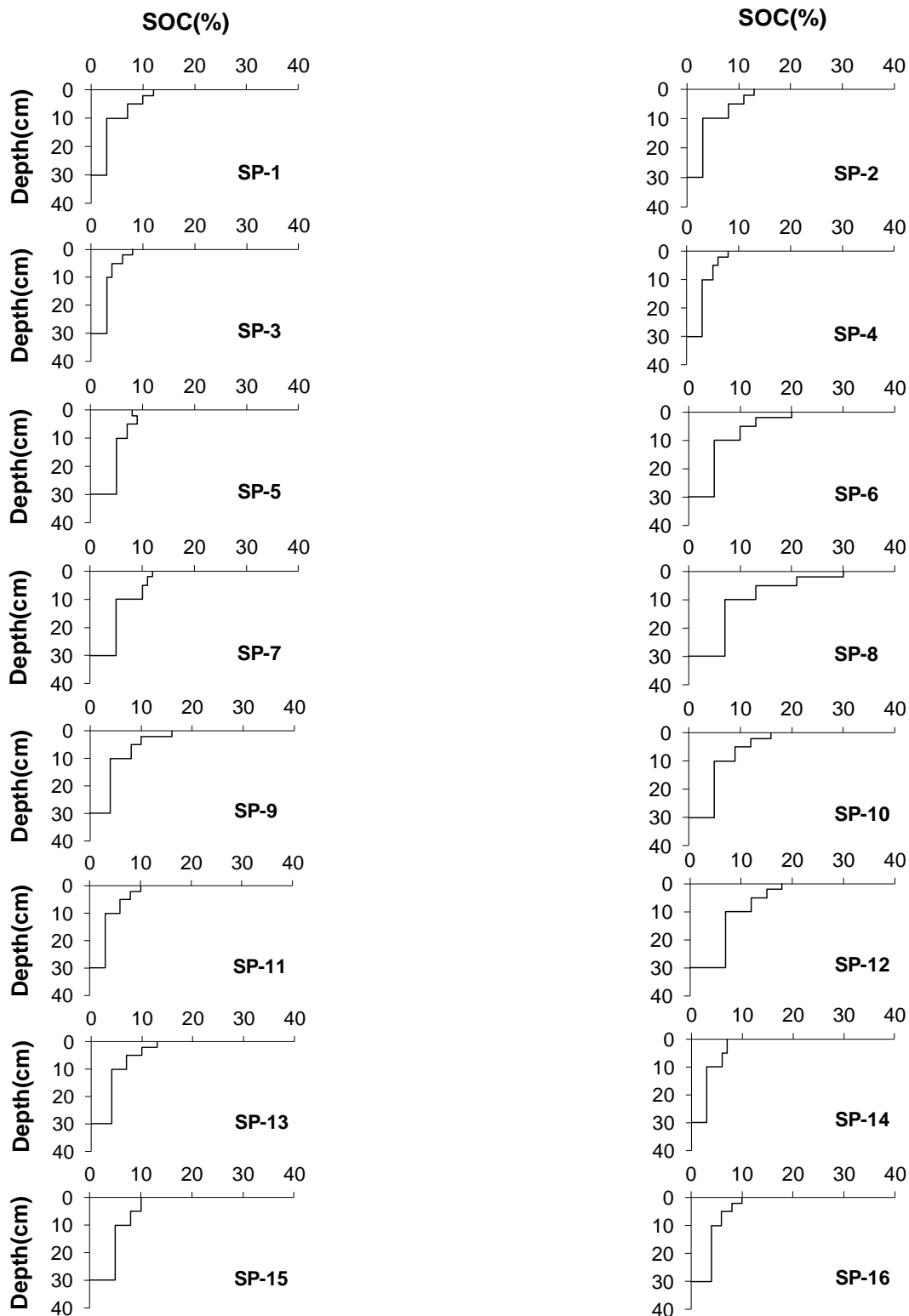


Figure 3.8 The depth distribution profile of SOC at each sampling point (SP-*i*'s) in the study

watershed. The depth profile shapes of both $^{210}\text{Pb}_{\text{ex}}$ (as indicated Figure 3.7) and SOC are almost similar at a given sampling point which implies that both are moving in similar

pattern by similar driving mechanism both in laterally (mainly driven by erosion) and vertically (governed by sedimentation of surface material to lower horizon by decomposition, bio-mixing, gravity, pipe-like conduction and gradient difference based diffusion like processes)

Annually renewed litter layer thickness in the forest floor decreases when SOC is produced by biological decay. When microbes attempt to obtain fresh litter from the renewed layer, the stable SOC form (often called recalcitrant carbon) and partially decomposed organic materials mix and move downward in the soil column. Dorr (1995) and Dorr and Munnich (1991) suggested that radiollead is immobile and its vertical migration is predominantly “passive,” i.e., it moves with its carrier without being mobilized in the liquid phase. In agreement with this, the observed similar depth profile distributions of SOC and $^{210}\text{Pb}_{\text{ex}}$ (see Figure 3.9a and b) in my study can be associated with passive migration which the momentum could be “bio-accelerated” (i.e., the movement mediated by the role of soil fauna). Comparable distribution of SOC and $^{210}\text{Pb}_{\text{ex}}$ throughout the watershed demonstrates that they are affected by similar surface processes, such as erosion. The analogous bi-directional movement (in the vertical soil shelf and on lateral soil surface) of SOC and $^{210}\text{Pb}_{\text{ex}}$ allows us to understand SOC transport based on $^{210}\text{Pb}_{\text{ex}}$ in a forested environment.

Since mid-1990’s global warming is dominating environmental agendas (Mol, 2012) and many climate change conventions are developing rapidly as the world community recognition on the issue increases (Lal, 2003). In this context, my findings can a kick start to identify the possible paths and store spots of SOC across different environments that can assist to develop management systems that could enhance carbon sequestration as a part of combating global warming. It can also generate valuable statistics that can be interpreted and used to reduce soil erosion-induced pollutions in different environmental units such as downstream water resource networks.

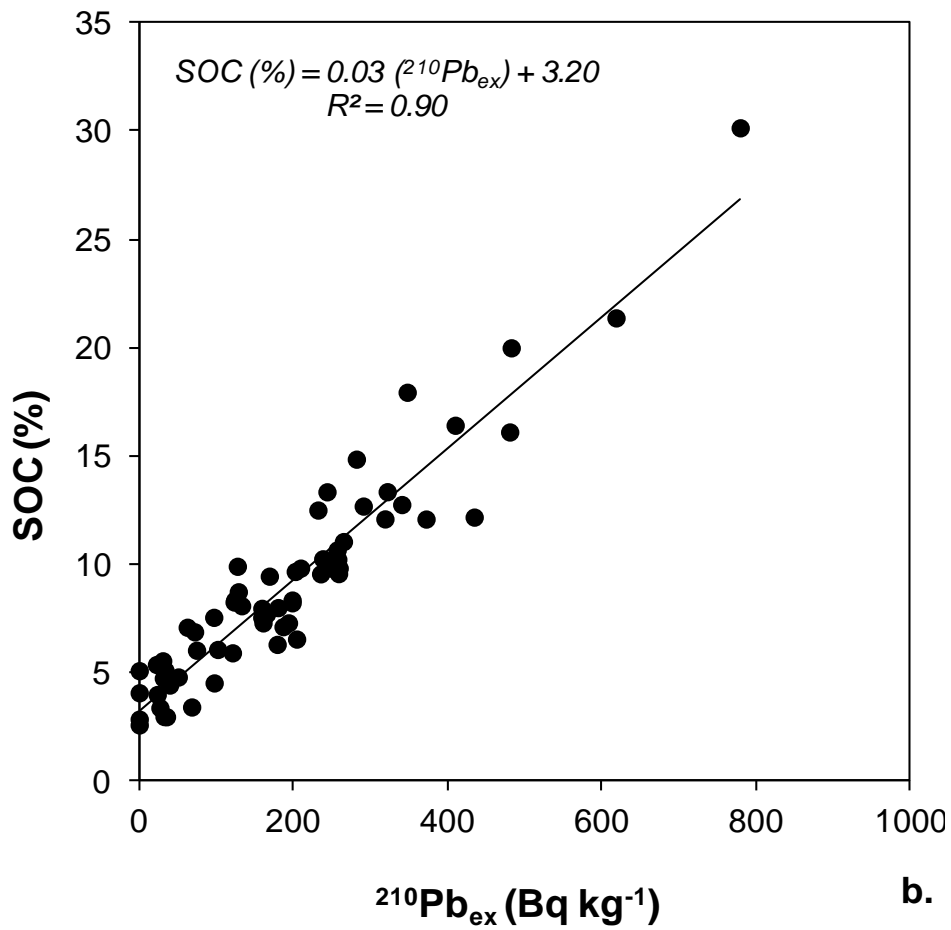
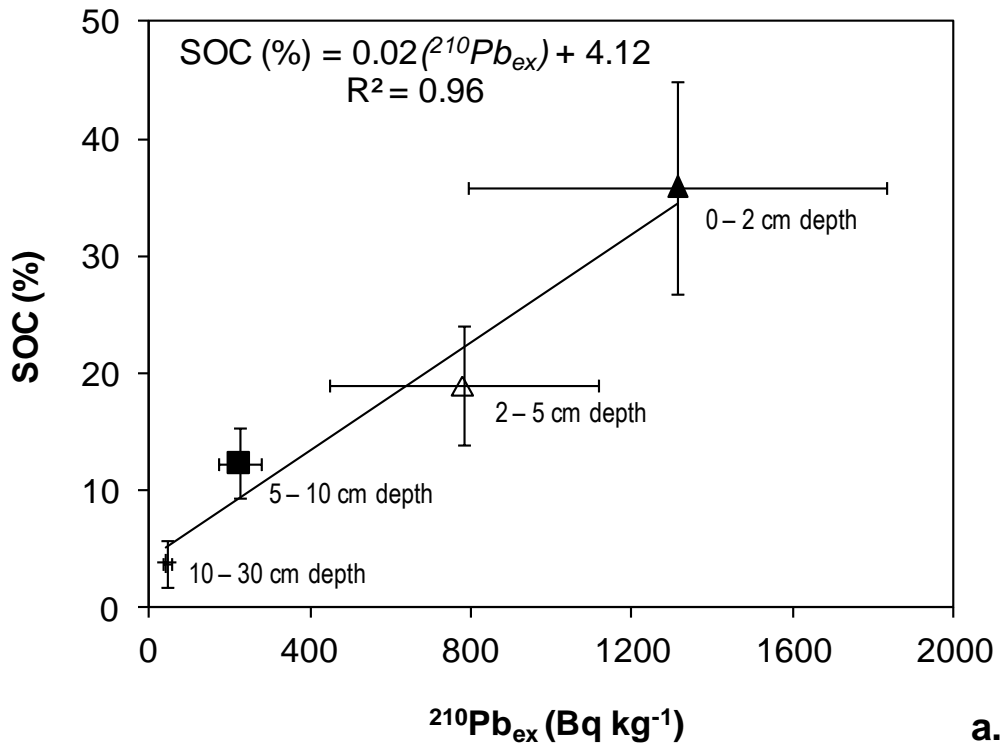


Figure 3.9 The relationship between $^{210}Pb_{ex}$ and SOC at (a) Reference site; (b) Hillslope

3.4 Conclusions

Previous studies have shown that $^{210}\text{Pb}_{\text{ex}}$ movement in forest soil is related to the movement of organic matter. However, organic matter is a mixture of thousands of chemical compounds, primarily organic carbon chains. My result suggests that $^{210}\text{Pb}_{\text{ex}}$ and SOC in forest soil have strong affinity and identical migration patterns. This result suggests that $^{210}\text{Pb}_{\text{ex}}$ distribution pattern could provide information about SOC and may be used to monitor and quantify the transport and distribution of SOC in forest soil. The strong relationship between SOC and $^{210}\text{Pb}_{\text{ex}}$ also indicates the possibility of developing models to predict SOC redistribution and provide highlights for management systems that encourage carbon sequestration. Due to morphological and physiological differences, the MRT of $^{210}\text{Pb}_{\text{ex}}$ in Japanese cypress canopy is shorter than that of Japanese cedar. However, after reaching the forest floor, erosion processes tends to influence the MRT of litter-fed $^{210}\text{Pb}_{\text{ex}}$ in forested hillslope condition. For example, I found that soil erosion shortens the MRT by approximately 8 to 24 years. This implies that transporting of litter-fed $^{210}\text{Pb}_{\text{ex}}$ by erosion is a potential source of contaminant on valuable natural resources located on the downstream side of the hillslope. Such kind of information can help to develop mechanisms to minimize the likely effects of soil erosion-driven contaminates on the downstream resources, more particularly on water resources. Given most of the world forests are located in mountainous and hillslope areas, the ubiquitous tracer, $^{210}\text{Pb}_{\text{ex}}$, could be a feasible tracer providing information that can be interpreted to such as possible approaches to enhance carbon sequestration capacity of forests at local, regional and global scales.

References

- Branford, D., Fowler, D., Moghaddam, M.V., 2004. Study of aerosol deposition at a wind exposed forest edge using ^{210}Pb and ^{137}Cs soil inventories. *Water, Air and Soil Pollution* 157, 107 – 116.
- Dorr, H., 1995. Application of ^{210}Pb in soils. *Paleolimnology* 13, 157 - 168.

- Dorr, H., Munnich, O.K., 1989. Downward movement of soil organic matter and its influence on trace-element transport (^{210}Pb , ^{137}Cs) in the soil. *Radiocarbon* **31**(3), 655 – 663.
- Dorr, H., Munnich, O.K., 1991. Lead and Cesium transport in European Forest soils. *Water, Air, and Soil Pollution* **57/58** 809 – 818.
- EI-Daoushy, F., 1988. A summary on the lead-210 cycle in nature and related applications in Scandinavia. *Environment International* **14**, 305 – 319.
- Fowler, D., Mourne, R., Branford, D., 1995. The application of ^{210}Pb inventories in soil to measure long-term average wet deposition of pollutants in a complex terrain. *Water, Air and Soil Pollution* **85**, 2113 – 2118.
- Fukuyama, T., Onda, Y., Takenaka, C. Walling, D., 2008. Investigating erosion rates within a Japanese cypress plantation using ^{137}Cs and $^{210}\text{Pb}_{\text{ex}}$ measurements. *Journal of Geophysical Research*, doi: 10.1029/2006JF000657.
- Intergovernmental Panel on Climate Change (IPCC), 2003. Good practices guidance for land use, land-use change and forestry. Institute for Global Environmental Strategies (IGES), Japan.
- Kato, H., Onda, Y., Tanaka, Y., 2010. Using ^{137}Cs and $^{210}\text{Pb}_{\text{ex}}$ measurements to estimate soil redistribution rates on semi-arid grassland in Mongolia. *Geomorphology* **114**, 508 – 519.
- Kaste, J.M., Bostick, B.C., Heimsath, A.M., Steinnes, E, Friedland, A.J., 2011. Using atmospheric fallout to date organic horizon layers and quantify metal dynamics during decomposition. *Geochimica et Cosmochimica Acta* **75**, 1642 – 1661.
- Lal, R., 1998. Soil erosion impact on agronomic productivity and environmental quality. *Critical Review in Plant Sciences* **17** (4), 319 – 464.
- Lal, R., 2003. Soil erosion and the global carbon budget. *Environment International*, 29, 437– 450.
- Lewis D., 1977. The use of ^{210}Pb as a heavy metal tracer in the Susquehanna River system. *Geochimica et Cosmochimica Acta* **41**(11), 1557 – 1564

- Likuku, A.S., 2009. Atmospheric transfer and deposition mechanisms of ^{210}Pb aerosols on to forest soils. *Water Air and Soil Pollution* **9**, 179 – 184.
- MolP, J.A., 2012. Carbon flows, financial markets and climate change mitigation. *Environmental Development* **1**, 10 – 24.
- Nagakura, J., Shigenaga, H., Akama, A., Takahashi, M., 2004. Growth and transpiration of Japanese cedar (*Cryptomeria japonica*) and Hinoki cypress (*Chamaecyparis obtusa*) seedlings in response to soil water content. *Tree Physiology* **24**, 1203 – 1208.
- Onda, Y., Gomi, T., Mizugaki, S., Nonoda, T., Sidle, R., 2010. An overview of the field and modeling studies on effects of forest devastation on flooding and environmental issues. *Hydrological Processes* **24**, 527 – 534.
- Osaki, S., Sugihara, S., Maeda, Y., Osaki, T., 2007. Behavior of ^7Be and ^{210}Pb deposited via rainwater on coniferous forest, a broad-leaved forest, and grassland. *Journal of Radioanalytical and Nuclear Chemistry* **272** (1), 147 – 152.
- Osaki, S., Tagawa, Y., Sugihara, S., Maeda, Y., Inokura, Y., 2003. Transfer of ^7Be , ^{210}Pb and ^{210}Po in a forest canopy of Japanese cedar. *Journal of Radioanalytical and Nuclear Chemistry* **255** (2), 449 – 454.
- Pricope, N.G., 2009. Assessment of spatial patterns of sediment transport and delivery for soil and water conservation programs. *Journal of Spatial Hydrology* **9**(1), 21 – 46
- Ritchie, C., McCarty, G., Venteris, E., Kaspar, T., 2007. Soil and soil organic carbon redistribution on the landscape. *Geomorphology* **89**, 163 - 171.
- Teramage, T.M, Onda, Y., Kato, H., Wakiyama, Y., Mizugaki, S., Hiramatsu, S., 2013. The relationship of soil organic carbon to $^{210}\text{Pb}_{\text{ex}}$ and ^{137}Cs during surface soil erosion in hillslope forested environment. *Geoderma* **192**, 59 – 67.

- Vaaramaa, K., Lasse, A., Solatie, D., Lehto, J., 2010. Distribution of ^{210}Pb and ^{210}Po in boreal forest soil. *Science of the Total Environment* **408**, 6165 – 6171.
- Van Oost, K., Quine, T., Govers, G., De Gryze, S., Six, J., Harden, J., Ritchie, J., McCarty, G. Heckrath, G., Kosmas, C., Giraldez, J., Marques da Silva, J., Merckx, R., 2007. The impact of agricultural soil erosion on the global carbon cycle. *Science* **318**, 626 – 229.
- Wakiyama, Y., Onda, Y., Mizugaki, S., Asai, Hiramatsu, S., 2010. Soil erosion rates on forested mountain hillslopes estimated using ^{137}Cs and $^{210}\text{Pb}_{\text{ex}}$. *Geoderma* **159**, 39 – 52.

Chapter 4: The migration of radiocesium in coniferous forest after Fukushima nuclear power plant accident

4.1 Introduction

A mega earthquake and the following tsunami on 11 March 2011 in the north-east part of Japan severely damaged the Fukushima daiichi nuclear power plant (hereinafter FDNPP), resulting in the discharge of various radionuclides into the atmosphere. This accident was recorded as the third episode of major nuclear crisis that injected anthropogenic radionuclide materials, such as radiocesium (^{134}Cs : $t_{1/2} = 2.1$ years and ^{137}Cs : $t_{1/2} = 30.2$ years), into the biosphere; the two previous episodes were the atomic bomb test and the Chernobyl nuclear power plant accident (26 April 1986 in Ukraine). According to the report of the Science Council of Japan (SCJ, 2011) on 2 May 2011, approximately 1.3×10^{16} Bq of ^{137}Cs was discharged into the environment between 11 March and 5 April 2011 (<http://www.scj.go.jp/en/index.html>). The released radioactive materials might have contaminated various terrestrial systems differently depending on the physical and biological components along the plume trajectories. In Japan, forested mountains and hills are the dominant land use and topographic features of its archipelago (Onda et al., 2010); which is very true for the majority of the contaminated land (Kato et al., 2012b). For example, heavily contaminated area, where $^{134,137}\text{Cs}$ deposit exceeds 1000kBq m^{-2} , was estimated about 4% of the forests in Fukushima prefecture (Hashimoto et al., 2012) and hence similar trends can be expected for the surrounding prefectures. So far, however, detail of radiocesium contamination in forest environment, including depth distribution has not been well understood yet.

Previous studies, however, have revealed that forests are critical environments that sink and recycle radionuclides for extended periods of time (Alexakhin et al., 1977; Tikhomirov, 1976). High atmospheric turbulence over forests results in the deposition of a larger amount of fallout

radionuclides on tree phytomass and forest floor than open lands (Bunzl et al., 1989*a*; Tikhomirov and Shcheglov, 1994). The intercepted radionuclides by forest canopy remain for some time and will slowly reach the forest floor mainly in association of hydrological process such as throughfall and stemflow (Bunzl et al., 1989*a*; Kato et al., 2012*b*). Although previous studies concluded hydrological pathways as the dominate transport of radiocesium from forest canopy onto forest floor, litterfall also can contribute year-round deposition of contaminated canopy materials (leaves, branches, twigs, fruits etc). Therefore, it is worth to consider the contribution and the subsequent influences of litterfall on the radiocesium dynamics in forest ecosystem.

The deposited fraction of radionuclides onto forest floor via different pathways then will undergo horizontal (pronounced in sloped lands) and vertical migration (pronounced in undisturbed sites). On flat undisturbed sites, the highest radiocesium concentration is at upper most soil layer and decreases exponentially down the soil depth. Exceptionally, litter layer in forest floor can play a unique role on the distribution of radiocesium, which typically lacks in most other land use types. In soil, the migration of radiocesium can be either slow or fast depending on various sets of factors. Both momentums can be a source for internal and external radiation dose (Almgren and Isaksson, 2006) for forest-dependent life chains, including human beings. As most of the heads of water resources (streams, rivers, springs, etc.) are located in forested watersheds and are intimately linked to downstream ecosystems (Gomi et al., 2002), specially fast vertical mobility of radiocesium in forest soil may quickly generate risks of contaminating soil and ground water. Therefore, understanding the radiocesium deposition and its subsequent migration in such distinctive environment is essential. Such a study can help to understand its behavior, use to inform decisions about possible countermeasures and set up environmental baselines, and to establish parameters to predict its movement in forested ecosystems.

Despite the importance of understanding the movement of radiocesium in forest soil, most previous studies focused on agricultural soil and undisturbed sites in non-forested environments such as pasture land (e.g., He and Walling, 1997; Kato et al., 2012a), and therefore little is known about forest soil (Bunzl et al., 1989a). Among the few studies on Chernobyl-affected forest soils, Karadeniz and Yaprak (2008) reported a relaxation length (i.e. the inverse of the rate of change of concentration) of 4 to 15 cm, and Poreba et al. (2003) indicated a relaxation length of 2.1 cm several years after the accident. However, their findings cannot be simply applied to the Japanese environment because of the difference in the climatic conditions, soil properties, orographic nature, vegetation types and nature of the accidents. More recently, Koarashi et al. (2012) has reported the vertical distribution of Fukushima-derived radiocesium in different land uses including two Japanese cedar forest located at 70 km northwest of the FDNPP. They vigorously identified major factors and processes that control the retention and migration of radiocesium in soil profile and other biological components found in the range of terrestrial ecosystems. Despite their extensive efforts, they have employed core soil sampling method with thicker soil section that ranges from 1 to 5 cm while Loughran et al., 2002 and Kato et al., 2012a have advised fine depth thickness to better describe depth distribution. In this regard, the above soil sectioning width appears to be too thick to describe the behavior of radiocesium migration. Besides, the composition and contamination density of radiocesium are expected to vary as the distance from the point of source so does its behavior in soil profile. Moreover, in addition to the tree species difference, their study lacks insights on the pre-Fukushima radiocesium distribution.

Therefore, this study examined and described the contribution and influences of litterfall on the radiocesium deposition from forest canopy onto forest soil. I also investigated the behavior of radiocesium in forest floor and defined its depth distribution in forest soil column. Estimation on radiocesium migration and soil-to-plant transfer rate were also made.

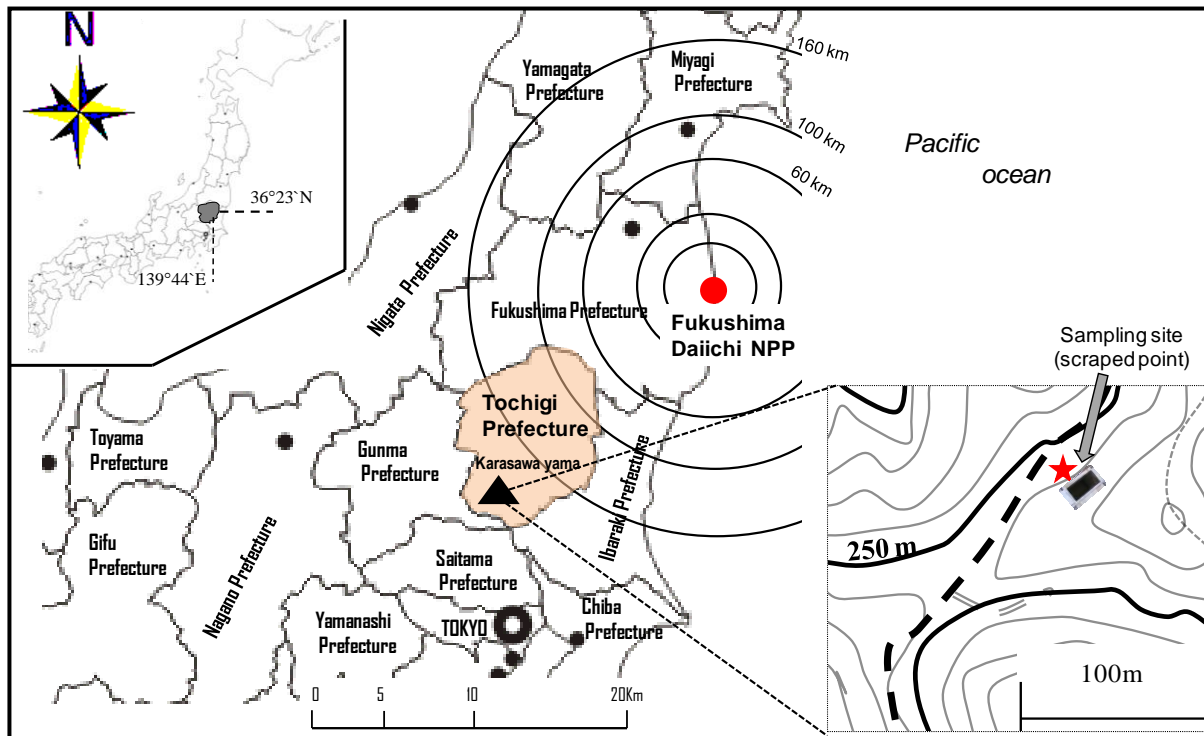


Figure 4.1 Map of the study area and location of the sampling point

4.2 Study site

The study was conducted in a 30-year-old Japanese cypress (*Chamaecyparis obtusa* Endl.) plantation forest stand located on Karasawa yama (139°44' E; 36°23' N), in the Tochigi prefecture of central Japan (Figure 4.1). The area is located 180 km southwest from the crippled FDNPP. The size of the catchment is 0.8 ha. This mountainous catchment is not only known for its economic and environmental importance but also often visited by hikers from the surrounding society.

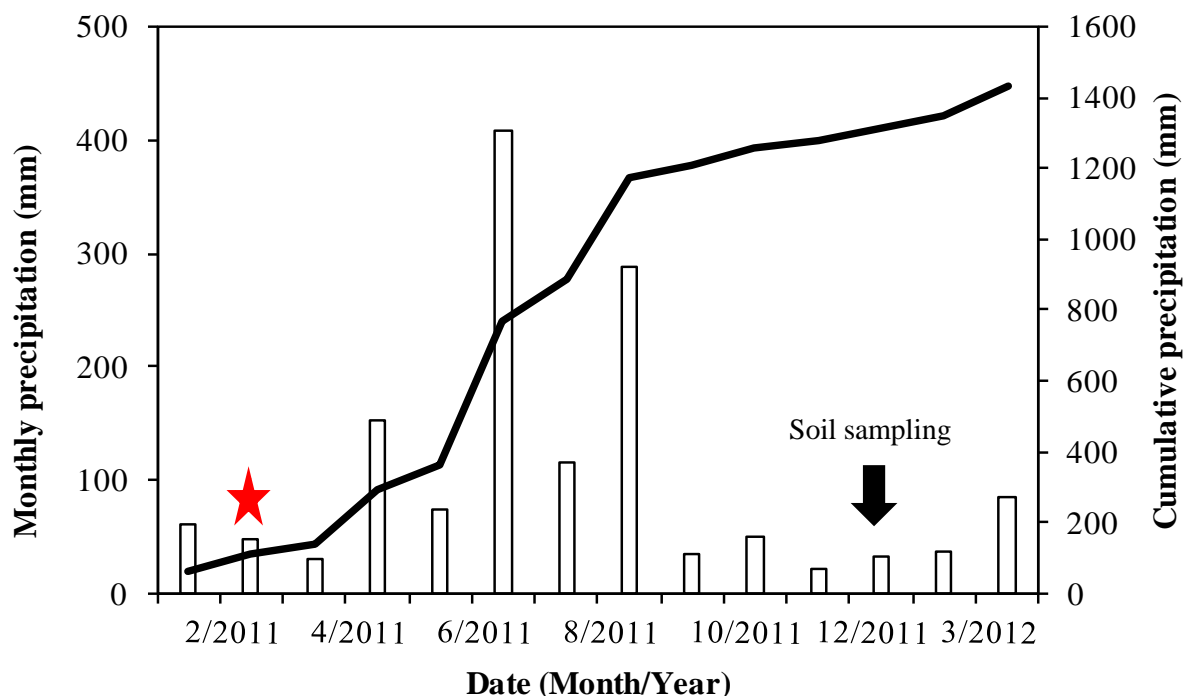


Figure 4.2 Monthly (bars) and cumulative (bold line) precipitation for one year duration at the study site. ★ = indicates arrival of the radionuclide plume at the study site on mid-March (2011) and the wet deposition was expected due to the precipitation from March 15 to the first two weeks April, 2011.

The climate of the area is humid temperate, with 1,259 mm mean annual rainfall and 14.1°C mean annual temperature. The soil type can be classified as an Orthic cambisols. The estimated stand density is approximately 2,500 trees per hectare. The forest floor is composed of sparsely grown marlberry (*Ardisia japonica* (Thunb.) Blume), herbs, and fallen broad and needle leaf litters.

A southeast wind blowing on 15 March 2011 drove a radionuclide plume that contaminated the northwest areas of the nuclear plant and spread widely to southwest regions, including the study site. According to the MEXT (2011) report, the plume that include the study site started around 23 March 2011 and deposited about 10 kBq.m⁻² of radiocesium. Low temperature at the time of accident and the large size composition (Hirose, 2012) of the radionuclide debris, kept the plume moving near to the ground surface, driven by local wind. Based on this situation, it is reasonable to assume that the deposition primarily occurred through a combination of wet deposition (snow and

rain droplets) and impaction on the forested mountains and hills of Japan's archipelago. Figure 4.2 shows monthly and cumulative total rainfall of the year 2011 around the time of accident and soil sampling date including the radiocesium deposition in the observation periods.

4.3 Materials and methods

4.3.1 Litterfall sampling

For the purpose of mentoring litterfall (*LF*) flux, four nylon nets with 1 m² area (each) litter-traps were suspended about 1m above the ground on the representative location of the study catchment about seven months before the accident (installed on 03August 2010). Following the FDNPP accident the litter traps' data was used to measure radiocesium deposition along with litterfall. This gave an exceptional opportunity to measure litter-derive radiocesium deposition starting from the very beginning. Litter traps were emptied regularly and the radiocesium activities were determined (discuss later) as a litterfall mass weighted mean activity from four replications to account for differences in *LF* mass during the observation period. The data for rainfall (*RF*), throughfall (*TF*) and stemflow (*SF*) were obtained from published material (for detail see Kato et al., 2012*b*) from the same study site and observation period (Table 4.1) and the results are complimented and compared.

4.3.2 Soil sampling

Soil samples were collected at an undisturbed flat area to minimize the effect of subsequent movement of radionuclides after fallout. The sampling point was purposely selected at the midpoints between tree lines to make it more representative and reduce the effect of coarse roots during sampling. I used a rectangular metal-framed scraper plate (internal dimensions of 15 cm x 30 cm) with an adjustable depth increment of 5 and 10 mm intervals. The sharp cutting edge of the plate can scrape the soil by rolling along the frame, guided by a re-positionable metal bar. This sampling

method permits us to collect a large number and volume of soil samples that encompasses and represents relatively wider microtopographic variability (Loughran et al., 2002; Kato et al., 2012a).

With this sampling scheme, I carefully separated understory vegetation and OI- (~3 cm thick) and Of- (~4.5 cm thick) horizons that were collected by hand and scissors (when necessary) to represent the forest floor. The understory vegetation was dominated by sparsely grown marlberry and annual herbs. The OI-horizon represented an organic horizon of litter in which the original shape of the components was easily recognizable and was composed of and built by periodically falling raw litter. The Of-horizon was an organic horizon located under the OI-horizon which was composed of an early fermented and fragmented litter component in which the original shapes of the litter were difficult to identify.

The radiocesium mobilization by understory plants is often estimated based on the horizon-to-plant transfer factor on dry weight base (TF_w) and aggregated transfer factor (T_{agg}) coefficients, which are defined as the ratio of average radionuclide concentration in plants ($Bq\ kg^{-1}$) to that in soil ($Bq\ kg^{-1}$) for TF_w or total soil profile inventory ($Bq\ m^{-2}$) in the case of T_{agg} (Calmon et al., 2009; Thiry et al., 2002; Kruyts et al., 2004). T_{agg} is more realistic for the medium-to-long term after deposition (IAEA, 2010) as radiocesium requires a long time to reach the tree root zone. Therefore, I assumed that the roots of understory vegetation in my study site can potentially explore the Of-horizon and the upper 2 cm soil, and it is reasonable to use TF_w instead of T_{agg} . Therefore, I used the radiocesium concentration in dried and bulked understory plants ($Bq\ kg^{-1}$) and the average concentration in Of-horizon and upper 2 cm soil layers ($Bq\ kg^{-1}$) to calculate TF_w .

The soil below the Of-horizon was scraped layer by layer in three major depth resolutions of 5, 10 and 20 mm. Although a 1 cm depth increment is recommended for the investigation of the depth profile of ^{137}Cs (Loughran et al., 2002), I employed a depth increment of 0.5 cm for the upper 5.0 cm. This helps to reduce the possible effects of soil thickness in defining the shape of the profile

in the highly contaminated upper soil section unlike that used by Koarashi et al. (2012). Then, the depths of soil from 5 to 10 cm and from 10 to 30 cm were sliced every 1.0 and 2.0 cm intervals, respectively. In the sampling depth, neither cracks nor big roots were encountered.

4.3.3 Laboratory analysis

Measurement of radiocesium activity

All samples were dried at 110°C for 24 h to determine the dry weight. The samples of litter, understory vegetation, Ol- and Of- horizons were then milled and mixed to ensure homogenous sample material for each respective sampling unit. The soil samples were disaggregated by gentle grinding and were then passed through a 2-mm sieve. Then, the milled understory vegetation, Ol-, Of-horizons and the < 2 mm soil fraction from each soil layer were placed in plastic U-8 bottles and sealed for assaying. The analysis was conducted in the laboratory of the University of Tsukuba, which was authorized for independent calibration checks during the worldwide open proficiency test in 2006 (IAEA/AL/171) prepared by the International Atomic Energy Agency (IAEA). The activities of ^{137}Cs and ^{134}Cs were determined using gamma ray spectrometry from a high purity n-type germanium coaxial gamma ray detector (EGC 25-195-R, Canberra-Eurysis, Meriden, USA) connected to an amplifier (PSC822, Canberra, Meriden, USA) and multichannel impulse separator (DSA1000, Canberra, Meriden, USA) using the counts at the 662 keV and 605 keV peaks, respectively. The absolute counting efficiency of the detector was calibrated using various weights of IAEA-2006-03 standard soil samples with background correction. The measured activities (Bq kg^{-1}) were converted to inventories (Bq m^{-2}) using the dry sample mass depth (kg m^{-2}) of each sampling layer. All measured activities were decay corrected to May 20, 2011.

Soil physiochemical property analysis

The physiochemical properties of the soil were determined for the < 2 mm soil samples. The particle size distribution (sand: 75 - 2000 μm ; silt: 5 -75 μm ; clay: < 5 μm) in each soil layer was analyzed using a laser diffraction particle size analyzer (SALD-3100, Shimadzu Co., Ltd., Kyoto,

Japan). The bulk density was determined from the dry weight and volume of soil in each layer. The organic matter content (OM) of the samples was determined by the weight loss after incineration of a known dry weight sample in a muffle furnace at 450 °C for 4 h. The pH was determined using a pH meter by mixing 5 g of dry soil with 50 ml of distilled water to a final 1:5 soil:water ratio.

4.4 Parameters for radiocesium depth profile

To investigate the vertical distribution of radiocesium, I applied a negative exponential profile function, which includes a number of simplified assumptions (Porto et al., 2001; Karadeniz and Yaprak, 2008; Kato et al., 2012a). This method can be appropriate for estimating the radiocesium movement in earlier stages after the fallout. Fitting an exponential function to the empirical data of the profile can provide parameter values that characterize the depth distribution of radiocesium. Importantly, in forest soil, the organic-rich upper layers could affect the theoretical exponential function. Therefore, I discussed the radiocesium concentration in the forest floor (which hereafter refers to the composition of the understory vegetation, OI-and Of-horizons) separately, while the depth penetration of radiocesium in soil below the Of-layer was assumed to approximately follow the exponential trend of the following general formula:

$$C(z) = C(0)e^{-\alpha z^p} \quad (4.1)$$

where z is the depth from soil surface (cm), $C(z)$ the concentration of radiocesium at depth z (Bq kg^{-1}); $C(0)$ is the radiocesium concentration (Bq kg^{-1}) in the surface soil; α (cm^{-1}) is the reciprocal of the relaxation depth; and p (*unitless*) is an experimentally determinable parameter depending on upper soil surface condition and form of transport. It also determines the shape of the depth distribution to be either straight, concave or convex (Isaksson and Erlandsson, 1995).

The parameter α depends on the characteristics of the radionuclides, soil type and its physiochemical characteristics, land use type, time elapsed and climatic conditions (Kato et al., 2012a). Its reciprocal value represents the relaxation length of the radiocesium in the vertical profile

(Karadeniz and Yaprak, 2008). The depth can be expressed either in linear (cm or m) or mass depth (kg m^{-2}). The linear relaxation depth, $1/\alpha$, represents the shape of the tail of the depth distribution, whereas the relaxation mass depth describes the penetration strength of radiocesium of soil mass per unit area. Considering the average bulk density, α (m^{-1}) can be reciprocally related to relaxation mass depth, h_0 (kg m^{-2}). When $p = 1$, the following function (Porto et al., 2001) can be used as an alternative to directly estimate h_0 by fitting the model to the empirical data of the reference site when z is expressed in mass depth.

$$C(z') = C(0)e^{-z'h_0} \quad (4.2)$$

Where z' is the mass depth from soil surface (kg m^{-2}); $C(z')$ is the concentration of radiocesium at depth z' (Bq kg^{-1}); $C(0)$ is the radiocesium concentration (Bq kg^{-1}) in surface soil; and h_0 can be easily determined using the linearized least square regression method.

4.5 Characterizing the pre-Fukushima ^{137}Cs

The observed ^{137}Cs concentration in the soil includes remnants of pre-Fukushima episodes, whereas due to its short half-life (2 years), the observed ^{134}Cs in the environment exclusively originates from Fukushima. To determine the pre-Fukushima ^{137}Cs concentration, I used a well-documented approach, the $^{134}\text{Cs} / ^{137}\text{Cs}$ ratio (e.g., Livens et al., 1992). The ratio was determined from litters which was taken immediately after the fallout and was found to be 1. Using this ratio, the pre-Fukushima ^{137}Cs residue in the soil profile was determined. Note that due to the physiochemical similarity of ^{137}Cs and ^{134}Cs , the behavior of ^{134}Cs , often indicated as radiocesium, described in this paper is also applicable to Fukushima-derived ^{137}Cs . For simplicity, I discussed ^{137}Cs as pre-Fukushima; otherwise it is indicated as the total ^{137}Cs in the soil profile to represent both pre and post Fukushima cesium altogether.

4.6 Diffusion and migration rates of radiocesium in mineral soil

Although the depth distribution of fresh fallout is often described by an exponential function as indicated in Eq. 4.1, the function fails to describe the downward transportation that occurs from the first instant of deposition, and unable to illustrate long-term distribution (Almgren and Isaksson, 2006). Redistribution of radiocesium within the soil profile is the result of a complex set of processes that the time-dependent model should consider, including physical, physico-chemical and biological processes (Almgren and Isaksson, 2006, Walling et al., 2002). Such transport mechanisms have been characterized by a diffusion coefficient (D , $\text{kg}^2 \text{m}^{-4} \text{y}^{-1}$) and a migration or convection rate (v , $\text{kg m}^{-2} \text{y}^{-1}$) that lump together all redistribution processes in the soil column (Walling et al., 2002). These transport coefficients can be also represented in the linear dimension (D , $\text{cm}^2 \text{y}^{-1}$; v , cm y^{-1}) if the effect of soil density (kg m^{-3}) is ignored. In this study, I estimated and evaluated these two parameters based on the formula proposed by Walling et al. (2002) as:

$$D \approx \frac{(N_z - W_z)^2}{2(t - t_0)} \quad (4.3)$$

$$V \approx \frac{W_z}{t - t_0} \quad (4.4)$$

Where:

t = sampling year

t_0 = maximum fallout year (e.g., 2011 for Fukushima, 1986 for Chernobyl, 1963 for bomb fallout)

N_z = mass depth (kg m^{-2}) or linear depth (cm) of the maximum radiocesium concentration

W_z = mass depth (kg m^{-2}) or linear depth (cm) of radiocesium concentration reduced to 1/e of the maximum concentration

4.7 Results and discussion

4.7.1 Radiocesium in litterfall and on tree canopy

Deposition of radiocesium via falling litter:

Within the observation period (March 11 to August 2011) the total *LF* was 150 g m^{-2} and its amount rose to 355 g m^{-2} up when the observation is extended until the first soil sampling date (January 16, 2012). Along with these, about 2472 and 3071 Bq m^{-2} radiocesium were deposited onto the forest floor, respectively. Kato et al. (2012b) has demonstrated that from 12 *RF* events (of total 719 mm rain), 81.2% was reached the Japanese cypress forest floor either via *TF* (71.5%) or *SF* (9.7%) which left deposits of 8030 Bq m^{-2} (*RF*), 2910 Bq m^{-2} (*TF*) and 119 Bq m^{-2} (*SF*) of radiocesium onto forest floor (Table 4.1). Of the total local fallout, *TF*, *SF* and *LF* pathways, respectively transported 5%, 0.2% and 5% radiocesium to forest floor during the first sampling period.

The radiocesium ratio of *LF* to rainfall ranged from 0.07 in early period to 2.2 in later period (Table 4.1), suggesting washing-off radiocesium from canopy via rainwater is reduced quickly and lived shortly after the fallout period. Note that some of the radiocesium in dripping rains might be deposit onto the litters that are already in the traps but it is assumed to be completely compensated by the washed outflow from litter surface by dripped water itself.

The deposited radiocesium by *LF* route for the first 160 days accounted for 30% ($\sim 2.5 \text{ kBq m}^{-2}$) of the local deposition density. This result is larger than the value ($\sim 7\%$) reported from 85-years old Norway spruce forest ($622 \text{ trees ha}^{-1}$) that has been investigated for the first 600 days following the Chernobyl accident (Bunzl et al., 1989a) in German. Figure 4.3 elucidates the radiocesium deposition ratio onto forest floor via *LF* route in Japanese cypress forest (after FDNPP accident, this study) and Norway spruce (after Chernobyl accident) over time. Although both have shown a logarithmic increase, the magnitude of *LF* contribution in cypress forest is higher by more than factor of 4. Indeed, several factors could be involved as possible reasons, including biological

and physiological nature the two tree species, but stand density is most likely related to the tree phenology and influences the light fluxes in forest; therein determines *LF* rate and amount. For example, Maguire (1994) concluded that forest under high stand densities released higher level of dead branch mass in the system. Hence, high stand density in cypress forest (> 4-folds) is the most conceivable factor to the observed difference.

Table 4.1 Deposition of radiocesium onto forest floor via Rainfall, Throughfall (TF), Stemflow (SF) and Litterfall (LF) at different sampling period

Sampling period	¹³⁷ Cs deposition (Bq m ⁻²)					¹³⁴ Cs deposition (Bq m ⁻²)				
	RF*	TF*	SF*	LF	LF/RF	RF*	TF*	SF*	LF	LF/RF
2011/3/11 - 3/28	5420	434	18.5	374	0.07	5150	385	24	376	0.07
2011/3/28 - 4/1	1010	389	9.47	-	-	1010	328	5.34	-	-
2011/4/1 - 4/13	400	180	36.5	352	0.88	359	189	30.9	357	0.99
2011/4/13 - 4/27	328	265	6.6	-	-	328	242	7.27	-	-
2011/4/27 - 5/20	345	483	<i>nd</i>	814	2.36	277	405	<i>nd</i>	814	2.94
2011/5/20 - 5/28	111	200	7.9	-	-	121	175	5.93	-	-
2011/5/28 - 5/30	71.2	137	<i>nd</i>	-	-	<i>nd</i>	141	21.2	-	-
2011/5/30 - 6/13	270	234	<i>nd</i>	582	2.16	195	216	<i>nd</i>	591	3.02
2011/6/13 - 6/22	75.6	112	<i>nd</i>	-	-	68.6	92.2	<i>nd</i>	-	-
2011/6/22 - 7/18	<i>nd</i>	328	40.7	-	-	<i>nd</i>	270	<i>nd</i>	-	-
2011/7/18 - 7/22	<i>nd</i>	52.9	<i>nd</i>	235	-	<i>nd</i>	13.2	<i>nd</i>	228	-
2011/7/22 - 8/19	<i>nd</i>	96.7	<i>nd</i>	39	-	<i>nd</i>	<i>nd</i>	<i>nd</i>	40	-
2011/8/19 - 10/11	-	-	-	76	-	-	-	-	78	-
Total	8031	2908	120	2472	0.31	7510	2460	95	2483	0.33

* Data adopted from Kato et al. (2012b) and compared with litterfall data.

nd stands for not detected of radiocesium in the sample.

Generally, the observations revealed that wet deposition mechanisms (specifically *TF*) dominates at the early sampling periods, and later on shifted to *LF* dominating pattern. Indeed, the contribution of falling litter pronounced to the extent that exceeds the flux in the *RF* by about a factor of more than two. Similarly, Witkamp and Frank (1964) demonstrated a three-fold increase of radiocesium in forest floor between September 1962 and June 1963 under tagged tulip poplar forest. Further, they showed that the contribution of falling litter raised from 8% (1962) to 42% (1963). In agreement, their result suggests that the radiocesium in tree crown needs time to fall upon the natural schedule of tree phenology.

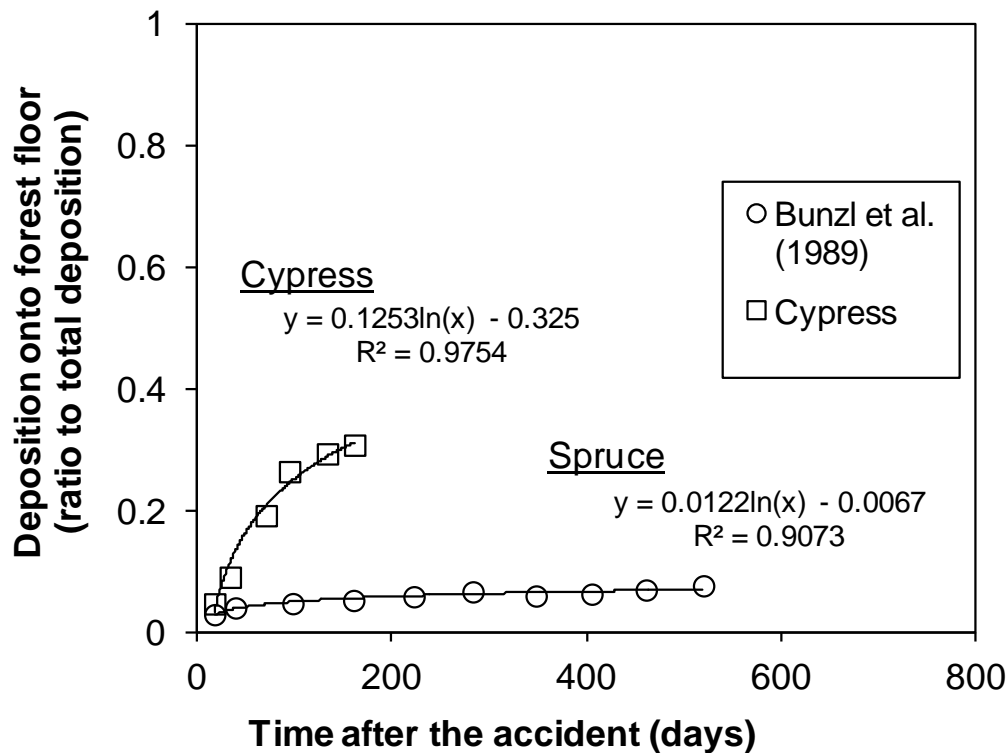


Figure 4.3 Comparison on deposition of radiocesium onto forest floor via literfall route in coniferous forest. The deposition in an old spruce forest was obtained from literature (*Bunzl et al. 1989*) studied immediately after Chernobyl power plant accident (April 1986) and compared to cypress forest investigated following FDNPP accident (March 2011).

Canopy interception ratio:

The cumulative radiocesium deposition ratio onto forest floor through *TF*, *SF* and *LF* was plotted against the time length after the accident and is illustrated in Figure 4.4. It shows that the radionuclides in the canopy were effectively removed and deposited onto the forest floor over time. As discussed above, it is very true that the radiocesium quantity in wet routes is highly reduced during the last observation periods (see Table 4.3). This implies that the retained radiocesium fractions in the canopy are strongly fixed possibly in a non-washable state that made falling litter as the potential transferring route onto forest floor. Taking the fallout deposition via *LF* in to account (Figure 4.4), the retained radiocesium in the canopy reported as more than 60% by Kato et al (2012b) was reduced by half (32 %) at the end the observation period and also lower than the values referred therein. The observed data indicates that the radiocesium deposition in the study forest tends to dominate by wet deposition during active fallout days in which the total precipitation was more than 700 mm (Figure 4.2). It has been indicated that radiocesium interception by tree crowns is much larger and effective for dry than wet deposition (Fraiture, 1992), which is unlikely for Fukushima case that wet deposition dominates (Hirose, 2012). Thus, lower value of retention fraction can be expected of which my result revealed.

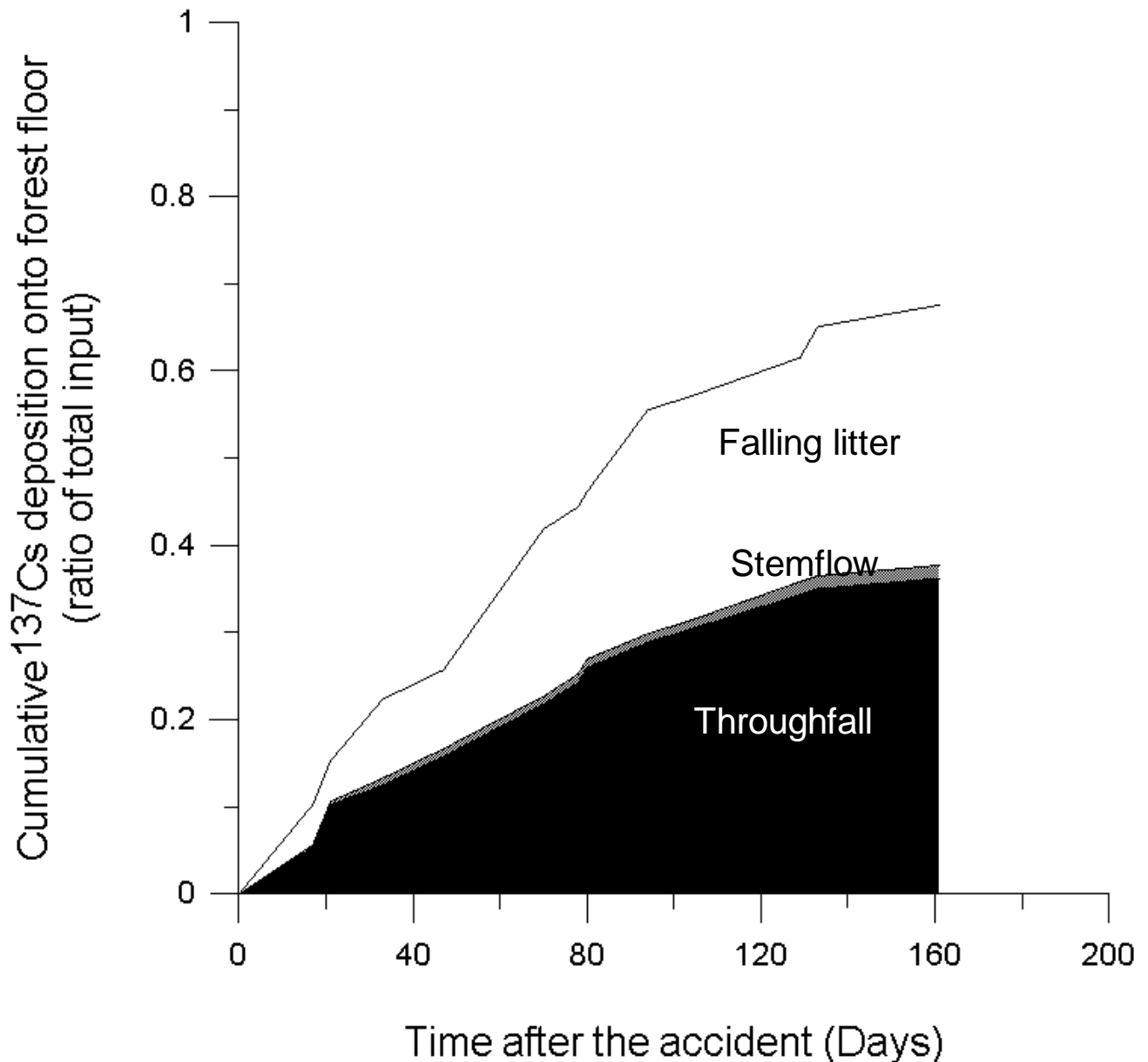


Figure 4.4 Deposition of radiocesium onto forest floor via different routes over time in cypress forest after the FDNPP accident. The net area under each respective curve roughly represents the cumulative deposition of radiocesium by each depositional route.

Half-life of radiocesium in tree canopy:

The half-life of radiocesium in the studied tree canopy for the observation period (160days) was reported as 620 days considering the wet deposition (Kato et al., 2012b). However, its half-life reduced by a factor of 4 (174 days) when *LF* routes is included in the analysis. Despite the

difference in species and site, several studies reported more or less similar half-life values. For example, Bunzl et al. (1989a) in German reported 90 days in spruce crowns for the first 130 days after deposition and 230 days between 131 and 600 observation days. Tobler et al. (1988) from Switzerland estimated its half-life in needle crown to be 115 and 175 days for the observation period of 50 – 240 days after the Chernobyl accident. These data indicate that the half-life of radiocesium tends to increase after the first phase of observation and the same trend can be expected in this study as radiocesium buys time to settle and strongly fixed to the crown structure.

It has been noted that, trees, especially coniferous trees are well known as effective scavengers and efficient interceptor of aerosol and radioactive particles than deciduous and grassland (Alexakhin et al, 1977; Allen, 1984; Bonnett and Anderson 1993; Bunzl and Kracke, 1988; Fesenko et al., 2005; Nimis, 1996; Tikhomirov, 1976). Given the fact that 70% of the Japan land is coniferous dominated mountainous forest (Onda et al., 2010) and this is true for the majority of the contaminated area, litterfall tends to operate as a sole source and a main transfer agent for radiocesium fraction in the canopy into forest floor. This most likely influences the concentration and distribution of radiocesium in the soil and the connected compartments for considerable time period.

4.7.2 Radiocesium in forest soil

Soil physiochemical properties

The soil type along the profile was found to be silt loam with a mean particle size distribution of 9.4 % (SD: 4) sand, 75% (SD: 3.6) silt and 15.6% (SD: 2.9) clay. The silt fraction dominated the soil texture composition in each examined layer, while the clay content showed a general increase with increasing soil depth. The bulk density and sand content showed no definite pattern (Table 4.2).

Organic matter contents of the O1-and Of-layers were 87.2 and 74.4%, respectively. Below these layers, the OM content decreased sharply and continuously with increasing depth. However, the OM content was greater than 10% in all soil layers in the upper 10 cm, with the highest proportion (27%) in the upper 0 – 0.5 cm. The pH of the soil was acidic and ranged from 5.10 to 5.92, showing a slight general increase below 5 cm soil depth (see Table 4.2).

Radiocesium inventory in soil

The total radiocesium inventory of the soil profile was found to be 13 kBq m^{-2} , of which the Fukushima accident contributed approximately 77% (10 kBq m^{-2}). The pre-Fukushima radiocesium in the studied forest was estimated to be 2.6 kBq m^{-2} which is in closed agreement with the reported values that ranges from 2 to 5 kBq m^{-2} (Koarashi et al., 2012; Yamamoto et al., 1983; Sakaguchi et al., 2010). As indicated above in section 4.1, litterfall deposited about 3.1 kBq m^{-2} in to forest floor which accounts for about 24% of the total radiocesium or 31% total Fukushima-derived soil inventory until the time of soil sampling. Spatial variability of soil radioactivity in forest is probably large immediately after fallout (Raitio and Rantavaara, 1994). However, as it can be observed from my data, the cumulative litterfall contribution to soil radiocesium increases and dominates over time (Figure 4.3). Therefore, it is reasonable that the spatial soil radioactivity caused by highly variable initial fallout can be even out in later time and litterfall may be taken as a homogenizing agent of the initial unequal fallout distributions.

Table 4.2 Physiochemical properties in each soil layer

Depth (cm)	Mass depth (kg m^{-2})	Bulk density (g cm^{-3})	Sand (%)	Silt (%)	Clay (%)	OM (%)	pH
Ol	0.7	0.02	-	-	-	87.2	4.93
Of	6.5	0.1	-	-	-	74.4	4.96
0.0 – 0.5	3.8	0.8	16	78	6	26.7	5.12
0.5 – 1.0	1.8	0.4	15	72	13	20	5.49
1.0 – 1.5	2.3	0.5	7	80	13	18	5.19
1.5 – 2.0	2.7	0.5	6	80	14	17	5.27
2.0 – 2.5	2.1	0.4	11	74	15	16	5.14
2.5 – 3.0	4.0	0.8	17	67	16	15	5.39
3.0 – 3.5	2.6	0.5	16	71	13	14	5.10
3.5 – 4.0	3.7	0.7	11	77	12	13	5.17
4.0 – 4.5	3.1	0.6	15	69	16	12	5.17
4.5 – 5.0	5.9	1.2	12	72	17	13	5.37
5.0 – 6.0	8.4	0.8	12	73	14	12	5.52
6.0 – 7.0	6.7	0.7	14	70	16	12	5.36
7.0 – 8.0	3.8	0.4	9	76	15	12	5.64
8.0 – 9.0	9.4	0.9	5	78	16	10	5.39
9.0 – 10	8.7	0.9	4	79	17	10	5.71
10 – 12	11.6	0.6	12	71	17	9	5.92
12 – 14	12.5	0.6	8	74	18	7	5.39
14 – 16	13.5	0.7	8	76	16	5	5.83
16 – 18	14.2	0.7	8	75	17	5	5.67
18 – 20	10.2	0.5	5	76	19	5	5.74
20 – 22	12.7	0.6	4	80	16	5	5.73
22 – 24	11.7	0.6	6	76	18	5	5.77
24 – 26	7.6	0.4	5	76	19	4	5.70
26 – 28	11.4	0.6	5	75	20	5	5.71
28 – 30	13.1	0.7	3	79	18	4	5.70

Radiocesium in forest floor

The forest floor was composed of understory plants (sparsely grown marlberry and other herbs) and the Ol- and Of-horizons. The biomass of the understory vegetation was 0.4 kg m^{-2} . The densities of the Ol- and Of-horizons were 0.7 kg m^{-2} and 6.5 kg m^{-2} , respectively.

Understory vegetation:

The Fukushima-derived radiocesium concentration in understory vegetation was $1.53 \pm 0.07 \text{ kBq kg}^{-1}$, and the TF_w ratio (Bq^{-1} in plant/ Bq kg^{-1} upper soil) was estimated to be 3.3. This implies that the concentration of radiocesium in a given dry-weight understory vegetation is more than three-fold higher than the average concentration found in the soil under consideration. Although I calculated the TF_w ratio for bulked understory plants, my result was slightly higher than the values reported by Zibold et al. (2009) - for ferns (1.2 to 3.2) and considerably different from that of blackberries (0.3 to 0.6). Note that because forest floor was a secondary receiver of radiocesium next to the phytomass at the time of fallout, the observed radiocesium in understory vegetation could be from two possible sources, i.e., via root up take from the forest floor and direct deposition on plant organs. Given that most of the understory vegetation has short lives (annual or biannual plants), it is more likely that the radiocesium entered into a relatively fast turnover phase and formed steady mobilize-remobilizing dynamics in this particular interphase.

Ol- and Of-horizons:

My results indicate that the radiocesium concentrations were the highest in Ol- and Of-layers. The retained fraction, defined as the ratio of inventory at each depth section to that of the total inventory of the soil, showed that the Of-horizon retained 47% of the radiocesium inventory of the soil profile (Table 4.3). Furthermore, the radioactivity in the forest floor is expected to increase in subsequent periods via litterfall as considerable proportion is still held in the canopy. Despite continues recharge of radiocesium by fallen litter from the canopy, only 5% of the total radiocesium content was found in the Ol-horizon at the observation point time. This is probably due to the

transfer of the O_l-horizon to the O_f-horizon through mechanical and biological breakdown (Llaurado et al., 1994; Rafferty et al., 2000) that discharges radiocesium together from fresh and nutrient-rich litters. Another reason could be the radiocesium concentration of the fallen litter is comparatively reducing overtime due to weathering (Bunzl et al., 1989a) and decaying processes at the canopy. However, litterfall likely continues to influence the inventory, vertical migration and subsequent distribution of radionuclides (Agapkina & Tikhomirov, 1991; Karpukhin, 1986; Kaurichev et al., 1977) in a manner similar to the movement of other nutrients.

Comparing my results with Chernobyl's can highlight the differences in the migration of the radiocesium in a forested environment. For example, Ipatyev et al. (1999) from Belarus reported that 96 - 99 % of the radiocesium was in the forest floor and the upper 5 cm of the pine forest soil two years after the accident. Fawaris and Johanson (1994), 5 years after the accident, demonstrated that more than 85% of the total radiocesium was in the top 5 cm of the coniferous forest soil in Sweden. For better contrast, I further compiled radiocesium retention in the litter layers (as a combination of the O_l and O_f- horizon) of previous studies from diverse locations and forest types over different time periods, which are displayed in Table 4.4. The retained ¹³⁷Cs proportion in litter layers varied over forest and soil types. The compiled values in Table 4.4 were plotted as a function of time elapsed between the accidents and sampling periods and are presented in Figure 4.5. It shows a general decline over time, obviously due to loss through ecological processes and physical decay. By comparison with these values, the migration of Fukushima-derived radiocesium in my sampled soil profile seems rapid, with about half of the total inventories already transported below the O_f-horizon in less than a year.

Table 4.3 The retention ^{137}Cs in the litter layer in different locations affected by Chernobyl power plant accident (% of the total soil inventory)

Reference	Location	Tree /forest type	Fallout density (kBq m ⁻²)	Sampling year	Retained ^{137}Cs in litter horizon (%)	Soil type
Witkamp and Frank (1964)	USA	Tulip poplar	-	1963	64	Slightly acid colluvial silt loam
Schimmack and Bunzl (1992)	Germany	Norway Spruce forest	30	April, 1989	85	Parabrown
		Scots pine forest	9	April, 1989	80	Sandy podsol
Tobler et al.(1988)	Switzerland	Norway spruce forest	8	October, 1986	56	Regosol
Tikhomirov et al. (1993)	Ukraine & Belarus	Birch-oak-pine mixed forest	210 - 250	August, 1987	95	Soddy podzolic sandy
				August, 1988	89	Soddy podzolic sandy
				August, 1989	85.3	Soddy podzolic sandy
				August, 1990	80.8	Soddy podzolic sandy
				August, 1991	76.6	Soddy podzolic sandy
Strebl et al.(1996)	Austrian	Norway spruce forest	-	1993	46	Dystric cambisol
Strandberg (1994)	Denmark	Scots pine forest	0.9	October, 1991	20	Podsolic
Melin et al.(1994)	Sweden	Pine forest	180	October, 1990	40	Podsol
Raitio & Rantavaara (1994)	Finland	Norway spruce forest	-	1991	21	-
		Scots pine forest	-	1991	45.5	-
Bunzl et al.(1998)	Germany	Norway spruce forest	20	1990	35	Podzolic parabrown
Fesenko et al.(2001)	Russia	Pine	800 - 2300	1996	8.8	Soddy podzolic loamy sand
		Pine and Birch mixed forest	890 - 2850	1996	12.5	Humic podozol gley loamy sand
		Pine and Birch mixed forest	1600	1996	11.5	Soddy podzolic loamy sand
This study	Japan	Japanese cypress forest	10	January, 2012	52	Orthic brown silt loam

In this comparison litter layer refers a combination of raw and partially fragmented litter layers

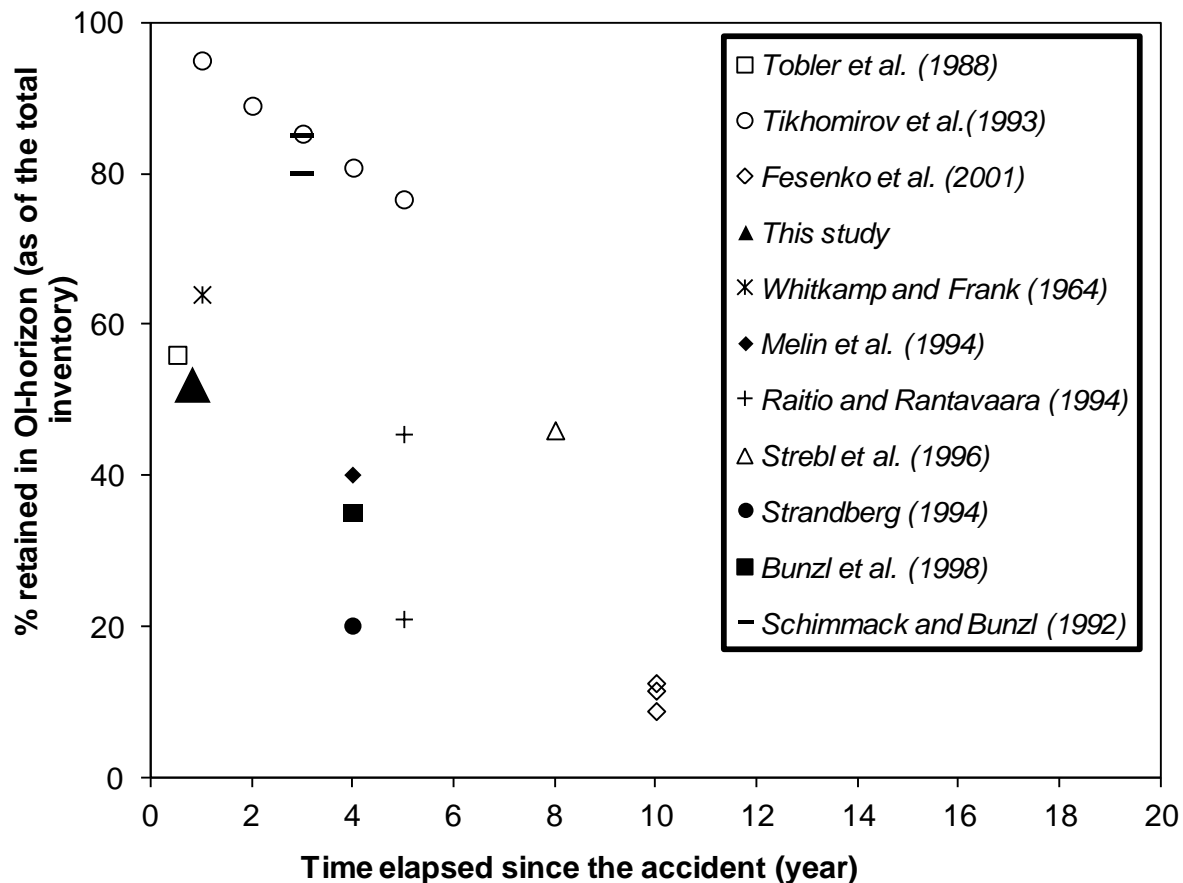


Figure 4.5 Retained ^{137}Cs in litter layer in different forest ecosystems over time. It compares my result to the reported values from different locations that were contaminated by Chernobyl accident (see also Table 4.3)

Generally, the retained fraction of radiocesium in the litter layer seems to depend on the fallout density of the area and the time length after the accident. More specifically, this can be clearly observed on the retained fraction values obtained on similar time length after Chernobyl accident regardless of the site differences such as 20% by Strandberg (1994) from Denmark in pine forest with contamination density of 0.9 kBq m^{-2} ; 40% by Melin et al. (1994) from Sweden in similar pine forest with contamination density of 180 kBq m^{-2} ; 35% by Bunzl et al. (1998) from Germany in spruce forest with a contamination density of 20 kBq m^{-2} ; and 81% by Tikhomirov et al. (1993) from Ukraine in mixed forest with fallout density of $210 - 250 \text{ kBq m}^{-2}$ (see Figure 4.5). Therefore the observed differences may partly be attributed to the variation of deposition density, in

which, the downward migration rate of radiocesium is likely masked, particularly in highly contaminated areas. For example, the fallout density in my study area (10 kBq m^{-2}) is far lower than that of the forested areas affected by Chernobyl, specifically compared to values reported by Tikhomirov et al. (1993), which ranged from $210 - 250 \text{ kBq m}^{-2}$. High radiocesium density in the latter case may contribute to an Ol-layer to be remained highly contaminated for longer time. Further, my result is in close agreement with the value reported from a similar contamination density (8 kBq m^{-2}) and time span after the accident, reported by Tobler et al. (1988) from Switzerland's Norway spruce forested area (see Table 4.4 and Figure 4.5). These provide evidences that the amount of radiocesium deposition density might have influenced the retained radiocesium fraction in an Ol-layer at a given time point. This should be taken in to account when comparing the migration rate in a forested environment.

4.7.3 Depth distribution of radiocesium inventory and Of- horizon

Comparing the ^{137}Cs inventory distribution to that of ^{134}Cs , the distinction between the two isotopes blurred in the upper soil layer but ^{137}Cs started run above ^{134}Cs profile in deeper soil section due to the presence of pre-Fukushima ^{137}Cs (Figure 4.6). The inventory peaks were located in the Of-horizon and then sharply dropped in the depths below, although also some quantity of radiocesium appeared at depths of 16 cm. The radiocesium inventory in the 0-0.5 cm soil layer (i.e., just below the peak) was approximately 3 times lower than that of the Of-horizon. This suggests that after the initial penetration, leaching of the radiocesium from the Of-horizon seems to be a slow process.

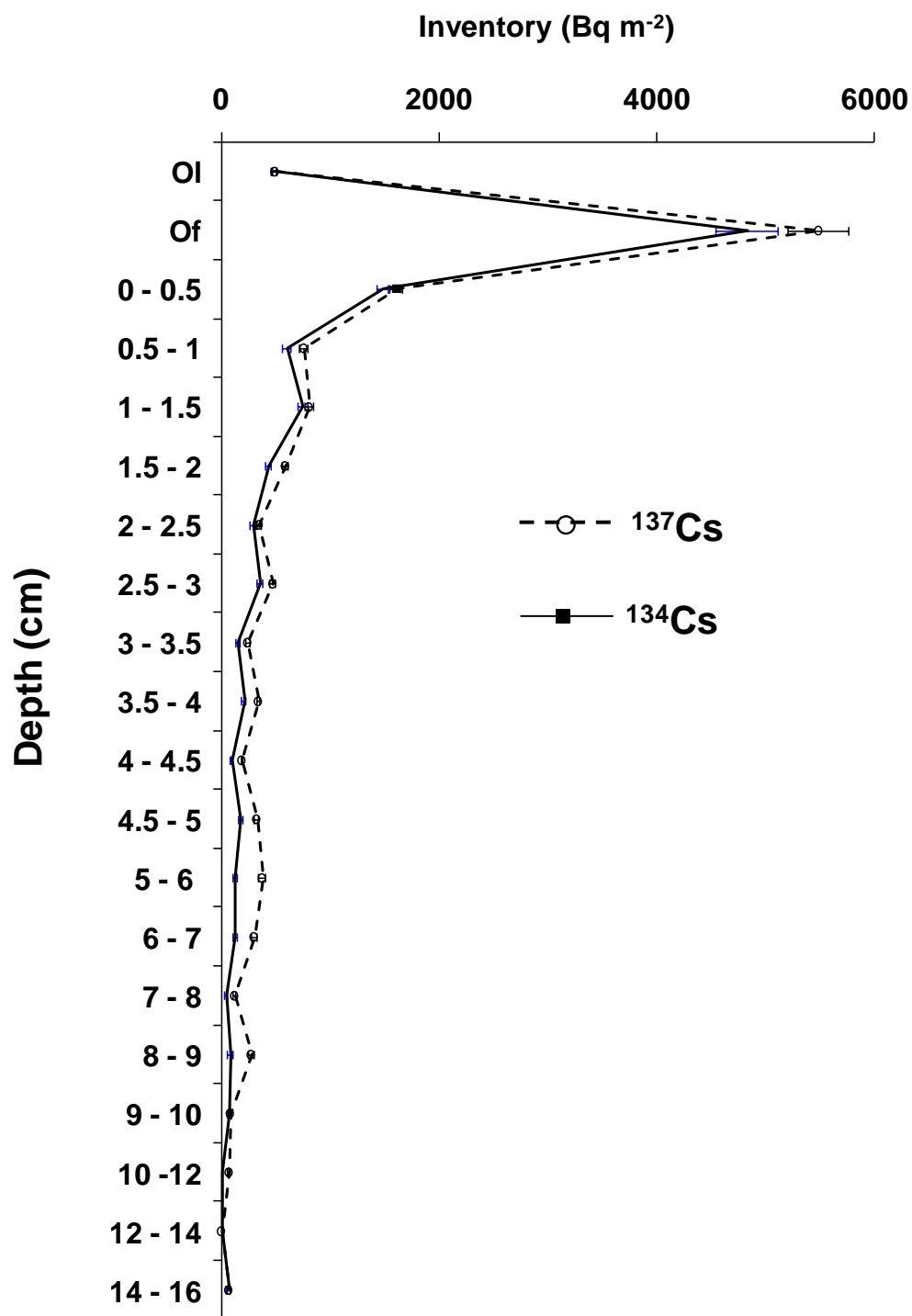


Figure 4.6 The vertical distribution of radiocesium inventory along the soil depth. The position of the peak is at Of -horizon. The ¹³⁷Cs inventory line runs above ¹³⁴Cs inventory more clearly in the deeper soil sections.

In a field study, Rafferty et al., (2000) evaluated the ^{137}Cs migration in a 35-year-old *Pinus contorta* forest stand under the influence of a full year of environmental conditions. They demonstrated that only 1% of ^{137}Cs migrates into mineral soil. In a sequential extractions experiment conducted by Brouwer et al. (1994) also demonstrated that on pure mineral substrate about 40% of the total ^{137}Cs was removed while the same procedure resulted only 8% from organic horizons. Sombre et al. (1994) have also reported similar trends in Spruce and Oak forest from Belgium. Similarly, several authors acknowledged that radiocesium is strongly fixed in the humic layer, which acts as a reservoir for plant uptake and retards the vertical migration in the soil profile of coniferous forest ecosystems (e.g., Fawaris and Johanson, 1994; Thiry and Myttenaere, 1993). These results clearly demonstrate that radiocesium is strongly fixed by organic fraction of soil. In consistent with this, higher proportion of radiocesium in Of-horizon observed in in this study supports and confirms that radiocesium barely leave organic horizons. This tendency is more likely determines the subsequent downward movement and bioavailability of radiocesium to plant roots that explore this soil section.

4.7.4 The distribution of pre-Fukushima ^{137}Cs in soil profile

The average ratio of $^{134}\text{Cs}/^{137}\text{Cs}$ in litter was found to be 1, and the pre-existing ^{137}Cs activities were obtained by deducting the measured ^{134}Cs from that of ^{137}Cs . Figure 4.7 illustrates the depth profile distribution of the total and pre-Fukushima ^{137}Cs . The pre-Fukushima ^{137}Cs peaked at 0.75 cm below the forest floor and tended to dominate in the deeper soil layers. The depth of the peak seems shallow compared to previously reported values as it was measured just below Of-horizon unlike of for example Fukuyama et al. (2010) and Wakiyama et al. (2010).

The pre-Fukushima ^{137}Cs depth distribution exhibited a general decreasing pattern with irregular profile shape (Figure 4.8). The potential reason for this could involve many complex

processes in the soil matrix, including the redistribution of radionuclides by percolating water and

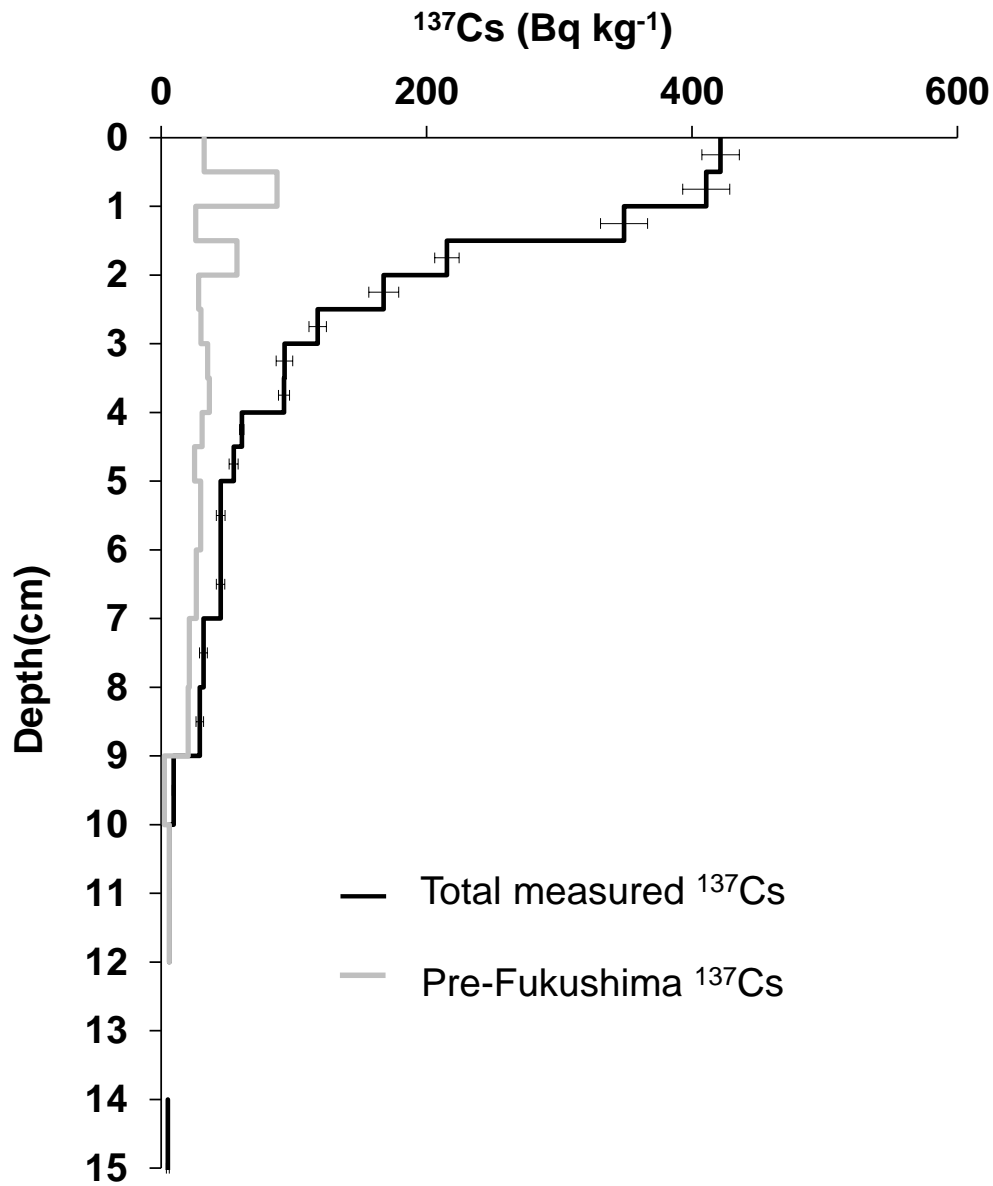


Figure 4.7 Total and pre-Fukushima ^{137}Cs depth distribution profile

bioturbation processes (Fujiyoshi and Sawmura, 2004) that likely cause heterogeneity along the soil depth. Furthermore, within a short depth interval, it has two peaks. The first longer peak appeared at a depth of approximately 0.75 cm, with a ^{137}Cs concentration of 87 Bq kg^{-1} , and the second peak emerged at a depth of 1.75 cm, with a concentration of 57 Bq kg^{-1} . About 10% of the pre-Fukushima radiocesium contained at the depth of 5 - 6 cm in which the first tick soil density (8.4 kg m^{-2}) was found (Figure 4.8 b)

Currently, it is difficult to clearly distinguish the Chernobyl ^{137}Cs from the atomic bomb ^{137}Cs . However, the two distinct peaks can generally represent the migration distance of pre-Fukushima radiocesium fallout events. Taking the displacement of the deeper pre-Fukushima derived ^{137}Cs peak in the soil and the time elapsed since the first radiocesium deposition on the earth surface (1963/1964), its downward velocity in the studied soil can be estimated about 0.4 mm y^{-1} .

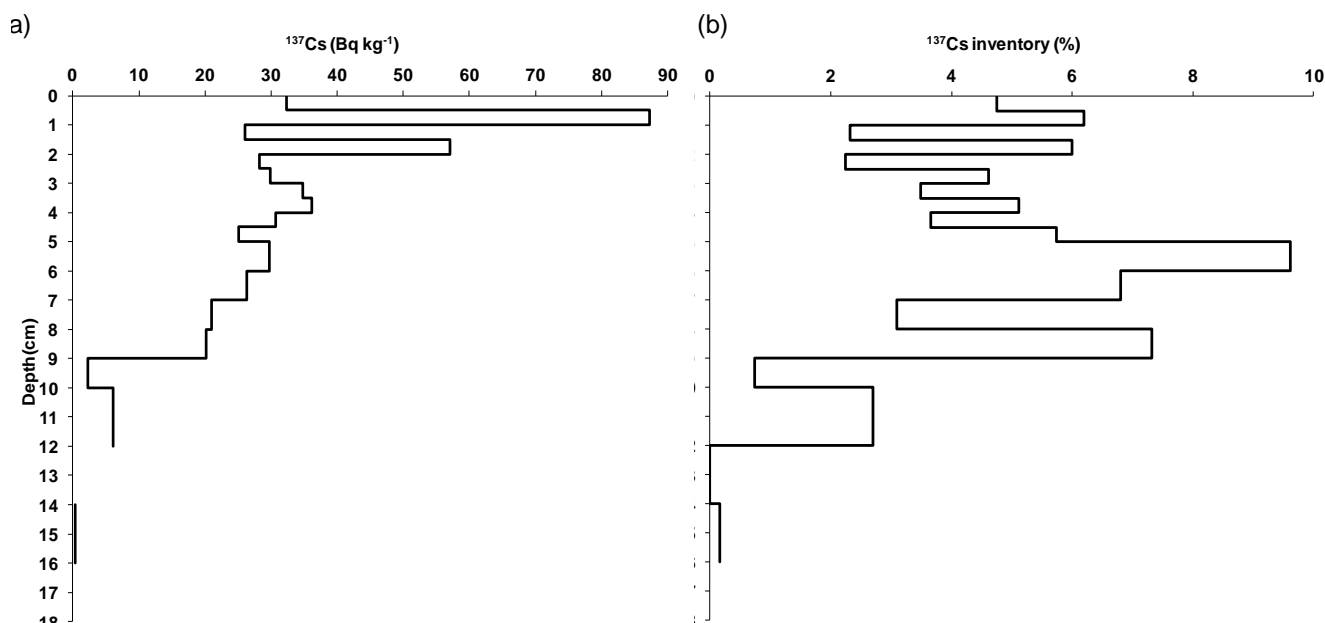


Figure 4.8 Pre-Fukushima ^{137}Cs depth profile (a) concentration distribution; (b) the corresponding inventory proportion

This migration rate is far lower as compared to previously results. For example, Schimmack et al. (1989) reported a long term migration of bomb-derived radiocesium that ranges from 0.7 to 10 mm y^{-1} in different soil layers which were sampled in spruce forest stand and grassland on 7 May 1986. Two decades ago, Dorr and Munnich (1991) reported that the average downward velocity of the bomb ^{137}Cs was 1.8 mm y^{-1} for undisturbed forest soil in Western Europe. Accordingly, pre-Fukushima ^{137}Cs peak in my observation was expected to be relatively deeper than observed in spite

of the likely differences in the study sites but did not. This implies that the downward velocity of pre-Fukushima ^{137}Cs shows no significant change, even after several years.

More interestingly, it was observed that almost all pre-Fukushima ^{137}Cs was contained in a soil layer in which the OM content occupied more than 10%, even after several years of deposition (Table 4.2 and Figure 4.7). Indeed, several researchers have demonstrated that forest soils have a strong tendency to retain radiocesium, and the majority of activities are distributed in organic-rich surface layers. For example, Schimmmack and Bunzl (1992) have reported that even three years after deposition, only 15 – 20% of the radiocesium activity in spruce and pine forest soils is found in upper 10 cm mineral soil while the rest is still in organic layer. Likewise, it seems that the downward migration of the radiocesium depends on the movement of the OM component of the soil, especially via microbial decomposition processes. This stage can be taken as a slow transport phase that is likely lasts from a year to several decades, depending on a set of factors governing the decomposition process. However, Yamaguchi et al. (2012) indicated that in forest and semi-natural ecosystems, large fractions of radiocesium are present in relatively mobile forms due to active biological recycling. This implies that in case of a forested hillslope scenario, the radiocesium active on soil surface can be transported downstream by runoff and has the potential to contaminate the nearby agricultural soils and water resources.

4.7.5 The distribution of Fukushima-origin radiocesium in soil profile

The depth distribution of the total ^{137}Cs concentration ran over the pre-existing ^{137}Cs depth profile line (Figure 4.7). The difference between the two profile shapes may represent the ^{137}Cs activity that originated from FDNPP accident. The general shape of the total ^{137}Cs activity depth profile is similar to those encountered in mostly undisturbed soils (He and Walling, 1997) and can represent the typical depth distribution exhibited in the early stage of fresh fallout.

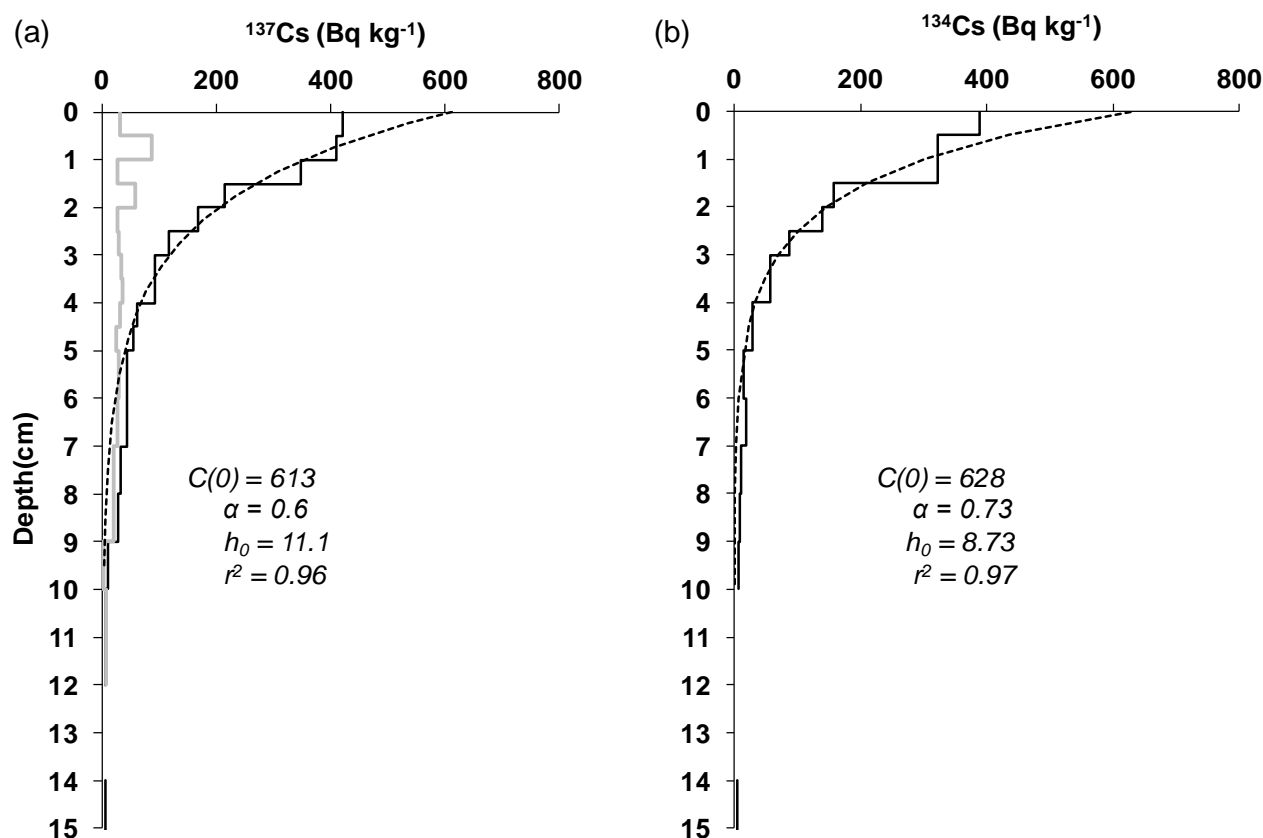


Figure 4.9 Depth distribution of Fukushima-derived radiocesium activity concentration below the Of-horizon of the forest soil; (a) ¹³⁷Cs and (b) ¹³⁴Cs concentrations profile. The black solid line shows the measured, gray solid line shows pre-Fukushima remains and the broken line is the fitting results by Eq.4.1.

The activities of ¹³⁷Cs and ¹³⁴Cs in the uppermost soil layer below the Of-horizon were 422 ± 15 Bq kg⁻¹ and 389 ± 15 Bq kg⁻¹, respectively, and the concentrations decreased with increasing depth (see Table 4.3 and Figure 4.9). This distribution pattern typically reflects the nature of radiocesium adsorption along the depth that the surface organic mat filtered and retained the majority of the radiocesium. The rest gradually attached to soil particles along the profile as the infiltration advanced during the period of fallout.

In fact, small quantities of Fukushima-derived radiocesium were observed in deeper soil layers. This is uncommon for fresh fallout, particularly in the context of the FDNPP accident, in which the fallout occurred during an ecological phase of rest when most biogeochemical processes

were inactive. Therefore, the most likely explanation of the observed fraction in the deeper soil section can be as follows: in stable, flat and organic-rich forest soil, good soil particle aggregates and stable soil structure are expected. This provides well-distributed macro and micro pore spaces for easy water infiltration for enclosed radiocesium. Furthermore, the released radionuclides from FDNPP were dominated by large particles (Hirose, 2012), which in turn require more time to dissolve and expose the radiocesium in ionic form to be fixed to soil particles. Moreover, based on Table 4.2, it is clear that the clay content in the layer beneath the Of-horizon is relatively small (6%), implying that the chance of radiocesium adsorption by clay particles from infiltrated water is low.

Taking this set of practical conditions and the time elapsed since fallout into consideration, it is reasonable to assume that the observed fraction of the radiocesium in the deeper soil was likely driven by radiocesium-circumscribed rainwater in the fallout period. This also implies that fixation of radiocesium in soil requires its own time which might make the process much slower particularly in forest soil (Bunzl et al. 1989*b*). Similarly, Schimmack et al. (1989) showed an unchanged depth distribution value of Chernobyl's radionuclides fallout between their first soil sampling on 13 June 1986 with a precipitation amount 200 mm and their second sample taken 4 months later, with a precipitation of 260 mm. They pointed out that the fraction of radionuclides observed in deeper layers is essentially the result of rain showers during the fallout period, as the later rain barely changed the depth distribution. In fact, this stage can contribute to a rapid initial downward migration (Rafferty et al., 2000) during the fallout period that likely depends on the intensity and duration of precipitation, the soil structure (particularly pore space size and distribution), radiocesium composition and the pre-existing soil moisture. Nevertheless, it cannot be used to describe the long-term radionuclide migration because it lasts only shortly after fallout.

4.7.6 Characteristics of the vertical distribution of radiocesium in soil profile

The vertical distribution behavior of radiocesium was examined based on the estimated coefficient of the parameters in Eq. 4.1 and Eq. 4.2 for soil below the Of-horizon. The value of p in Eq. (4.1) is often chosen to be 1 in most studies. However, Isaksson and Erlandsson (1995) and Karadeniz and Yaprak (2008) have indicated that it can also be 0.75 for a lichen carpet, 2.00 in the case of purely diffusional transport, or even lower for active transport processes. As I dealt with the forest floor separately in the preceding sections, p was chosen as 1, and the empirical data was fitted using Eq. 4.1.

The parameter that represents the inverse of the relaxation length (α) of ^{134}Cs was found to be 0.7 cm^{-1} (Figure 4.9a and b), which was equivalent to a 1.4 cm linear relaxation length. Considering the total ^{137}Cs activity in the soil profile, the value of α was lower, at 0.6 cm^{-1} (or a 1.7 cm relaxation length). Obviously, this difference can be attributed to the present of pre-Fukushima radiocesium. The relaxation mass depths of the Fukushima-derived radiocesium in the study soil profile (h_0 , kg m^{-2}) were determined by Eq. 4.2 and found to be 8.7 and 11.1 kg m^{-2} for ^{134}Cs and the total ^{137}Cs , respectively. The observed small difference in both estimated parameters between the total and Fukushima-derived ^{137}Cs indirectly implies relatively rapid migration of the latter source of radiocesium.

It is hard to compare my results with previous studies in which the reported values are either from agricultural fields or that are conducted several years after the Chernobyl accident. For example, 18 years after Chernobyl accident, Karadeniz and Yaprak (2008) reported relaxation lengths that ranged from 4 to 15 cm with an equivalent relaxation mass depth (h_0) of 56 to 200 kg m^{-2} in slightly acidic, organic-rich undisturbed coniferous forest soil in Turkey. Similarly, 16 years after the Chernobyl accident, Poreba et al. (2003) observed a relaxation length of 2.1 cm ($\alpha = 0.481 \text{ cm}^{-1}$) in acidic soil with an average OM content of 4% in spruce and beach forest soil in Poland.

More recently, Kato et al. (2012a) found relatively higher values of h_0 ($9.1 \text{ kg}\cdot\text{m}^{-2}$) and α (1.2 cm^{-1}) for radiocesium from an untilled (at least since 2010) home garden located 40 km from the crippled FDNPP. Koarashi et al. (2012) have also investigated the distribution Fukushima-derived radiocesium in different land uses conditions including two broadleaf (both Japanese oak) and three coniferous (one Japanese red pine and two Japanese cedar) forests located ~ 70 km from FDNPP. They reported a relaxation length (cm) that ranges from 1.43 to 2.9 and relaxation mass depth (kg m^{-2}) of 7.4 to 10.9 for forest land uses. Given the difference in sampling techniques mentioned earlier, my results are almost in consistent with that of the latter authors. However, the observed slight difference in the profile distribution parameters can be attributed to the sets of difference in the sampling date, land uses and cover type, soil type, precipitation and the like. The differences of these effects are reflected in the value of α , and it can be generalized that the higher the value of the coefficient α , the harder the set of condition for radiocesium to penetrate the soil and vice versa.

4.7.7 Diffusion and migration rates of radiocesium in the soil profile

Unlike the diffusion coefficient (D), which considers the expected depth displacement of the maximum concentration by a factor of $1/e$, the migration rate (v) for young fallout is not noticeable. The values of D and v in this study were approximated based on Eq. 4.3 and 4.4, and the results are illustrated in Table 4.4 with the reported values from literatures, while Figure 4.10 demonstrates the depth position of input parameters used for both pre-Fukushima and Fukushima-derived radiocesium.

As indicated, the linear values of D and v were found to be $1.5 \text{ cm}^2 \text{ y}^{-1}$ and 0 cm y^{-1} for Fukushima-derived cesium, and $0.24 \text{ cm}^2 \text{ y}^{-1}$ and 0.03 cm y^{-1} for pre-Fukushima cesium, respectively (Table 4.4). Specifically, the value of D reflects the lump sum effects of at least three major processes: molecular diffusion, hydrodynamic dispersion and physical mixing (Schimmack

and Marquez, 2006). Further, these authors took soil profiles at ten sampling dates since Chernobyl accident between 1986 and 2001 in undisturbed grassland in Bavaria and demonstrated that the D value generally reduces over time. In a good agreement, higher value of D for Fukushima-derived cesium was observed compared to the pre-Fukushima, suggesting faster diffusion-like downward transportation tends to dominate in my study site in the aftermath of the accident. Rosen et al. (1999) have also reported similar trends for ν -value from Swedish undisturbed grassland soil profiles after Chernobyl accident ($0.5 - 1.0 \text{ cm y}^{-1}$ for the first year and $0.2 - 0.6 \text{ cm y}^{-1}$ thereafter). Moreover, regardless of the influential set of factors that emerge from climatic and site differences, my results are also in consistent with the range of values reported by Almgren and Isaksson, (2006) (Table 4.5) and most of the references therein which were determined based on convection-diffusion equation. These imply that the general trends to be similar in such that higher in first years following the nuclear accident until the adsorption by soil particles begin and slow down then after.

Table 4.4 Values of diffusion and migration coefficients

Derived source	W_p		N_p		ν		D		Reference
	Mass depth	Depth	Mass depth	Depth	$\text{kg m}^{-2} \text{y}^{-1}$	cm y^{-1}	$\text{kg}^2 \text{m}^{-4} \text{y}^{-1}$	$\text{cm}^2 \text{y}^{-1}$	
	(kg m^{-2})	(cm)	(kg m^{-2})	(cm)					
Pre-Fukushima	-	-	-	3.6	0.2 - 1	-	20 - 50	-	Walling et al.(2002)
Pre-Fukushima	-	-	-	-	-	0 - 0.35	-	0.06 - 2.63	Almgren and Isaksson (2006)
Pre-Fukushima	-	-	-	-	-	0 - 0.52	-	0 - 2.7	Schimmack and Marquez (2006)
Pre-Fukushima	5.7	0.75	26.1	4.25	0.2	0.03	8	0.24	This study
Fukushima	3.8	0	12.8	2	0	0	4.5	1.5	This study

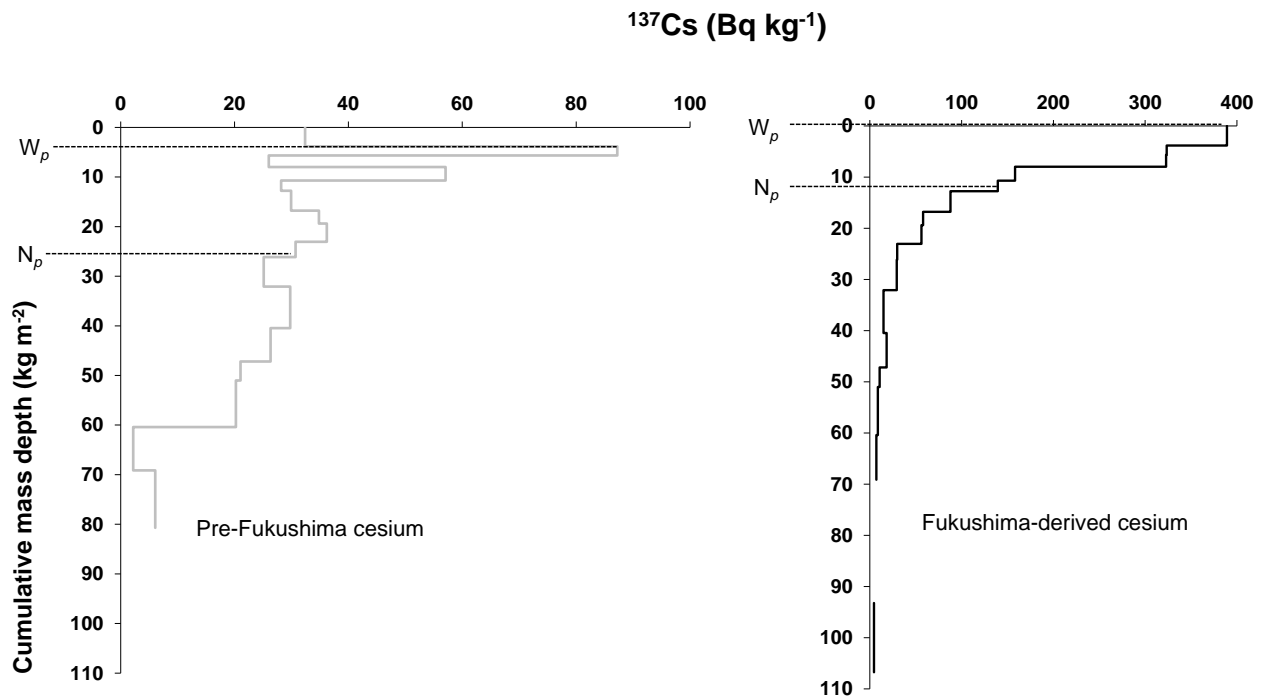


Figure 4.10 Comparative position of the input parameters used for determination of Diffusion (D) and Migration rate (v) coefficients in soil depth profile distribution of Pre- and Fukushima-derived radiocesium.

Combining all the parameters used to describe the depth distribution behavior, it is possible to provide an insight into the vertical migration of radiocesium in the forest environment. However, a considerable proportion (30%) of the radiocesium is still held in the forest canopy. Therefore, the concentration of radiocesium in the forest floor and soil are expected to increase at a slow rate, chiefly through litterfall input. This will affect the subsequent distribution of radiocesium in the forest ecosystem. Schimmack and Marquez (2006) have concluded for a time-series observations that the convection and dispersion coefficients determined from the first years profiles after a nuclear accident could mislead the long term radiation predictions as they depend on time and depth. These difficulties clearly expected to be complicated in forest ecosystem as more complex factors taking part in the process unlike of grassland soils. Therefore, a continuous monitoring and precise predicting models has to be conducted and investigated.

4.8 Conclusions

Given the specific conditions at the time of the FDNPP accident, the deposition of the radionuclides in the forest canopy and forest soil are most likely occurred by a combination of wet and impaction mechanisms. Litterfall depositional route tends to remain the main radiocesium transferring agent in congested forest like in this study. Its influence enhanced in later time and is expected to even out the possible unequal initial fallout. In the forest floor, the understory plants and the upper few centimeters of soil can be taken as an active radiocesium remobilization inter-phase, chiefly due to the short life-span of the plants. Almost all radiocesium activity (99% of the total inventory) was found in the upper ~10 cm in which the OM content was above 10%. The raw organic layer (Ol+Of) holds 52 % of Fukushima-derived at the time of soil sampling and the rest is distributed in soil below Of-layer. Specifically, the Of-horizon tends to accumulate radiocesium (47%) more tightly and retards subsequent migration, implying the dynamics and periodical changes in the Of-horizon will likely determine the migration, the residence time and bioavailability of the radiocesium. In this context, the Of-horizon can be taken as a crucial soil segment in the discipline of forest radioecology, especially for long-lived ^{137}Cs . Such information can help to understand and predict the movement of radiocesium within the forest ecosystem, to estimate radiation dose exposure, to identify sources of contamination to downstream resources and to develop possible countermeasures and environmental baselines.

References

- Agapkina, G.I, Tikhomirov, F.A., 1991. Radionuclide-organic compounds in soil liquors and their role in radionuclide uptake by plants. *Ecologia* **6**, 22 – 28.
- Alexakhin, R.M, Naryshkin, M.A., 1977. Radionuclide Migration in Forest Biogeocenoses. *Nauka* 1977, Moscow.

- Allen, S.E., 1984. Radionuclides in natural terrestrial ecosystems. *Science of the Total Environment* **35**, 285 – 300.
- Almgren, S., Isaksson, M., 2006. Vertical migration studies of ^{137}Cs from nuclear weapons fallout and Chernobyl accident. *Journal of Environmental Radioactivity* **91**, 90 – 102.
- Bonnet, P.J.P., Anderson, M.A., 1993. Radiocesium dynamics in a coniferous forest canopy: a mid-wales case study. *Science of the Total Environment* **136**, 259 – 277.
- de Brouwer, S., Thiry, Y., Myttenaere, C., 1994. Availability and fixation of radiocesium in forest brown acid soil. *Science of the Total Environment* **143**, 183 – 191.
- Bunzl, K., Kracke, W., 1988. Cumulative deposition of ^{137}Cs , ^{238}Pu , $^{239+240}\text{Pu}$ and ^{241}Am from global fallout in soils from forest, grassland and arable land in Bavaria (FRG). *Journal of Environmental Radioactivity* **8**, 1 – 14.
- Bunzl, K., Kracke, W., Schimmack, W., Zelles, L., 1998. Forms of fallout ^{137}Cs and $^{239+240}\text{Pu}$ in successive horizons of forest soil. *Journal of Environmental Radioactivity* **39** (1), 58 – 68.
- Bunzl K, Schimmack, W, Kreutzer, K, Schierl, R., 1989a. Interception and retention of Chernobyl-derived ^{134}Cs , ^{137}Cs and ^{106}Ru in Spruce stand. *Science of the Total Environment* **78**, 77 – 87.
- Bunzl, K, Schimmack, W, Kreutzer, K, Schierl, R., 1989b. The migration of fallout ^{134}Cs , ^{137}Cs and ^{106}Ru from Chernobyl and of ^{137}Cs from weapons testing in forest soil. *Z.pflanzenernaehr. Bodenk.*, **152**, 39 – 44.
- Calmon, P, Thiry, Y, Zibold, G, Rantavaara, A, Fesenko, S., 2009. Transfer parameter values in temperate forest ecosystems: a review. *Journal of Environmental Radioactivity* **100**, 757 – 66.
- Dorr, H, Munnich, O.K., 1991. Lead and Cesium transport in European Forest soils. *Water, air, and Soil Pollution* **57 - 58**, 809 – 18.

- Fawaris, B. H, Johanson, K.J., 1994. Radiocesium in soil and plants in a forest in central Sweden. *Science of the Total Environment* **157**, 133 – 38.
- Fesenko, S.V, Soukhova, N.V, Sanzharova, N.I, Avila, R, Spiridonov, S.I, Klein D, et al. 2001. Identification of processes governing long-term accumulation of ^{137}Cs by forest trees following the Chernobyl accident. *Radiation and Environmental Biophysics* **40**, 105 – 13.
- Fesenko, S.V, Voigt G., Spiridonov, S.I., Gontarenko, I.A, 2005. Decision making frameworks for application of forest countermeasures in the long term after the Chernobyl accident. *Journal of Environmental Radioactivity* **85**, 143 - 166 – 66.
- Fraiture, A., 1992. Introduction to the Radioecology of Forest Ecosystems and Survey of Radioactive Contamination in Food Products from Forests. *Commiss. Eur. Comm., Rad. Prot. Rep.***57**, 1 - 103.
- Fujiyoshi, R, Sawamura, S., 2004. Mesoscale Variability of vertical profiles of environmental radionuclides (^{40}K , ^{226}Ra , ^{210}Pb and ^{137}Cs) in temperate forest soils in Germany. *Science of the Total Environment* **320**, 177 – 88.
- Fukuyama, T., Onda, Y., Gomi, T., Yamamoto, K., Kondo, N., Miyata, S., Kosugi, K, Mizugaki, S., Tsubonuma, N., 2010. Quantifying the impact of forest management practice on the runoff of the surface-derived suspended sediment using fallout radionuclides. *Hydrological Processes* **24**, 596 – 607.
- Gomi, T, Sidle, R.C, Richardson, J.S., 2002. Understanding processes and downstream linkages of head water systems. *Journal of BioScience* **52** (10), 905 – 16.
- Hashimoto, S., Ugawa, S., Nanko, K., Shichi, K., 2012. The total amounts of radioactively contaminated materials in forests in Fukushima, Japan. *Scientific Reports* **2**, 416; doi: 10.1038/srep00416

- He, Q., Walling, D.E., 1997. The distribution of fallout ^{137}Cs and ^{210}Pb in undisturbed and cultivated soils. *Applied Radioactivity Isotopes* **48**, 677 – 90.
- Hirose, K., 2012. 2011 Fukushima dai-ichi nuclear power plant accident: Summary of regional radioactive deposition monitoring results. *Journal of Environmental Radioactivity* **111**, 13 - 17.
- IAEA, 2010. Handbook of parameter values for the prediction of radionuclide transfer in terrestrial and freshwater environments. *Technical Reports Series* **472**, 1–194
- Ipatyev, V, Bulavik I, Baginsky V, Goncharenko G, Dvornik A.,1999. Forest and Chernobyl: forest ecosystems after the Chernobyl nuclear power plant accident: 1986 -1994. *Journal of Environmental Radioactivity* **42**, 9 – 38.
- Isaksson, M., Erlandsson, B., 1995. Experimental determination of the vertical and horizontal distribution of ^{137}Cs in the ground. *Journal of Environmental Radioactivity* **27** (2), 141–160.
- Karadeniz, O, Yaprak, G., 2008. Vertical distribution and gamma dose rates of ^{40}K , ^{232}Th , ^{238}U and ^{137}Cs in the selected forest soils in Izmir, Turkey. *Journal of Radiation Protection Dosimetry*, **1 – 10**, doi:10.1093/rpd/ncn185.
- Karpukhin, Al., 1986. Complexes of organic matter with some metal ions. *Doctoral Thesis*, Moscow.
- Kaurichev, I.S, Karpukhin, A.I, Stepanova, L.V., 1977. Qualitative composition of water-soluble organic compounds in the soil water. *Doklady TSKhA* **253**, 53 –5.
- Kato, H, Onda, Y, Teramage, M., 2012a. Depth distribution of ^{137}Cs , ^{134}Cs and ^{131}I in soil profile after Fukushima Daiichi Nuclear power plant accident. *Journal of Environmental Radioactivity* **111**, 59 –64.
- Kato, H, Onda, Y, Gomi, T., 2012b. Interception of the Fukushima reactor accident-derived ^{137}Cs , ^{134}Cs and ^{131}I by coniferous forest canopies. *Geophys. Res. Lett* **39**, L20403, doi:10.1029/2012GL052928.

- Koarashi, J., Atarashi-Andoh, M., Matsunaga, T., Sato, T., Nagao, S., Nagai, H., 2012. Factors affecting distribution of Fukushima accident-derived radiocesium in soil under different land-use conditions. *Science of the Total Environment* **431**,392 – 401.
- Kruyts, N, Titeux, H, Delvaux, B., 2004. Mobility of radiocesium in three distinct forest floors. *Science of the Total Environment* **319**, 241 – 52.
- Livens, F.R, Fowler, D, Horrill, A.D., 1992. Wet and dry deposition of ^{131}I , ^{134}Cs and ^{137}Cs at an upland site in northern England. *Journal of Environmental Radioactivity***16**, 243 – 54.
- Llaurado, M., Vidal, M., Rauret, G., Roca, C., Fons, J., Vallejo, V.R., 1994. Radiocesium behavior in Mediterranean conditions. *Journal of Environmental Radioactivity* **23**, 81 – 100.
- Loughran, R.J, Wallbrink, P.J, Walling, D.E, Appleby, P.G., 2002. Chapter 3: Sampling method. In: Zapata, F.,editor. Handbook for the Assessment of Soil Erosion and Sedimentation using Environmental Radionuclides. The Netherlands: Kluwer Academic Publishers; p. 41 – 57.
- Maguire, D.A., 1994. Branch mortality and potential litterfall from Douglas-fir trees in stands of varying density. *Forest Ecology and Management* **70**, 41 – 53.
- Melin, J., Wallberg, L., Suomela, J., 1994. Distribution and retention of cesium and strontium in Swedish boreal forest ecosystems. *Science of the Total Environment* **157**, 93 – 105.
- MEXT, 2011. Ministry of Education, Culture, Sports, Science and Technology, Japan (MEXT). Corrections to the Readings of Airborne Monitoring Surveys (Soil Concentration Map) based on the Prepared Distribution Map of Radiation Doses, etc. By MEXT. <http://radioactivity.mext.go.jp/old/en/1270/2011/08/1270_083014-2.pdf> (accessed 29 November 2011).
- Nimis, P.L., 1996. Radiocesium in plants of forest ecosystems. *Studia Geobotanica* **15**, 3 – 49.

- Onda, Y, Gomi, T, Mizugaki, S, Nonoda, T, Sidle, R., 2010. An overview of the field and modeling studies on effects of forest devastation on flooding and environmental issues. *Hydrological Processes* **24**, 527 –534.
- Poreba, G, Bluszcz, A, Snieszko, Z., 2003. Concentration and vertical distribution of ^{137}Cs in agricultural and undistributed soil from Chechlo and Czarnocin areas. *Journal on Methods and application of Absolute Chronology* **22**, 67 – 72.
- Porto, P., Walling. D.E., Ferro, V., 2001. Validating the use of caesium -137 measurements to estimate soil erosion rates in a small drainage basin in Calabria, Southern Italy. *Journal of Hydrology* **248**, 93 – 108.
- Rafferty, B, Brenna, M, Dawson, M, Dowding, D., 2000. Mechanism of ^{137}Cs migration in coniferous forest soils. *Journal of Environmental Radioactivity* **48**, 131 – 43.
- Raitio, H., Rrantavaara, A., 1994. Airborn radiocesium in Scots pine and Norway spruce needles. *Science of the Total Environment* **157**, 171 – 180.
- Rosen, K., Oborn, I., Lonsjo, H., 1999. Migration of radiocesium in Swedish soil profiles after Chernobyl accident, 1986 – 1995. *Journal of Environmental Radioactivity* **46**, 45 – 66.
- Sakaguchi, A., Kawai, K., Steier, P., Imanaka, T., Hoshi, M., Endo, S., Zhumadilov, K., Yamamoto, M., 2010. Feasibility of using ^{236}U to reconstruct close-in fallout deposition from the Hiroshima Atomic Bomb. *Science of the Total Environment* **408**, 5392 – 5398.
- Schimmack, W, Bunzl, K., 1992. Migration of radiocesium in two forest soils as obtained from field and column investigations. *Science of the Total Environment* **116**, 93 – 107.
- Schimmack, W, Bunzl, K, Zelles, L., 1989. Initial rates of migration of radionuclides from the Chernobyl fallout in undisturbed soils. *Geoderma* **44**, 211 – 18.

- Schimmack, W, Marquez, F.F., 2006. Migration of fallout radiocesium in grassland soil from 1986 to 2001; Part II: Evaluation of activity-depth profiles by transport models. *Science of the Total Environment* **368**, 863 – 874.
- SCJ. 2011. Report to the foreign academies from Science Council of Japan (SCJ) on Fukushima daiichi nuclear power plant accident. <<http://www.scj.go.jp/en/index.html>>(accessed 1 July 2011).
- Sombre, L., Vanhouche, M., de Brouwer, S., Ronneau, C., Lambotte, J.M., Myttenaere, C., 1994. Long-term radiocesium behavior in spruce and Oak forests. *Science of the Total Environment* **157**, 59 – 71.
- Strandberg, M., 1994. Radiocesium in a Danish pine forest ecosystem. *Science of the Total Environment* **157**, 125 – 132.
- Strebl, F., Gerzabek, M.H., Karg, V., Tataruch, F., 1996. ¹³⁷Cs-migration in soil and its transfer to roe deer in an Austrian forest stand. *Science of the Total Environment* **181**, 237 – 247.
- Tobler, L, Bajo, S, Wytttenbach, A., 1988. Deposition of ^{134,137}Cs from Chernobyl fallout on Norway spruce and forest soil and its incorporation in to spruce twigs. *Journal of Radioactivity* **6**, 225 – 45.
- Thiry, Y, Myttenaere, C., 1993. Behavior of radiocaesium in forest multilayered soils. *Journal of Environmental Radioactivity* **18**, 247 – 57.
- Thiry, Y, Goor F, Riesen T., 2002. The true distribution and accumulation of radiocesium in stem of Scots pine (*Pinus sylvestris* L.). *Journal of Environmental Radioactivity* **58**, 243–59.
- Tikhomirov, F.A., 1976. Radioecological problems in forest biogeocenoses; Biological effects of low doses of ionizing irradiation. *Syktvykar* **70** - 85.
- Tikhomirov, F.A, Shcheglov, A.I., 1994. Main investigation results on the forest radioecology in the Kyshtym and Chernobyl accident zones. *Science of the Total Environment* **157**, 45 – 57.

- Tikhomirov, F.A, Shcheglov, A.I, Sidorov, V.P., 1993. Forests and forestry: radiation protection measures with special reference to Chernobyl accident zone. *Science of the Total Environment* **137**, 289 – 305.
- Wakiyama, Y., Onda, Y. Mizugaki, S. Asai, H., Hramatsu, S., 2010. Soil erosion rates on forested mountain hillslopes estimated using ^{137}Cs and $^{210}\text{Pb}_{\text{ex}}$. *Geoderma* **159**, 39 – 52.
- Walling, D.E, He, Q, Appleby, P.G., 2002. Conversion models for use in soil-erosion, soil-redistribution and sedimentation investigations. In: Zapata, F. (Ed.), *Handbook for the Assessment of Soil Erosion and Sedimentation using Environmental Radionuclides*. Kluwer Academic Publishers, Dordrecht, Netherlands, pp. 111– 64.
- Witkamp, M., Frank, M.L., 1964. First year movement, distribution and availability of ^{137}Cs in the forest floor under tagged Tulip Poplars. *Radiation Botany* **4**, 485 – 495.
- Yamaguchi, N, Takata, Y, Hayashi, K, Ishikawa, S, Kuramata, M, Eguchi, S, et al., 2012. Behavior of radiocesium in soil-plant system and its controlling factor: A review. *Bulletin of National Institute for Agro-environmental Sciences* **31**, 75 –129 (in Japanese with English abstract).
- Yamamoto, M., Komura, K., Sakanoue, M., 1983. ^{241}Am and Plutonium in Japanese rice-field surface soils. *Journal of Radiation Research* **24**, 237–249.
- Zibold, G, Klemt, E, Konopleva, I, Konoplev, A., 2009. Influence of fertilizing on the ^{137}Cs soil-plant transfer in a spruce forest of Southern Germany. *Journal of Environmental Radioactivity* **100**, 489 – 96.

Chapter 5: The use of ^{134}Cs : ^{137}Cs ratio to trace the migration of surface materials since the Fukushima accident

5.1 Introduction

The introduction of radiocesium to the environment, particularly short-lived ^{134}Cs ($t_{1/2} = 2.1$ year), following the Fukushima nuclear power accident on 11 March 2011, leaves an opportunity to have additional and further analysis on environmental processes. More specifically, since the existing ^{134}Cs is only from Fukushima, it could make it possible to study more recent process that occurred since the accident such as soil forming process.

In forested ecosystem, radiocesium temporary trapped by forest canopy and later-on reach to forest floor through different mechanism (e.g Bunzl et al., 1989; Bonnett and Anderson, 1993; Kato et al., 2012). Falling litter is vital for the productivity of forest land and major component of global carbon and other nutrient cycle (Aerts, 1997; Couteaux et al., 1995; Prescott, 2005; García-Palacios et al. 2013). However, Braakhekke et al. (2013) have reported that the current lack of understanding of soil system forms is a bottleneck and sources of uncertainty in terrestrial carbon cycle predictions. In forest, soil organic matters are supplied by litter upon decomposition through biological activities that destruct plant litter constituents. Then the materials migrates in solid and solution down to mineral soil matrix which results a typical and basic sequence of soil horizons as O_l, O_f, O_h and A. This process affects the organic and upper soil horizons thereby affect the migration and distribution of radionuclides that has been absorbed and adsorbed with litter and migrate together along the soil profile (Figure 5.1). Hence, radionuclides may be more effective to understand the process because of two major advantages. Firstly, loss through radioactive decay is constant and can be exactly calculated and corrected. Secondly, inputs occur only at the soil surface, no direct input at the depth

unlike of, for example of carbon isotopes (^{13}C & ^{14}C – commonly used to study such process) via root.

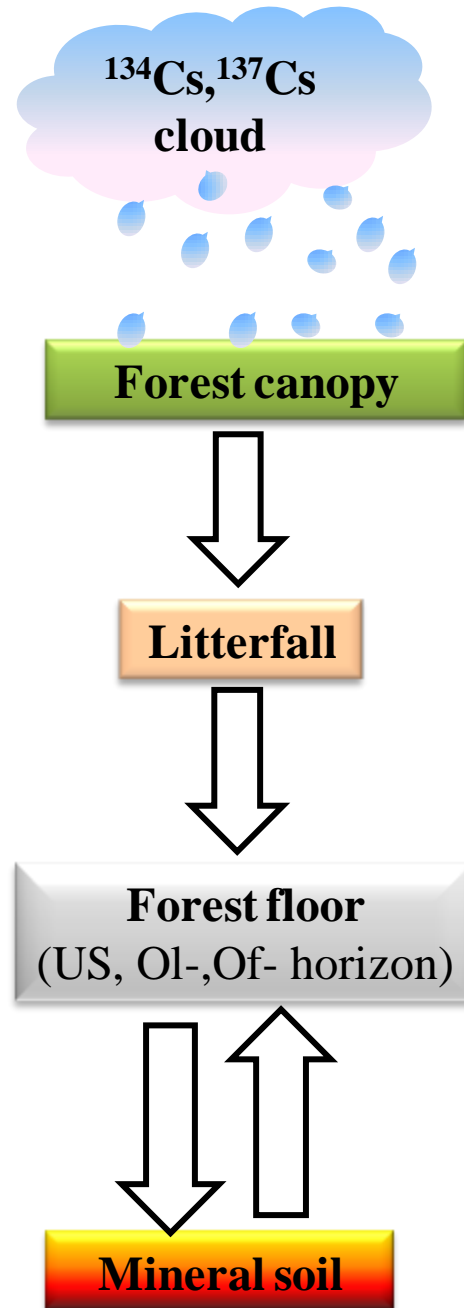


Figure 5.1 Simple pictorial model representing radiocesium depositions via litterfall and its subsequent possible pathways in stable site. (*US*: understory vegetation; *Ol*:- litter horizon and; *Of*:- fermented horizon)

Therefore, it is very reasonable to hypothesize that “Fukushima-derived $^{134}\text{Cs}:$ ^{137}Cs ratio can be used to trace the recent migration of surface organic materials therein SOC along the soil profile in stable site”. The hypothesis bases on the following assumption and consideration: (1) the total radiocesium initially deposited and remained completely in the first layer and propagated later-on as litter does. (2) ^{134}Cs is only originated from Fukushima accident. (3) In the deeper soil layer the ratio is low due to the presence of the remnants of pre-Fukushima ^{137}Cs (Figure 5.2). (4) Although both cesium have different half-life and decaying rate, their decay corrected ratio is relatively constant. For example, Ruhm et al. (1997) have successfully located the location of fungi mycelium in forest soil horizon by matching the $^{137}\text{Cs}:$ ^{134}Cs ratio in fungi collected from forest floor to the ratio in different soil horizons. With similar analog, if the $^{134}\text{Cs}:$ ^{137}Cs ratio is tend to be higher in association with increasing organic matter at the specific soil horizon, it can be reasonably inferred that it is due to the migration of cesium coded surface material since the introduction of ^{134}Cs .

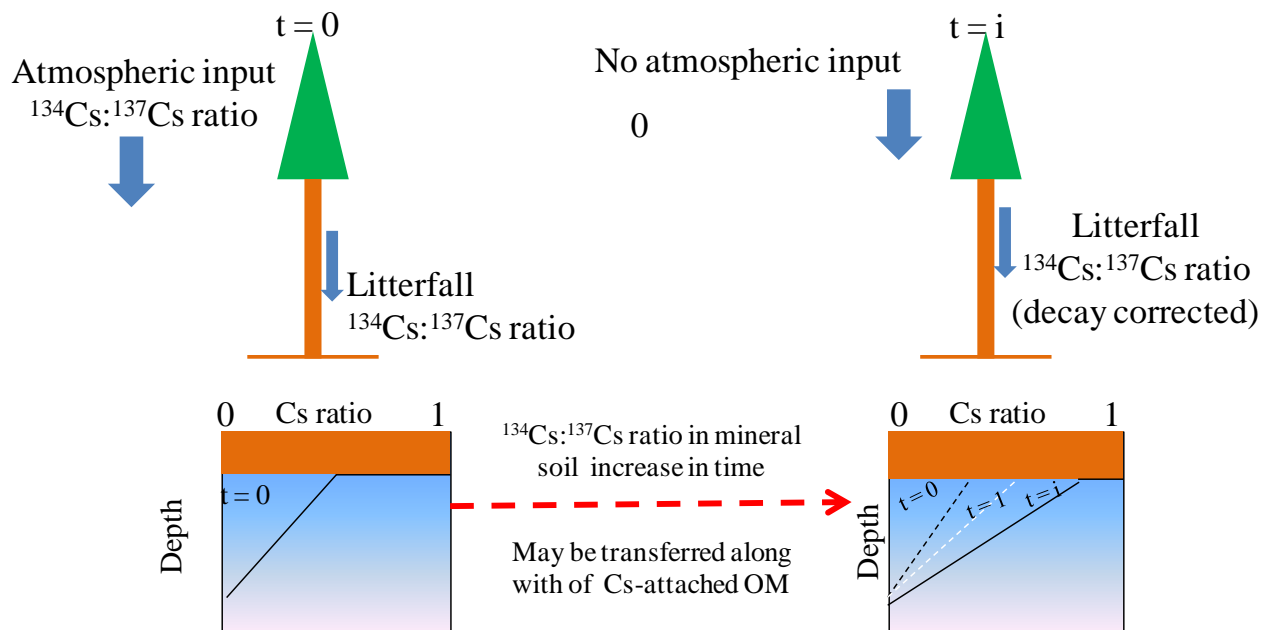


Figure 5.2 Expected $^{134}\text{Cs}:$ ^{137}Cs ratio over time along the vertical strata of forest

The objective of present study is therefore to evaluate the hypothesis that $^{134}\text{Cs}:^{137}\text{Cs}$ ratio can be a useful tool to trace the migration of surface organic material along soil profile.



Figure 5.3 The model of initial theory. The direction of arrows shows the trends of the level. (OM stands for organic matter)

5.2 Study site

The study was conducted in the same area of Chapter 4 in a 30-year-old Japanese cypress (*Chamaecyparis obtusa* Endl.) plantation forest stand located on Karasawa yama (139°44' E; 36°23' N), Tochigi prefecture (Figure 5.4). The area is located 180 km southwest from the crippled FDNPP. The size of the catchment is 0.8 ha. This mountainous catchment is not only known for its economic and environmental importance but also often visited by hikers from the surrounding society. After the FNPP accident, the contamination density of the area was reported about 8 kBq m^{-2} (Kato et al., 2012)

The climate of the area is humid temperate, with 1,259 mm mean annual rainfall and 14.1°C mean annual temperature. The soil type can be classified as an Orthic cambisols. The estimated stand density is approximately 2,500 trees per hectare. The forest floor is composed of sparsely grown marlberry (*Ardisia japonica* (Thunb.) Blume), herbs, and fallen broad and needle leaf litters.

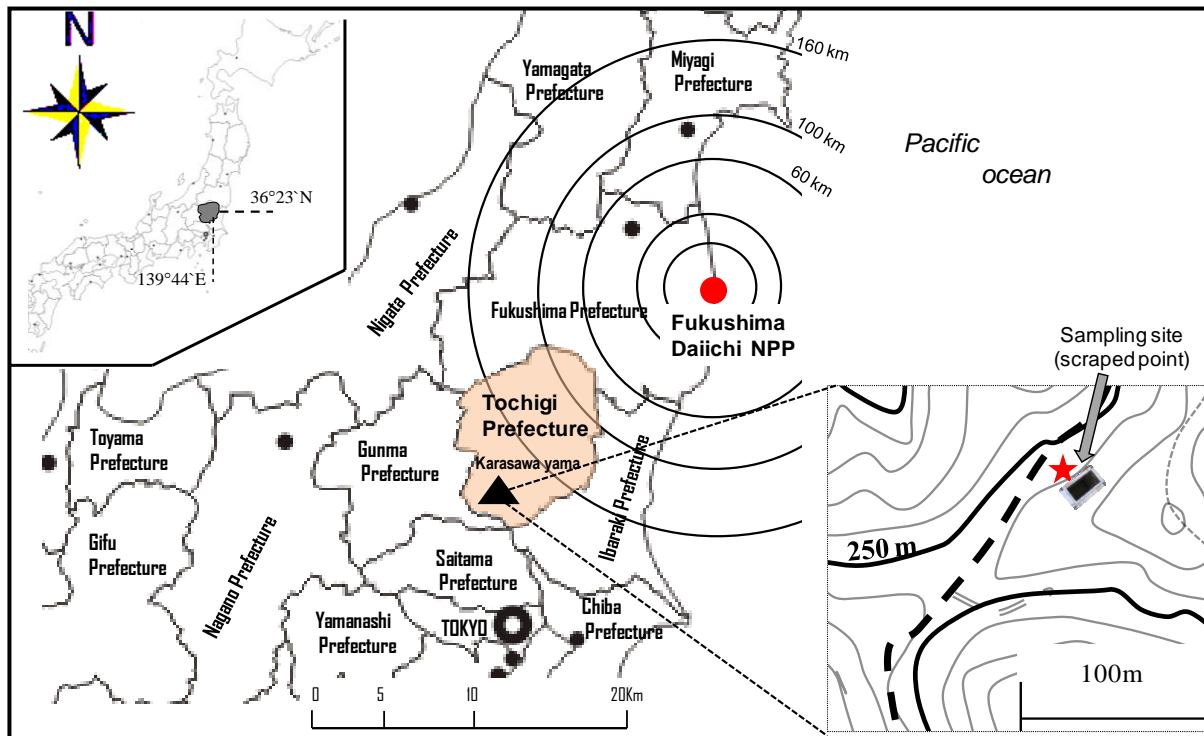


Figure 5.4 Map of the study area and location of the sampling point

Thinning was carried out within the observation period that put-off the experiment for about 24 days (11 October 2011 to 04 November 2011). Strip thinning with 50% thinning intensity was employed in a pattern that left-off every two tree lines in alternative fashion and reduced the tree density by half. The instruments were reinstalled again on 4 November 2011 and the experiment has been resumed again.

5.3 Materials and methods

5.3.1 Litterfall sampling

For the purpose of mentoring litterfall (*LF*) flux, four nylon nets with 1 m² area (each) litter-traps were suspended about 1m above the ground (Figure 5.5) on the representative location of the study catchment about seven months before the accident (installed on 03August 2010). Following the Fukushima nuclear power plant accident, the litter traps' data was used to measure radiocesium deposition along with litterfall. This gave an exceptional opportunity to measure litter-derive

radiocesium deposition starting from the very beginning. Litter traps were emptied regularly and the radiocesium activities were determined as a litterfall mass weighted mean activity from four replications to account for the observed differences in *LF* mass during the observation period. The values are used to determine the ^{134}Cs : ^{137}Cs ratio in the falling litter as well as to estimate the total radiocesium deposition onto forest floor via this route.

5.3.2 Soil sampling

Soil samples were collected at an undisturbed flat area to minimize the effect of subsequent movement of radionuclides by runoff after fallout. Scraper soil sampling was carried out for four consecutive sampling dates between January and October 2012. The sampling points were purposely selected at the midpoints between tree lines to make it more representative and reduce the effect of coarse roots during sampling. I used a rectangular metal-framed scraper plate (internal dimensions of 15 cm x 30 cm) with an adjustable depth increment of 5 and 10 mm intervals. With this sampling scheme, I carefully separated understory vegetation and O_l- (~3 cm thick) and O_f- (~4.5 cm thick) horizons that were collected by hand and scissors (when necessary) to represent the forest floor. The understory vegetation was dominated by sparsely grown marlberry and annual herbs. The O_l-horizon represented an organic horizon of litter in which the original shape of the components was easily recognizable and was composed of and built by periodically falling raw litter. The O_f-horizon was an organic horizon located under the O_l-horizon which was composed of an early fermented and fragmented litter component in which the original shapes of the litter were difficult to identify (Figure 5.5).



Figure 5.5 Photographs of the components of forest floor collected during soil sampling

The soil below the Of-horizon was scraped layer by layer in three major depth resolutions of 5, 10 and 20 mm. Although a 1 cm depth increment is recommended for the investigation of the ^{137}Cs depth profile (Loughran et al., 2002), I employed a depth increment of 0.5 cm for the highly contaminated upper 5.0 cm soil layer. Then, the depths of soil from 5 to 10 cm and from 10 to 30 cm were sliced every 1.0 and 2.0 cm intervals, respectively (Figure 5.6). In the sampling depth, neither cracks nor big roots were encountered.

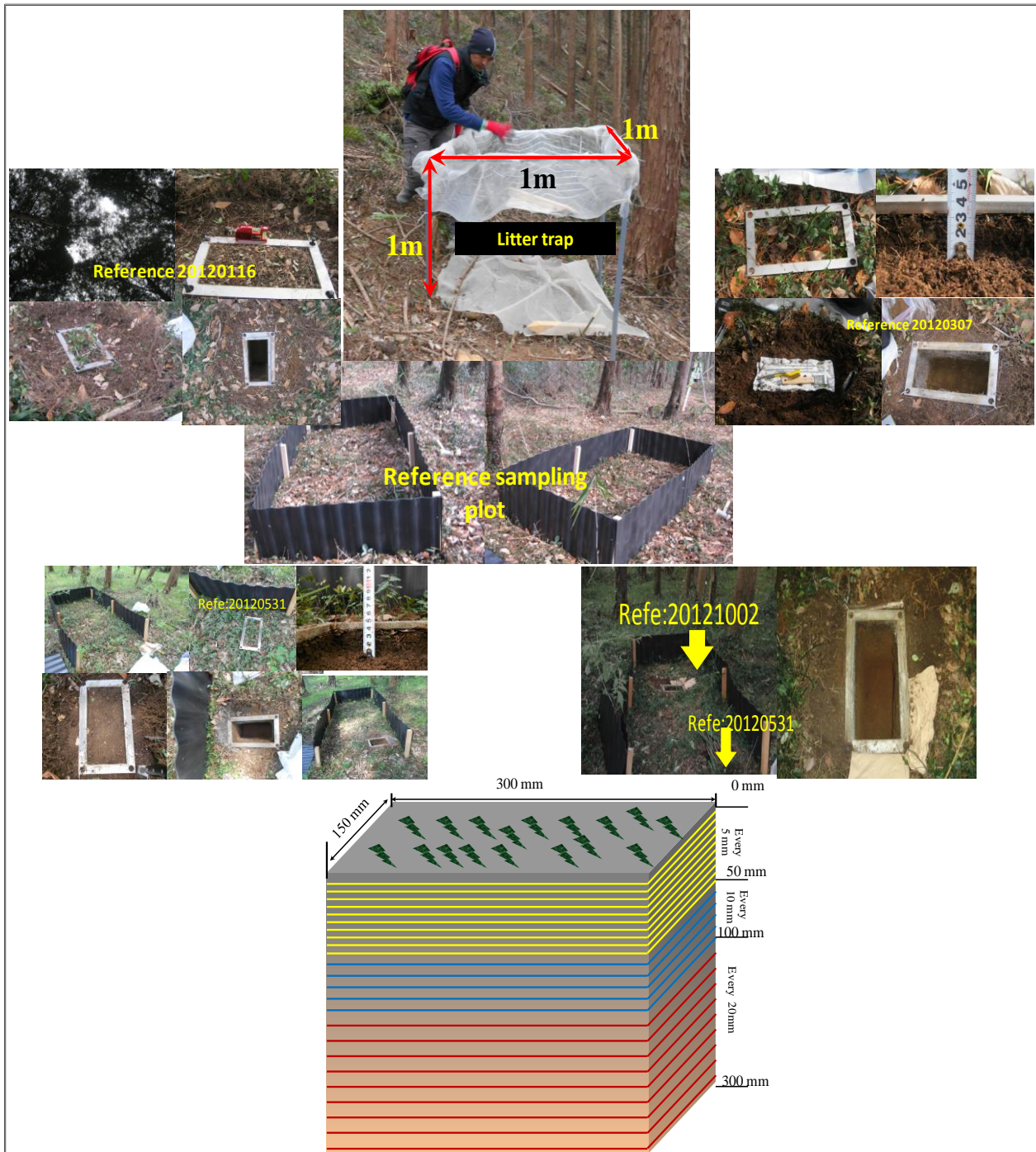


Figure 5.6 Photographs of litter trap and scraper soil sampling setups in coniferous forest at references site

5.3.3 Laboratory analysis

As illustrated in Figure 5.7, all samples were dried at 110°C for 24 h to determine the dry weight. The samples of litter, understory vegetation, Ol- and Of- horizons were then milled and mixed to ensure homogenous sample material for each respective sampling unit. The soil samples were disaggregated by gentle grinding and were then passed through a 2-mm sieve. Then, the milled understory vegetation, Ol-, Of-horizons and the < 2 mm soil fraction from each soil layer were placed in plastic U-8 bottles and sealed for assaying. The analysis was conducted in the laboratory of the University of Tsukuba, which was authorized for independent calibration checks during the worldwide open proficiency test in 2006 (IAEA/AL/171) prepared by the International Atomic Energy Agency (IAEA). The activities of ^{137}Cs and ^{134}Cs were determined using gamma ray spectrometry from a high purity n-type germanium coaxial gamma ray detector (EGC 25-195-R, Canberra-Eurysis, Meriden, USA) connected to an amplifier (PSC822, Canberra, Meriden, USA) and multichannel impulse separator (DSA1000, Canberra, Meriden, USA) using the counts at the 662 keV and 605 keV peaks, respectively. The absolute counting efficiency of the detector was calibrated using various weights of IAEA-2006-03 standard soil samples with background correction. The measured activities (Bq kg^{-1}) were converted to inventories (Bq m^{-2}) using the dry sample mass depth (kg m^{-2}) of each sampling layer. All measured activities were decay corrected to May 20, 2011. The organic matter (OM) of the samples was determined through loss-on-ignition method.

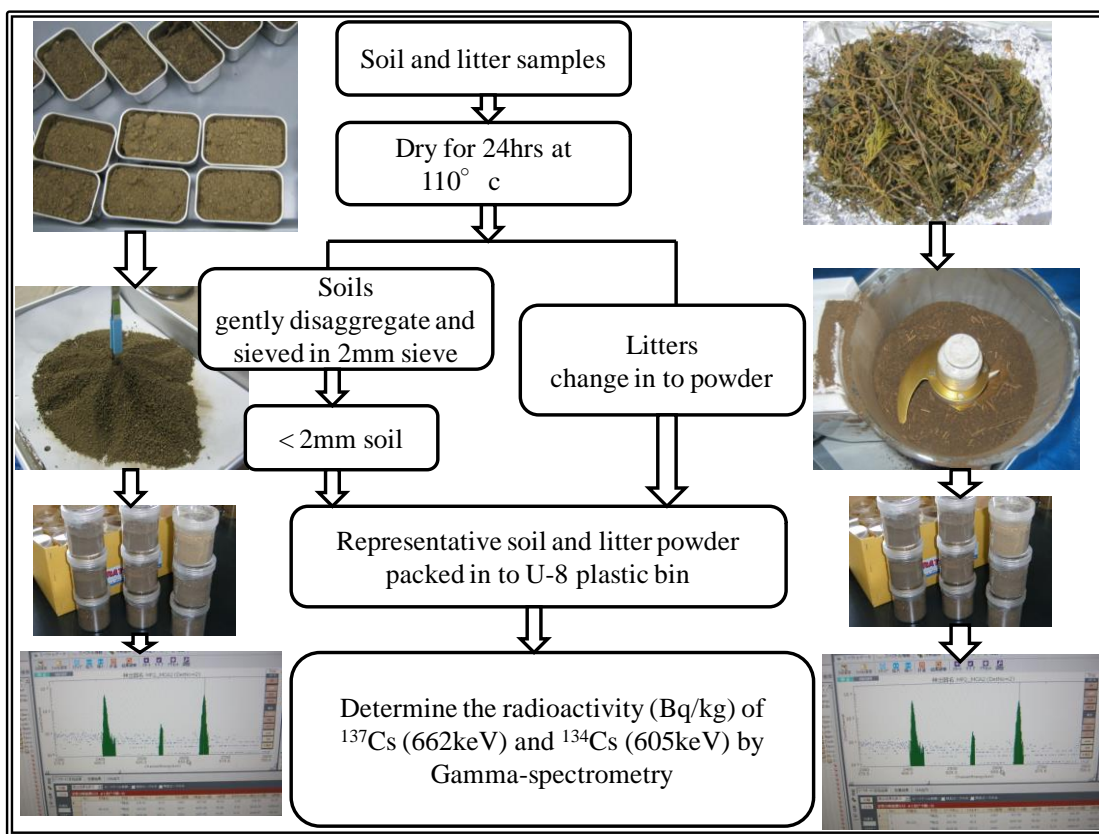


Figure 5.7 Laboratory procedures for soil and litter samples for radioactivity analysis

5.4 Results and discussion

5.4.1 ^{134}Cs : ^{137}Cs ratio in litterfall

Litterfall flux and its associated radiocesium were monitored using four litter traps for about one year and nine months. In average, 85 g m^{-2} litterfall per observation period provided an average of 9.6 kBq kg^{-1} radiocesium onto forest floor (Table 5.1). The radiocesium activity that deposited along with litter showed a general decreasing trend during the observation period regardless of the litterfall flux and thinning operation. This is possibly due to losses through weathering process, decaying (e.g Bunzl et al., 1989; Kato et al., 2012; Bonnett and Anderson, 1993) and also absorption and translocation by foliage at the canopy (Fesenko et al., 2001). However, the trends of deposition seem highly variable in temporal scale compared to spatial variability (Figure 5.8), possibly due to

the difference in litterfall flux according to their physiological responses to climatic bands across seasons.

Table 5.1 The amount of litterfall and associated radiocesium activity

Sampling period	Litterfall (g m ⁻²)	Activity		^{134:137} Cs ratio
		¹³⁷ Cs (Bq kg ⁻¹)	¹³⁴ Cs (Bq kg ⁻¹)	
2010/08/03 - 11/5	41±29	<i>nd</i>	<i>nd</i>	Before the accident
2010/11/05 - 2011/3/4	664±110	<i>nd</i>	<i>nd</i>	
2011/3/4 - 3/28	15±3	24933±6330	25257±6348	1.01
2011/3/28 - 4/1	-	-	-	-
2011/4/1 - 4/13	14±3	25143±6384	25471±6401	1.01
2011/4/13 - 4/27	-	-	-	-
2011/4/27 - 5/20	32±6	25438±6458	25143±6319	0.99
2011/5/20 - 5/28	-	-	-	-
2011/5/28 - 5/30	-	-	-	-
2011/5/30 - 6/13	23±4	25304±6425	25978±6529	1.03
2011/6/13 - 6/22	-	-	-	-
2011/6/22 - 7/18	-	-	-	-
2011/7/18 - 7/22	30±3	7833±1878	7664±565	0.98
2011/7/22 - 8/19	12±4	3250±677	3291±88	1.01
2011/7/22 - 10/11	23±9	3304±689	3327±89	1.01
2011/10/11 - 11/4	Thinning period			
2011/11/4 - 12/28	205±52	2819±698	3435±903	1.22
2011/12/28 - 2012/2/19	87±8	1594±342	1909±492	1.20
2012/02/19 - 4/6	331±48	1512±149	1828±198	1.21
2012/4/6 - 5/31	220±77	1378±128	1429±157	1.04
2012/5/31 - 8/28	28±11	1061±495	1120±579	1.06
2012/8/28 - 11/13	63±14	1430±386	1452±383	1.02
Average	85*	9615	9792	

* calculated starting from accident. *nd*: not detected

Litterfall showed an irregular pattern and its rate was generally higher and relatively variable both in time and space after thinning (Figure 5.8). Probably as a result of changes in aerodynamics in the forest ecosystem specially related to the speed and strength of the wind. Obviously, one can expect faster and stronger wind in post-thinning than that in pre-thinning environment which might easily break already weakened branches, twigs and leaves during intensive competition during pre-thinning time period.

The inventories of radiocesium deposition along with litter more or less follow a similar pattern with the litterfall flux (Figure 5.8). Comparatively, the cumulative radiocesium deposition during the observation period (first 641 days) via litter accounts for more than 60 % of the local fallout density (8 kBq m^{-2}). This result is far larger than the value reported by Bunzl et al. (1989). They reported only about 7% of the local fallout reached the forest floor by litter in 85-years old spruce forest during the first 600 days after the Chernobyl accident. This difference can be explained in terms of leaf area index (LAI) that could indicate the availability of solar radiation in forest ecosystem (Bonan, 1993). This can determine the amount and pattern of the falling leaf and therein the amount of radiocesium. For example, higher LAI refers larger leaf area or more leaves present per unit ground area (Jordan, 1969), implying closed canopy leads to less available solar radiation to the lower canopy components that could cause higher litterfall flux and vice versa. However, stand density is the only available information at the moment and cannot be directly mean higher LAI because LAI is directly depend on the size of leaf or number of leaf per unit ground area. Hence, it needs additional observation, further analysis and consideration to convert the stand density information to LAI so as to justify the observed differences. Regarding to the difference in stand density, the detail discussion can be referred in Chapter 4 section 4.7.1.

^{134}Cs : ^{137}Cs ratio in the falling litter over time showed almost similar values that range from 0.96 to 1.22 (Table 5.1). Its overall mean value during the observation period was found to be

approximately 1. Ohno et al. (2012) have reported similar values (0.97 - 1.0) from litter samples taken from 60 km west of the crippled Fukushima nuclear power plant. Therefore, I use the ratio value to be one and used in the analysis and discussion wherever needed.

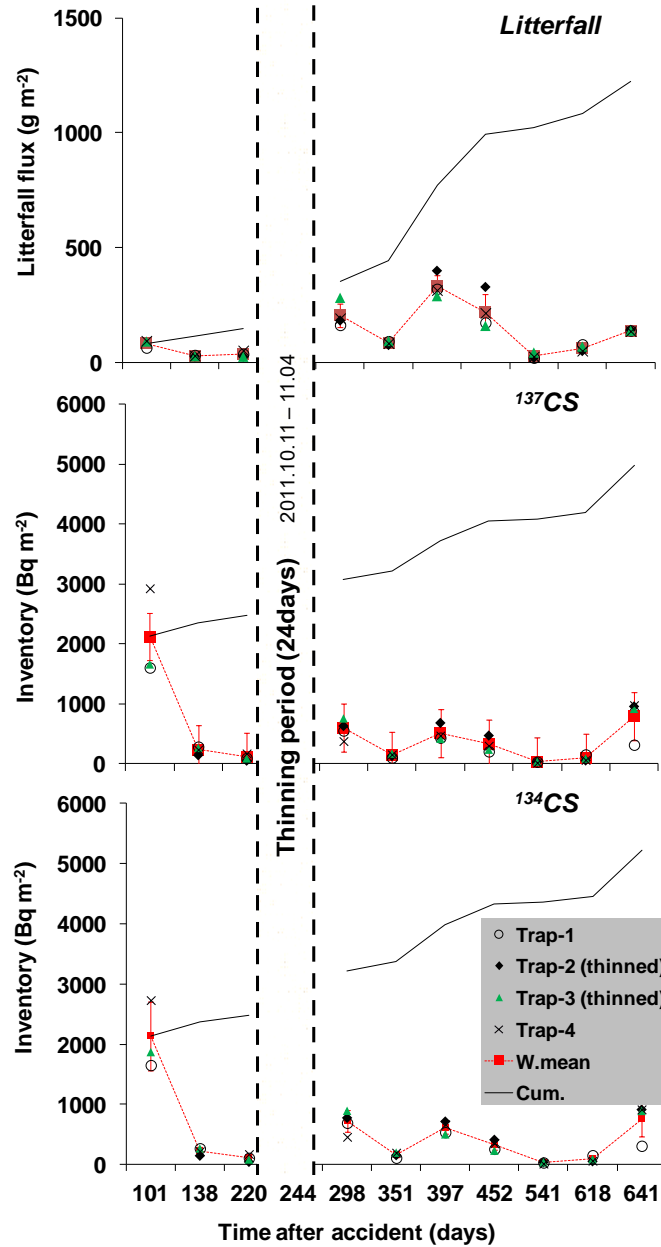


Figure 5.8 Temporal and spatial deposition pattern of litter and associated radiocesium after Fukushima accident. The red and broken line represents the weighted mean of the four litter traps during each respective observation period and the solid line shows the cumulative deposition.

5.4.2 Vertical distribution of radiocesium in soil profiles over time

The radiocesium in forest soil was found to be more active in forest floor section. Figure 5.9 illustrates radiocesium activity depth distribution over time. It can be observed that in the three components of forest floor (UG, Ol- and Of-layers), the radioactivity was more than 500 Bq kg⁻¹ and fluctuates with different magnitude among the sampling time steps. This implies that radiocesium tends to stay and circulated in this sub interface for considerable time period.

In fact several previous studies also revealed radiocesium tends to stay in the organic soil horizon. For example, Dorr and Munich (1991) suggested that radiocesium is mainly more active and bounded to SOM and its mobility decrease as the depth where turnover of OM is limited. In a good agreement, both the concentration and inventory of radiocesium (Table 5.2) in Of-horizon showed a general increasing trend over time, implying the input of radiocesium in this layer is higher than output. It is also clear and very true that just below Of-horizon (see Figure 5.9), the radioactivity sharply declined down the depth in all sampling dates, indicating radiocesium barely leave this layer over time. Similarly, Rafferty et al. (2000) have also evaluated the ¹³⁷Cs migration in a 35-year-old *Pinus contorta* forest stand under the influence of a full year of environmental conditions and found only 1% of ¹³⁷Cs was migrated in to mineral soil. Therefore, forest floor in generally and Of-horizon in particular (Figure 5.9b) can, at least be taken as a temporary sink of radiocesium and might be bioavailable to plant roots that potentially explore particularly this horizon. As shown in Table 5.2, the total radiocesium density fluctuates across the sampling dates while expected to increase. This kind irregular pattern can partly be explained by the presence of micro-spatial variability among the sampling soil profiles.

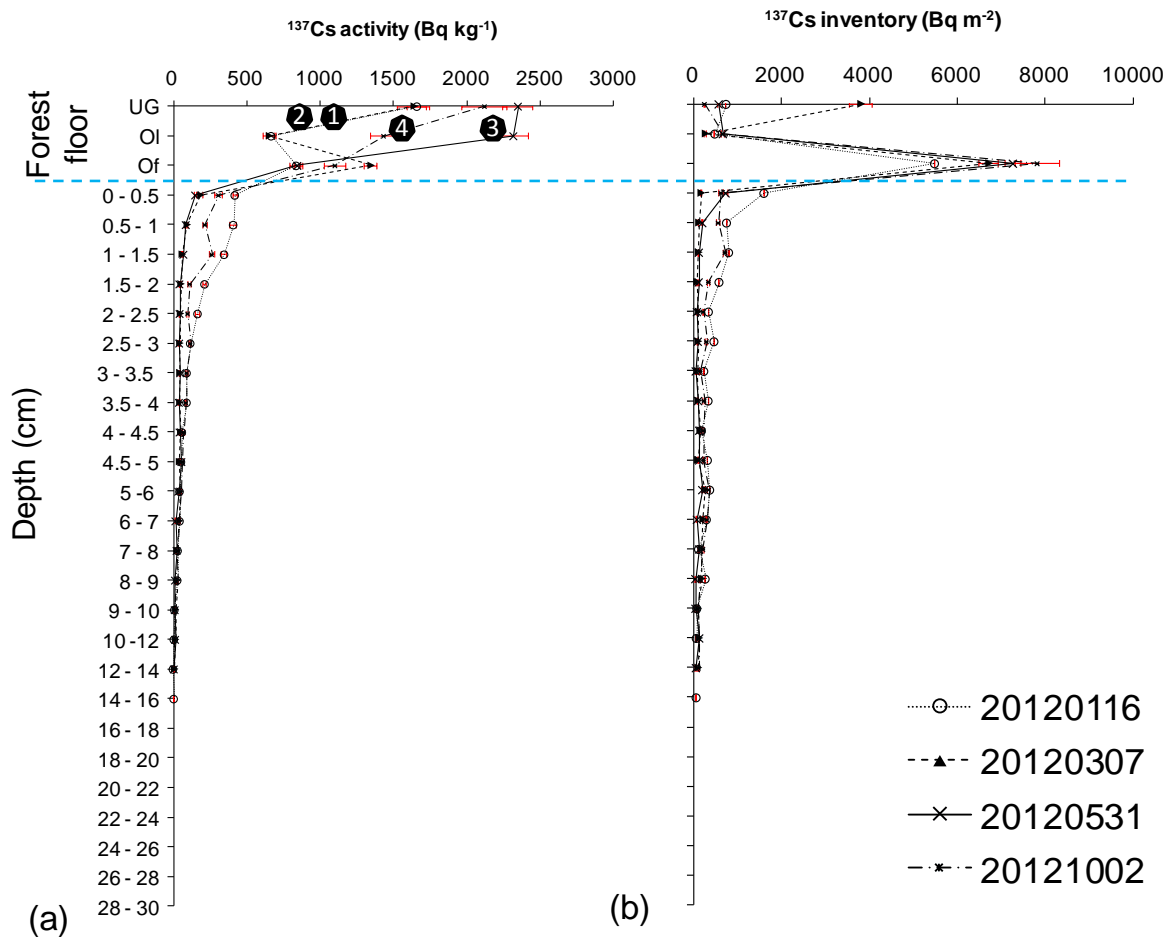


Figure 5.9 The depth distribution of the radiocesium activities (a) and the corresponding inventory (b) at the reference soil profiles in four different sampling dates. The number indicates the order of sampling time step sequence.

In forest floor components the following general order can be identified based on the evolution of radioactivity concentration over time:

UG: $3 > 4 > 1 > 2$ (highest in 3rd sampling profile => might be due to the sample was taken during active growing period)

Ol-layer: $2 > 4 > 1 \& 2$ (highest in 3rd sampling profile might be due to high Cs content in falling plant organs)

Of-layer: $2 > 4 > 1 \& 3$ (highest in the 2nd sampling => might be due to low root uptakes as plants are biologically in phase of rest)

From the above radiocesium activity evolution, it is possible to infer that sampling period might be an important factor to determine its concentration in specific time point and govern in defining its shape along soil profile.

Table 5.2 The proportion of radiocesium inventory in forest soil over time

		Sampling date				Mean mass depth (kg m ⁻²)
¹³⁷ Cs (% of total inventory)		2012.01.16	2012.03.07	2012.05.31	2012.10.02	
Forest soil layer	<i>Forest floor</i>					
	UG	5	29	5	2	0.2
	Ol	4	2	6	5	0.5
	Of	40	51	66	57	6.8
	<i>Mineral soil</i>					
	Below Of-layer	51	18	23	37	5.1
Total inventory (Bqm⁻²)		13690	13143	11096	13804	
<hr/>						
¹³⁴ Cs (% of total inventory)						
Forest soil layer	<i>Forest floor</i>					
	UG	6	27	5	2	0.2
	Ol	4	2	6	6	0.5
	Of	44	65	73	68	6.8
	<i>Mineral soil</i>					
	Below Of-layer	46	6	17	24	5.1
Total inventory (Bqm⁻²)		11030	11961	11371	12416	

5.2.1 Temporal behavior of ¹³⁴Cs:¹³⁷Cs ratio and soil organic matter along the soil profile

Given the micro spatial variability among sampling points, the ratio profile showed a general decreasing trend along the depth (Figure 9.10) which are the typical shapes for reference sites and the pattern is almost alike reported by Ohno et al. (2012) that the ratio decrease due to the presence of pre-Fukushima ¹³⁷Cs. The ratio generally increases just below the surface over time, confirming the presence of gradual migration of radiocesium from surface soil. However, the sampling time band seems not relaxing enough to clearly observe this effect.

As stated above Ruhm et al. (1997) have used radiocesium ratio to identify the potential soil layer where the fungi mycelium is located. With similar analog to test my hypothesis, the radiocesium ratio is plotted with the corresponding organic fraction along soil depth over time. Figure 5.10 illustrated the depth distribution of radiocesium ratio and the corresponding OM fraction of four sampling dates in fine depth interval. Both are high in the upper most surface soil layers and decreases in exponential pattern along the depth. The ratio in upper most soil surface is more or less similar to the ratio value in litterfall, indicating the dominate source of contamination of this soil section is the radiocesium deposited along with falling litter. Accordingly, matching radiocesium ratio seems more likely working on the upper soil horizon.

However, exceptionally higher (almost similar ratio values of the surface organic material) ratio was observed around the depth of 9 - 16 cm whereas the corresponding SOM fraction did not show any change from the normal trend (Figure 5.10). If this had transported with surface organic materials, the SOM fraction would have increased too. Previous studies reported that rapid migration phase are common just immediately after fresh fallout associated with percolating rainwater of the direct deposits. This input in solution makes the most rapid contribution of downward migration (Bunzl and Kracke 1988; Rafferty et al., 2000) before adsorption started. Therefore, the observed higher ratio in the specified depth in all four depth profiles is possibly caused by such rapid migration phase. In such cases, however, the ratio matching technique seems not feasible. Figure 5.11 demonstrates the evolution of radiocesium ratio and SOM fraction in coarse soil layers over time. From the figure it is clearer that radiocesium variability is intense as observed in fine depth profiles (Figure 5.10) at deeper soil sections and its evolution over time seems independent of the OM fraction (Figure 5.11). Still the coarse soil depth is unable to reduce the ratio variability over time in the deeper soil section. Braakhekke et al. (2013) suggested that different mechanism may be operating in different layers within one profile. This may lead to large

uncertainty and oversimplification as the result of generalization or neglecting of several factors for the sake of simplification. This further implies that the process of radiocesium migration is still not well understood and many questions remained unanswered.

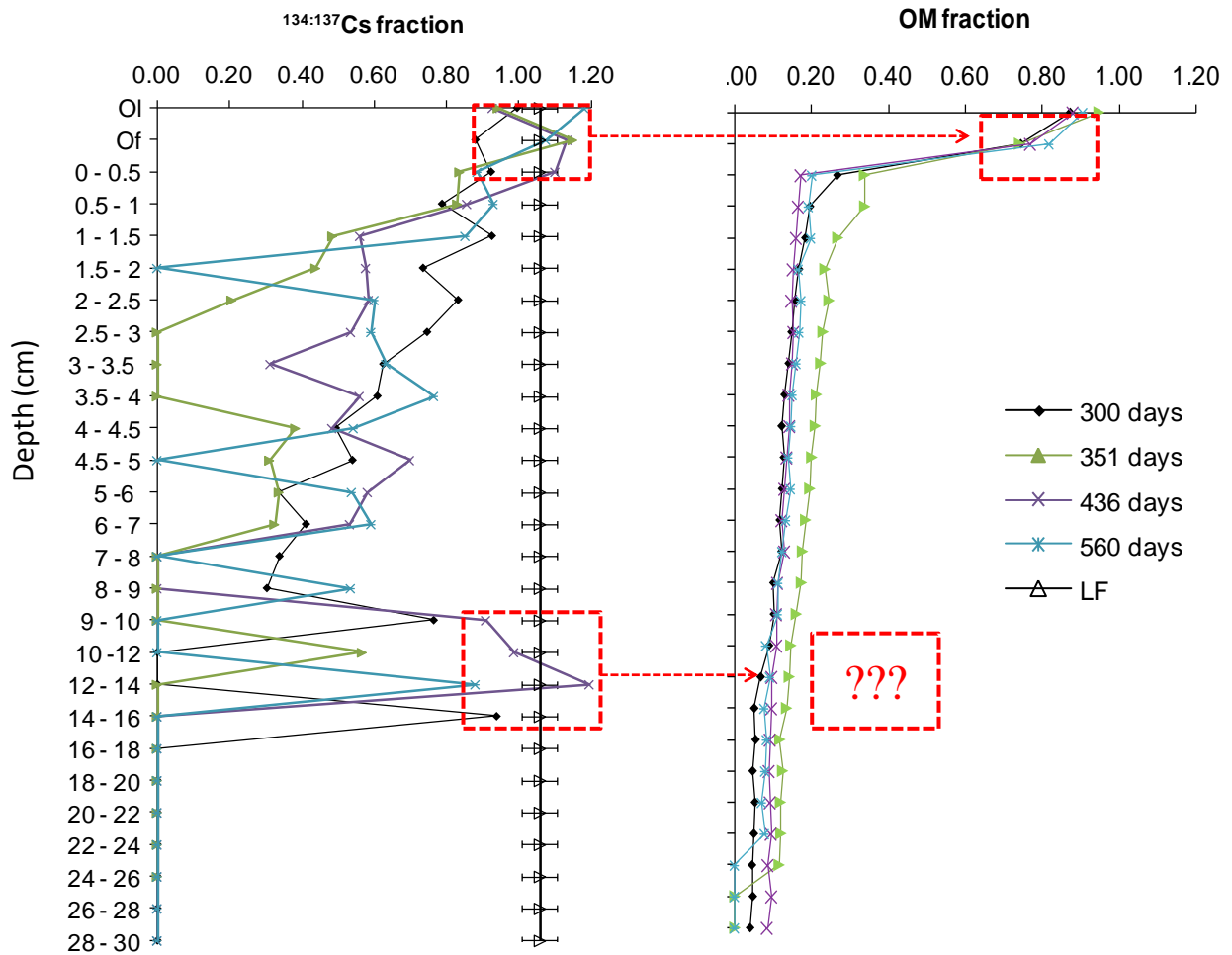


Figure 5.10 Vertical distribution of $^{134}\text{Cs}:$ ^{137}Cs ratio and the corresponding OM fraction along fine soil depth resolution over time. LF stands for the ratio in the falling litter which assumed to be constant across the sampling dates.

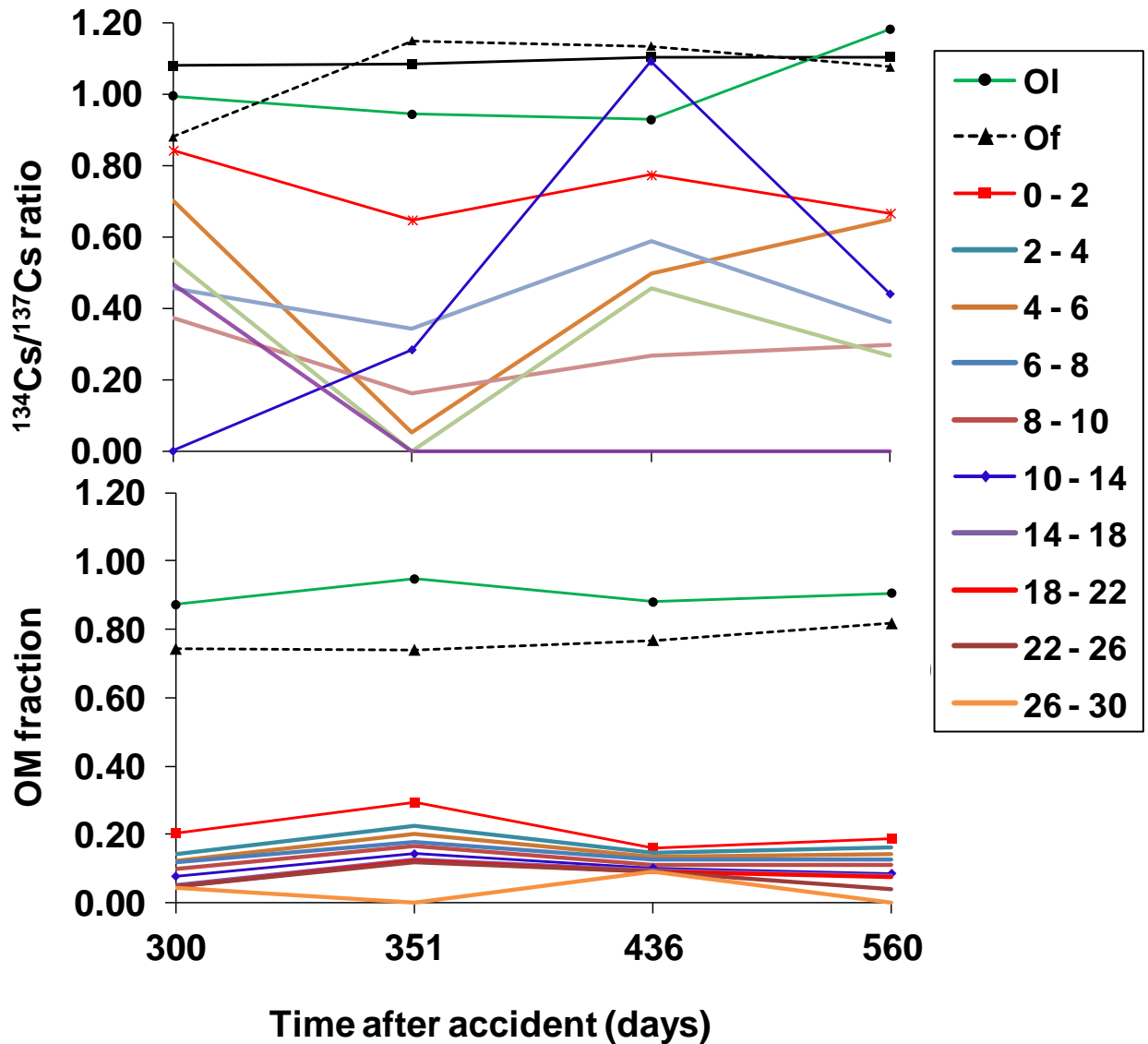


Figure 5.11 The evolution of $^{134}\text{Cs}:^{137}\text{Cs}$ ratio and SOM fraction in coarse soil section over time

5.5 Conclusions

Against the reported values, the contribution of litterfall path to deliver radiocesium is considerably high due to the obvious reason of stand density differences. However, stand density may not be directly related to the canopy closure or leaf area or more leaves. Therefore, I suggest that it is better to relate it the value of LAI which can explain better the radiation interception at the forest canopy.

Forest floor in general and Of-horizon in particular can, at least be taken as a temporary sink of radiocesium which might be bioavailable to plant roots that potentially explore this horizon. Below this soil section, the radiocesium is sharply decline with depth. Hence, the subsequent migration seems to depend on the migration of this soil section. Taking this unique behavior I proposed the use of $^{134}\text{Cs}:$ ^{137}Cs ratio matching along with the SOM fraction to trace the migration of surface materials along the soil profile. The technique seems working for the upper most dynamic soil horizons but failed to explain exceptionally high ratio observed in deeper soil section, which probably caused by rapid migration phase during the initial fallout associated with rain water percolation. This implies that still the process is not well understood. Therefore, further and detailed studies are needed to investigate how this principle can be workable. Besides, the behavior of radiocesium during decomposition processes is the central element to answer most of the basic questions associated to chemical and physical interaction of radiocesium with soil organic matter and organic carbon molecules. Doing so, such type of approach can help to estimate the migration of SOC from the time of decomposition on soil surface up to the deeper soil layer where it permanently locked. And most importantly this information can be linked and can supply supplemental evidences to the observed strong relationship between SOC and $^{210}\text{Pb}_{\text{ex}}$ which have been discussed in Chapter 2 and 3 to understand carbon cycle in forest ecosystem.

References

- Aerts, R., 1997. Climate, leaf litter chemistry and leaf litter decomposition in terrestrial ecosystems: a triangular relationship. *Oikos* **79**, 439–449
- Bonan, B.G., 1993. Imprtnance of leaf area index and forest type when estimating photosynthesis in boreal forests. *Remote Sensing Environment* **43**, 303 – 314.
- Bonnet P.J.P., Anderson M.A., 1993.Radiocesium dynamics in a coniferous forest canopy: a mid-wales case study. *Science of the Total Environment* **136**, 259 – 277.

- Braakhekke, M.C., Wutzler, T., Reichstein, M., Kattge J., Beer C., Schrump, et al., 2013. Modeling the vertical soil organic matter profile using Bayesian parameter estimation. *Biogeosciences* **10**, 399 - 420
- Bunzl, K., Kracke, W., 1988. Cumulative deposition of ^{137}Cs , ^{238}Pu , $^{239+240}\text{Pu}$ and ^{241}Am from global fallout in soils from forest, grassland and arable land in Bavaria (FRG). *Journal of Environmental Radioactivity* **8**, 1 – 14.
- Bunzl, K, Schimmack, W, Kreutzer, K, Schierl, R., 1989. Interception and retention of Chernobyl-derived ^{134}Cs , ^{137}Cs and ^{106}Ru in Spruce stand. *Science of the Total Environment* **78**, 77 – 87.
- Couteaux, M. M., Bottner, P., Berg B., 1995. Litter decomposition, climate and litter quality. *Tree* **10** (2), 63 - 65
- Dorr, H, Munnich, O.K., 1991. Lead and Cesium transport in European Forest soils. *Water, air, and Soil Pollution* **57 - 58**, 809 –18.
- Fesenko, S.V, Soukhova, N.V, Sanzharova, N.I, Avila, R, Spiridonov, S.I, Klein, D, et al. 2001. Identification of processes governing long-term accumulation of ^{137}Cs by forest trees following the Chernobyl accident. *Radiation and Environmental Biophysics* **40**, 105 – 13.
- Garcia-Palacios, P., Milla, R, Delgado-Baquerizo, M., Martin-Robles, N., Alvaro-Sanchez, M, Diana, H. Wall, D. H., 2013. Side-effects of plant domestication: ecosystem impacts of changes in litter quality. *New Phytologist* **198**, 504 – 513
- Hillel, D., 1998. Environmental Soil Physics. Academic press, New York.
- Jordan, C.F., 1969. Derivation of Leaf-Area Index from quality of light on the forest floor. *Ecology* **50**(4), 663 – 666.
- Kato, H, Onda, Y, Gomi, T., 2012. Interception of the Fukushima reactor accident-derived ^{137}Cs , ^{134}Cs and ^{131}I by coniferous forest canopies. *Geophys. Res. Lett* **39**, L20403, doi:10.1029/2012GL052928.

- Loughran, R.J, Wallbrink, P.J, Walling, D.E, Appleby, P.G., 2002. Chapter 3: Sampling method. In: Zapata, F., editor. Handbook for the Assessment of Soil Erosion and Sedimentation using Environmental Radionuclides. The Netherlands: Kluwer Academic Publishers; p. 41 - 57.
- Ohno, T., Muramatsu, Y., Miura, Y., Oda, K. Inagawa, N., Ogawa, H., Ymazaki, A., Toyama, C., Sato, M. 2012. Depth profiles of radioactive cesium and iodine released from Fukushima Daiichi nuclear power plant in different agricultural fields and forest. *Geochemical* **46**, 287 – 295.
- Prescott, C. E., 2005. Do rates of litter decomposition tell us anything I really need to know? *Forest Ecology and Management* **220**, 66 - 74
- Rafferty, B., Brenna, M, Dawson, M, Dowding, D., 2000. Mechanism of ¹³⁷Cs migration in coniferous forest soils. *Journal of Environmental Radioactivity* **48**, 131 – 43.
- Ruhm, W., Kammerer, L., Hiersche, L., Wirth, E., 1997. The ¹³⁷Cs/¹³⁴Cs ratio in Fungi as an indicator of the major mycelium location in forest soil. *Journal of Environmental Radioactivity* **35**(2), 129 – 148.

Chapter 6: General discussion and Conclusions

6.1 Main Findings of the study and their intra-linkage

The study was aimed to evaluate the relationship between fallout radionuclides and soil organic carbon in coniferous forest. For this purpose, observations were carried out at plot scale in three forest types (Japanese cypress, Japanese cedar and broad-leaved forest (BLF)) to get pre-hand information and at watershed scale (Japanese cypress forest) to confirm the persistency of the results obtained at plot scale. Due to the introduction of new radiocesium to the environment following Fukushima nuclear power plant accident, additional and supplemental analysis were carried out on its migration in forested system to trace more recent environmental processes like migration of organic matter (OM) along the soil profile. The main findings of each Chapter are discussed below and their linkages are illustrated in Figure 6.1.

In chapter 2, the relationship of SOC to $^{210}\text{Pb}_{\text{ex}}$ (natural radionuclide) and ^{137}Cs (artificial radionuclide) during soil erosion in hillslope forested environment were closely examined using runoff plots in three different forest types. High soil erosion was observed in Japanese cypress forest followed by BLF and Japanese cedar. Similar order of magnitude was also reported by Wakiyama et al. (2010). However, the SOC content in the eroded materials follow a reverse order, indicating the role of SOC budget in reducing soil erosion. Therefore, it is possible to conclude that the lower the soil erosion the higher the SOC content at the point of source. Regarding to the discharged radionuclides by runoff, comparatively, $^{210}\text{Pb}_{\text{ex}}$ and SOC have shown strong linear relationship across the examined forest types and move together when erosion impacted them. This partially explained by the advantage of the chemical property it possesses towards the cation exchanging sites than ^{137}Cs . Several researchers appreciated the existence of strong correlation between OM to radiocesium (Dorr, 1995; Vaaramaa et al., 2010) and so does in this study to SOC.

As indicated in the preceding Chapter, $^{210}\text{Pb}_{\text{ex}}$ has shown strong affinity with SOC in the course of soil erosion. At the same time, Japanese cypress stand was identified as highly eroded forest, caught attention for further investigation. Hence, detailed analysis was done to evaluate this strong relationship at wider scale. In Chapter 3, the dynamics and relationship of SOC and $^{210}\text{Pb}_{\text{ex}}$ starting from the very beginning of deposition from forest canopy was examined. As a result, I found out again strong relationship between them both in spatial and vertical distribution. Then I proposed a qualitative model called “*Inverted –U-Shape model*” for both stable and hillslope scenario to represent the dynamic of SOC and radiollead pathways in forested environment as a modification of the common compartment model used in several studies (e.g. Likuku, 2009; Osaki et al., 2003).

Collectively, it is reasonable to propose $^{210}\text{Pb}_{\text{ex}}$ as a potential radionuclide candidate to trace and study SOC process in forested environment due to the following major advantages:

1. As it has a natural source, it can deposit as a continuous input from atmosphere and canopy along with the falling litter. In forest environment, falling litter is a sole input source of SOC and radiollead, giving a good opportunity to deposit, interact and move together in biogeochemical processes.
2. In both observation scales it demonstrated strong correlation with SOC due to its unique chemical advantage (Hillel, 1998)
3. Its ubiquitous nature makes it possible for global application unlike of area-specific artificial radiocesium

In fact I identified litterfall as the major pathway of radiollead input to the forest floor. However, radiollead in the soil is the lump sum of direct fallout, hydrological inputs and litterfall routes while the sources of SOC are almost from falling litter. Hence, the potential limitation is lack of technique to separate the radiollead deposited with litterfall in the soil which requires further study

at least to develop the correction coefficient to split out litter-fed radiolabel and look at its relationship with SOC originated from the litter in the course of decomposition. One possible approach could be laboratory experiment to see the behavior of radiolabel attached to litter and develop a correction coefficient to correct the field experiment.

In Chapter 4 and 5 I dealt with Fukushima-derived radiocesium for the purpose of supplemental and additional information to understand more recent environmental events such as soil forming processes and migration of highly contaminated soil section along the soil profile. Since litter is the main input sources of SOC and other nutrients, it can play a great role in transferring, depositing and distributing radionuclides from forest canopy to forest floor (Bunzl et al. 1989, Prescott, 2005) in similar ways for other nutrients. On top of this, the falling litter found to be the dominant transferring mechanism of radiocesium from forest canopy to forest floor and prolonged to operate after other mechanism had stopped. My result is against the value reported by Bunzl et al. (1989) from spruce stand. One possible reason could be the difference in stand age and density. Indeed leaf area index (LAI) can be a more realistic comparison tool for the observed differences. It actually express the area covered by leaf in the canopy which can be related to amount of light that potentially reach the lower canopy parts and forest floor. However, it needs to change the available stand density information to LAI which in turn demands conversion factor. Therefore, additional study and analysis is required in the future to develop and outline procedures and protocols to utilize the stand density characteristics and information to LAI to estimate eventually the amount of light flux available for forest environment below the upper front of forest canopy.

The evolution of $^{134}\text{Cs}:^{137}\text{Cs}$ ratio in the organic horizons and matching it along the depth might be a useful indicator to trace the movement of soil organic fraction. This method seems worth particularly to estimate the migration of SOC upon decomposition. Because the date of introduction

of ^{134}Cs in the environment is definitely known, possesses short half-life with known decaying rate and totally deposited on surface soil before it propagated down the depth. This offers a good opportunity to examine recent migration of OM/SOC to the deeper soil horizon that probably locked permanently and able to estimate its stock as well as its vertical cycle in soil profile in better way. Although $^{210}\text{Pb}_{\text{ex}}$ is under researched topic, especially this ratio approach might be helpful to validate and complements the natural $^{210}\text{Pb}_{\text{ex}} - \text{SOC}$ relationship found in Chapter 2 and 3 in this study. However, still the concept is young and surrounded by various uncertainties and questions in the course of developing protocols, models and working principles out of it. Questions including: how radiocesium behave during litter decomposition? What is the physical and mechanical interaction between radiocesium and litter decomposition products? What and how other migration mechanisms affect the radiocesium budget in a given soil horizon? What are the roles of decomposing community on radiocesium migration? and so forth?

6.2 Conclusions

In response to lack of methods to understand the carbon cycle as an interface that involves many complex factors, interacted processes and surrounded by uncertainty, I studied starting from identifying a very simple relationship between SOC and fallout radionuclides as best strategy to step on to the next level. The deriving point is that there are several isotope-based studies available in agricultural field but even simple evaluation is lacking in forest ecosystem particularly regarding to the natural radiolead due to the mostly obvious reason- the complexity of forest environment. Within these circumstances, I found a permissible and strong linear relationship between SOC and $^{210}\text{Pb}_{\text{ex}}$ at:

- (1) Plot scale: where I examined the relationship between SOC and radionuclides (radiolead and radiocesium) during soil water induced-erosion process. The result revealed that the

discharged radiolead and SOC moved together than did SOC and radiocesium, indicating radiolead has a tendency of fixing on SOC complex.

- (2) Watershed scale: where the spatial and depth distribution SOC and radionuclide (radiolead & radiocesium) and their relationship have been evaluated started from falling litter as deposition mechanism. The data of falling litter revealed that litterfall transfers more than half of $^{210}\text{Pb}_{\text{ex}}$ that deposits on forest canopy annually whereas radiocesium was not detected at all. Given that a continuous type of input of $^{210}\text{Pb}_{\text{ex}}$ and litter as main input source of SOC, falling litter operates as a main transferring agent that deposits simultaneously $^{210}\text{Pb}_{\text{ex}}$ mechanically and organic carbon physio-chemically onto forest floor. This provides an opportunity for both to interact and move together in the subsequent biogeochemical processes. The results in this study revealed that physically $^{210}\text{Pb}_{\text{ex}}$ and SOC are moving together and chemically (based on literature, Hillel, 1998) are strongly bounded than ^{137}Cs .

Hence, I proposed $^{210}\text{Pb}_{\text{ex}}$ as a potential radionuclide candidate to trace and study SOC dynamics in forested environment and developed a qualitative model called Inverted-U shaped model (IUS-model) to represent the $^{210}\text{Pb}_{\text{ex}}$ and carbon cycles in forested environment. The model gives a simple way of representing the radiolead and organic carbon flows in forested environment and helps to quantify the amount of radiolead budget at different components in the forest in stepwise pattern. However, correction factor is required to amend the radiolead deposited by other mechanisms such as hydrological process to better understand the fate of litter-fed radiolead component in the soil after deposition, possibly in the course of decomposition process.

Fukushima –derived radiocesium is found to be retained in forest canopy and litterfall still dominating its transfer pathways to forest floor. In soil, Fukushima-derived radiocesium tends to stay in upper soil layer where OM is above 10%. It seems that the subsequent migration is to depend on

the movement of this soil fraction. Although the principle is young and not well understood, the introduction of ^{134}Cs into the environment following the Fukushima nuclear power plant, could provide additional opportunity to analysis more recent processes like the migration of OM/SOC along the soil profile. ^{134}Cs : ^{137}Cs ratio matching with OM therein SOC along soil profile to trace the recent migration of surface materials were examined and seems working in the upper most soil layers. Given the need of detailed and additional studies, ratio matching can be used as supplementary information for the carbon cycle along the vertical soil profiles. Together with the $^{210}\text{Pb}_{\text{ex}}$, radiocesium ratio could be a possible tool to trace the transfer rate of SOC from upper soil horizons to deeper horizon where it is permanently locked. Such information can be useful to estimate the carbon sequestration rate by forest soil and provide better and essential inputs and can serve as a tool for different global, regional and local climate and environmental programs.

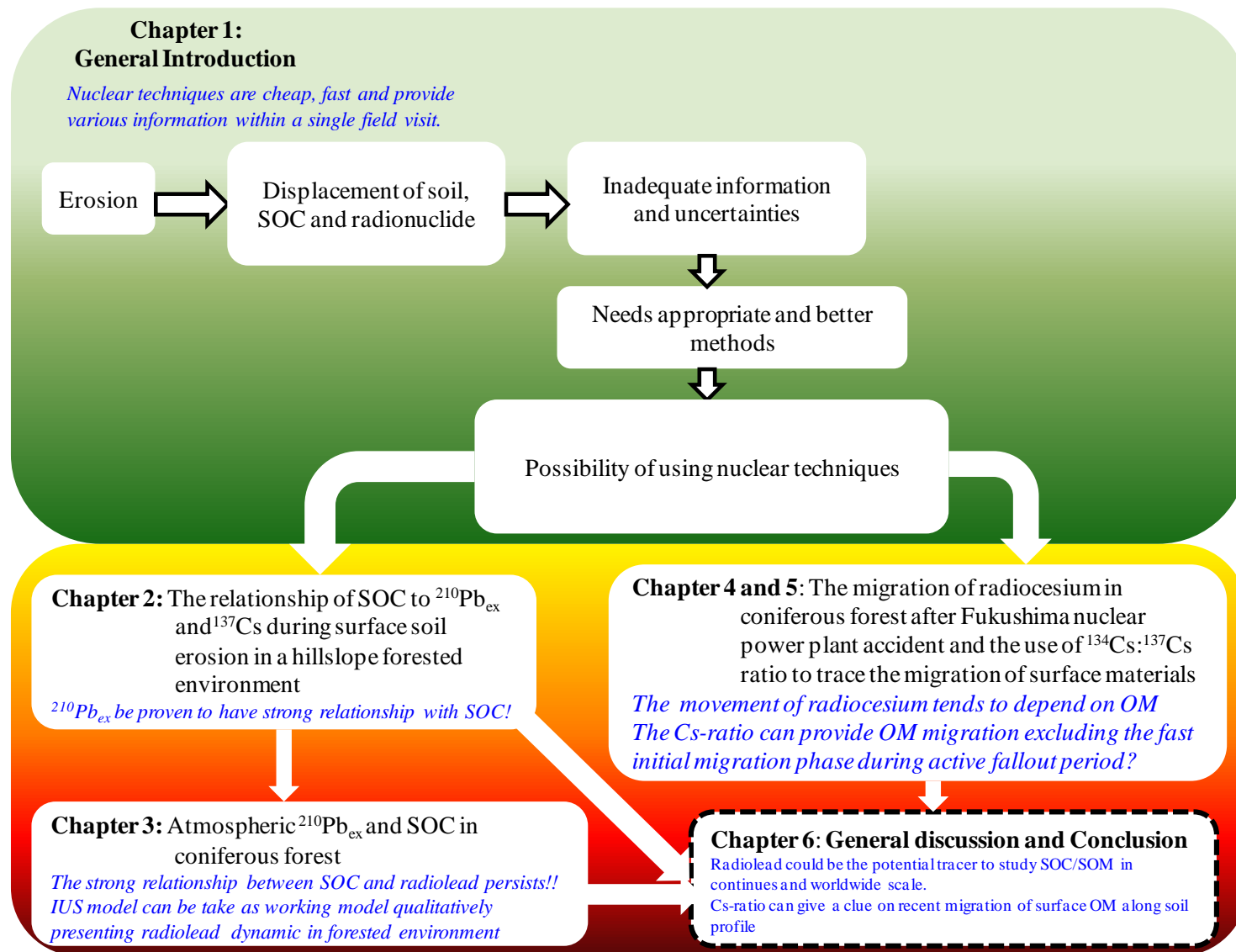


Figure 6.1 A framework of logical connectivity across the topics of the chapters with their main findings in this study. *SOC*: Soil organic carbon; *SOM*: soil organic matter

References

- Bunzl, K, Schimmack W, Kreutzer K, Schierl R., 1989a. Interception and retention of Chernobyl-derived ^{134}Cs , ^{137}Cs and ^{106}Ru in Spruce stand. *Science of the Total Environment* **78**, 77 – 87.
- Dorr, H., 1995. Application of ^{210}Pb in soils. *Paleolimnol* **13**, 157 - 168.
- Hillel, D., 1998. Environmental Soil Physics. Academic press, New York.
- Likuku, A.S., 2009. Atmospheric transfer and deposition mechanisms of ^{210}Pb aerosols on to forest
Soils. Water Air and Soil Pollution **9**, 179 – 184.
- Osaki, S., Tagawa, Y., Sugihara, S., Maeda, Y., Inokura, Y., 2003. Transfer of ^7Be , ^{210}Pb and ^{210}Po in a forest canopy of Japanese cedar. *Journal of Radioanalytical and Nuclear Chemistry*, **255** (2), 449 – 454.
- Vaaramaa, K., Lasse, A., Solatie, D., Lehto, J., 2010. Distribution of ^{210}Pb and ^{210}Po in boreal forest
Soil. Science of the Total Environment **408**, 6165 - 6171.
- Wakiyama, Y., Onda, Y., Mizugaki, S., Asai, Hiramatsu, S., 2010. Soil erosion rates on forested mountain hillslopes estimated using ^{137}Cs and $^{210}\text{Pb}_{\text{ex}}$. *Geoderma*, **159**, 39 - 52.

Acknowledgments

In the last five years I have received and earned a great of knowledge and character from my laboratory members and surrounding community in Tsukuba and the hospitality I received from the peoples of Japan where ever I traveled. I have been so fortune and I wish to take this opportunity to acknowledge as many peoples as possible though I would be happy to thank each and every person whom I received kind supports.

Uppermost, I applaudably and plausibly indebted to my supervisor Professor Dr. Yuichi Onda for unlimited direction, assistance and all round supports in the course of this study. Without his help, it is just unthinkable. I am very thankful to Professor Takehiko Fukushima, Associate Professor Bunkei Matsushita, Associate Professor Teruyuki Maruoka and Lecturer Ryo Anma, Associate professor Hirota Matsu for their constructive comments which helped me a lot to shape this study. My special thanks extend to Dr. Yoshifumi Wakiyama who strongly helped me in all processes starting from planning, field work and laboratory analysis. His support was time and space unlimited. Indeed no words can satisfy me to thank Dr. Hiroaki Kato. I am totally indebted for his unlimited support, guidance and advise specially dealing with the Fukushima cases and his support even extended out of the science edges. It was worthy for me all the time I spent with him, Thank you, Dr. Kato. I am also grateful to Associate professor Takashi Gomi and Dr. Jeremy Patin for taking their valuable time for reading and commenting on manuscript.

I pleased to express my gratitude for Dr. Abrar Juhar Mohammed for his encouragement and valuable advices along the course of this study. I am also thankful to Dr. Shigeru Mizugaki, for his support in laboratory work, data analysis procedure and general advices. My special gratitude goes to the sampling crew Dr. Tajirou Fukuyama, Dr. Yoshifumi Wakiyama, Ms. Furukawa Tomomi, Ms. Natsuki Tanigawa and Mr. Tomohiro Narisawa. Without this crew's helps and comments, it is hard to come up and realized the part of this study. I am also grateful to staffs and students from

environmental soil chemistry laboratory of the University Tsukuba particularly Mr. Takashi Kanda who assisted me in SOC analysis and Professor Teruo Higashi, Associate Professor Tamura Kenji and Ms. Maki Asano who arranged and allowed me to participate in soil seminars.

I am immensely pleased for warm cooperation and support in my study and laboratory life from Mr. Shinya Takahashi (my Tutor), Mr. Shigeaki Baba, Ms. Furukawa Tomomi, Dr. Yoshifumi Wakiyama, Dr. Hiroaki Kato, Dr. Kazuki Nanko, Ms. Marino Hiroaka, Mr. Yoshitaka Komatsu, Mr. Yusuke Noguchi, Dr. Tomoyuki Iida, Dr. Kazuya Yoshimura, Dr. Nicolas Loffredo, Dr. Akiko Hirata, Dr. Sho Iwagami, Mr. Cristobal M. Padilla, Mr. Yoshitaka Komatsu, Mr. Xinchao Sun, Mr. Yukio Takeuchi, Mr. Hiroki Yoda, Ms. Ayumi Kawamori, Mr. Ryo Manome, Mr. Shimpei Kawaguchi, Mrs. Minako Takase, Mrs. Fumi Kono, Mrs. Noriko Maekawa, Mrs. Takako Sato, Mrs. Asami Okazaki, Mrs. Keiko Sumiya, Mrs. Fumiko Koiwa, Mrs. Kazumi Fujii, Mrs. Yoko Matsui, Mrs. Noriko Oshima, Mrs. Yuko Takakuwa, Mrs. Maki Hayashi, Mrs. Tomiko Horie, Mrs. Masumi Aizawa, Mrs. Miyuki Abe, Mrs. Atsuko Kojima, Mrs. Yukari Taguchi, Mrs. Yuri Kojina.

My family, my love and my wife, thank you for your priceless support and being me a father. I dedicated this study for my lovely wife, my baby boy, my sisters and my late parents, you-all deserve it.

This study is the part and parcel of the Core Research for Evolutional Science and Technology (CREST) project of Japan entitled 'Development of innovative technologies for increasing in watershed runoff and improving river environment by the management practice of devastated forest plantation' and this work was also funded from the distribution-mapping project financially supported by the Ministry of Education, Culture, Sports, Science and Technology of Japan. I gratefully acknowledged their support.

I am so grateful to the government of Japan for offering me Monbukagakusho (MEXT) scholarship which is the part of bi-lateral agreements signed with the government of Ethiopia. Last

but not least, I also highly appreciate innumerable individuals, institutions and organizations' directly and indirectly for their contribution towards the success of this study. Thank you-ALL.

Above all, how I honor Him! Praise be to God! He made it possible, Thank you!